Development of Analytical Framework for MIMO-OFDM System in Fading Environment

A Thesis

submitted in partial fulfillment of the requirements for the award of the degree of

Doctor of Philosophy

in

Department of Electronics and Communication Engg.

by

Daljeet Singh
(Reg no: 951306004)

under the supervision of

Dr. Hem Dutt Joshi
Associate Professor

Thapar Institute of Engineering and Technology
Patiala, India
July 2018

Candidate Declaration

I hereby certify that the work, which is being presented in the thesis, entitled **Development of Analytical Framework for MIMO-OFDM System in Fading Environment**, in partial fulfillment of the requirements for the award of the degree of **Doctor of Philosophy** in Electronics and Communication Engineering from Thapar Institute of Engineering and Technology, Patiala is an authentic record of my own work carried out during the period **Jan 2014** to **July 2018** under the supervision of Dr. Hem Dutt Joshi. I have also cited the reference about the text(s)/figure(s)/table(s) from where they have been taken. The matter presented in this thesis has not been submitted elsewhere for the award of any other degree or diploma from any institution.

Date: 10/07/19

Daljeet Singh
Candidate

This is to certify that the above statement made by the candidate is correct to the best of our knowledge.

Date: 10/07/19

Dr. Hem Dutt Joshi
Associate Professor
Supervisor

.....to my parents, to my wife and to our son PavitAradh

Abstract

The use of wireless communication has extended from traditional voice calling and short message service to high-speed internet, machine-to-machine communication, and real-time applications like online gaming, video conferencing, e-commerce transactions, voice over internet protocol, chatting, and instant messaging. As a result, the number of distinct users who communicate through wireless media has increased substantially over the last few years. These recent innovations in mobile systems have pushed the current fourth-generation communication systems to achieve even higher throughput. Maintaining the required quality of service for reliable and secure communication is the major challenge among the research fraternity.

In order to fulfill these needs of wireless communication, many current and future standards have adopted multicarrier techniques like orthogonal frequency-division multiplexing (OFDM) along with multiple-input-multiple-output (MIMO) system. This combination is known as MIMO-OFDM system, which has advantages of both MIMO and OFDM. MIMO can be implemented effectively with the help of different coding techniques in time and/or frequency domain.

In this dissertation, an analytical framework for MIMO-OFDM systems is presented. It includes the study of different types of MIMO-OFDM systems and the various sub-blocks that are used to implement these systems. With the aid of the analytical framework devised in this work, the performance of MIMO-OFDM systems is calculated. The second contribution of this thesis is the introduction of a unified approach for obtaining the performance analysis of MIMO-OFDM system. This approach was introduced for both space frequency block coded and space time block coded OFDM systems. The performance of MIMO-OFDM systems can be calculated for any given fading scenario using the proposed approach due to the usage of generalized channels. The third contribution of this thesis is the study of MIMO-OFDM systems under the effect of channel impairments like carrier frequency offset and unavailability of perfect channel state information. The analytical results obtained from the derived expressions are verified using Monte Carlo simulations. The results obtained by the proposed unified approach are obtained mostly in closed-form expressions. In some cases, numerical integration is required to be calculated over finite limits. This is very easily implemented with ignorable error using tools like MATLAB and Mathematica.

List of Publications

SCI Journal

1. D. Singh and H. D. Joshi, "BER Performance of SFBC OFDM System over TWDP Fading Channel," *IEEE Commun. Lett.*, vol. 20, no. 12, pp. 2426-2429, 2016.

2. D. Singh and H. D. Joshi, "Performance Analysis of SFBC-OFDM System with Channel Estimation Error Over Generalized Fading Channels," *Trans. Emerg. Telecommun. Technol.*, vol. 29, no. 3, pp. e3293, 2018.

3. D. Singh and H. D. Joshi, "Generalized MGF Based Analysis of Line-of-Sight Plus Scatter Fading Model and its Applications to MIMO-OFDM Systems," *Int. J. Electron. and Commun.*, vol. 91, pp. 110-117, 2018.

4. D. Singh and H. D. Joshi, "Error Probability Analysis of STBC-OFDM Systems with CFO and Imperfect CSI over Generalized Fading Channels," *Int. J. Electron. and Commun.*, vol. 98, pp. 156-163, 2019.

International Conference

1. D. Singh, H. D. Joshi, and B. Gupta, "Performance of SFBC-OFDM Systems in Fading MIMO Channels," in *Proc. of the* 10^{th} *INDIACom,* 4^{th} *Int. Conference on Computing for Sustainable Global Development*, New Delhi, Mar. 2017, pp. 819-821.

2. D. Singh and H. D. Joshi, "ABER Analysis of SFBC-OFDM System with Different Detection Schemes over Fading Channels," in 15^{th} *Int. Symp. on Wireless Communication Systems (ISWCS)*, Portugal, Aug. 2018.

Acknowledgements

Any task as onerous and challenging as Ph.D. dissertation cannot expect to see its fruition but for the consistent support and contributions from a lot of people. Therefore, there are a number of people that must be acknowledged for the successful compilation of this dissertation.

I owe an extreme debt of gratitude to my Ph.D. guide Dr. Hem Dutt Joshi who has always supported and motivated me to go in the right direction. This Ph.D. would not have been possible without the contribution of numerous technical criticisms, ideas, and suggestions given by him that found their way into the final dissertation. I could not have asked for a more supportive and knowledgeable Ph.D. guide. Further, I am also obliged to everyone in my Ph.D. committee: Dr. Rajesh Khanna, Dr. Amit Kumar Kohli and Dr. Neeraj Kumar whose valuable suggestions helped me to give the final shape to the dissertation.

I am extremely fortunate to have very helpful and talented friends at Thapar Institute of Engineering and Technology. What wonderful people I have worked with over the years. There are friends I would like to single out for their help and unconditional friendship throughout my Ph.D.: Manish Deshwal, Dr. Gaurav Madhu, Atul Kumar, Dr. Pradeep Teotia, Chandanpreet Kaur and Atul Sharma.

No words of thanks are enough to express my deepest gratitude and sincerest love to my parents whose rock solid faith in me kept me strong in all circumstances. I am also thankful to my wife Dilshad, my brother Gurpreet for their wholehearted and endless support and patience. Last but not least, I bow my head before the Almighty God for showering His mercy on me for each and every moment.

Daljeet Singh

Table of Contents

List of Figures

List of Tables

List of Notations

In this dissertation, the matrices are represented by uppercase boldface letters, and lowercase boldface is used for vectors, whereas scalars are shown with un-boldface letters.

w	Additive white Gaussian noise
$\bar{\gamma}$	Average SNR
Δf	Carrier frequency offset
$\mathbf{H}_{m,n}[k]$	Channel matrix between m^{th} transmit and n^{th} receive antenna on k^{th} sub-carrier
R_C	Code rate
$\mathbb{G}$	Coding matrix of MIMO
$p\left(e/\gamma\right)$	Conditional BER
$p_s\left(e/\gamma\right)$	Conditional SER
δ	Error in estimating the channel
$\mathbb{E}[\cdot]$	Expectation operator
$\|\|[\cdot]\|\|_F^2$	Frobenius norm
s_k	ICI coefficient
$\gamma_{i,j}$	Instantaneous SNR between i^{th} transmit and j^{th} receive antenna
γ	Instantaneous SNR
P_{in}	Interference power due to ICI
α_i	Magnitude of channel from i^{th} antenna
$\mathbb{M}(\cdot)$	Moment generating function
M	Modulation order
P_z	Noise power due to AWGN
N_0	Noise power
ϵ	Normalized frequency offset
γ_T	Normalized instantaneous SNR for MIMO-OFDM with channel impairments
R_x	Number of receiving antennas
N	Number of sub-carrier in one OFDM symbol
T_x	Number of transmitting antennas
τ	Propagation delay of channel
σ_δ^2	Quality of channel estimation
$\Re[\cdot]$	Real part operator
γ_{IN}	SINR

γ_I	SIR
γ_t	SNR of SFBC-OFDM
E_s	Symbol energy
$\mathbf{x}_i$	Symbol generated from MIMO encoder for i^{th} antenna
$\mathbf{s}_i$	Symbol generated from OFDM modulator
$\mathbf{x}$	Symbol generated from symbol mapping
P_t	Transmit power
T_u	Useful duration of one OFDM symbol

List of Abbreviations

AWGN	Additive white Gaussian noise
AF	Amount of fading
ABER	Average bit error rate
BPSK	Binary phase shift keying
CF	Characteristic function
CFO	Carrier frequency offset
CSI	Channel state information
CDF	Cumulative distribution function
CP	Cyclic prefix
DFT	Discrete Fourier transform
EGC	Equal gain combining
ECC	Error control coding
FFT	Fast Fourier transform
FER	Frame error rate
FSK	Frequency shift keying
FSO	Free space optical
FDMA	Frequency division multiplexing access
FD-MIMO	Full dimensional MIMO
GA	Genetic algorithm
GSC	Generalized selection combining
GTR	Generalized two-ray
IID	Independent and identically distributed
IEP	Index error probability
ITS	Intelligent traffic systems
ICI	Inter carrier interference
IDFT	Inverse discrete Fourier transform
IMT-A	International mobile telecommunications advanced
IMT	International mobile telecommunications
ITU	International telecommunication union
IoT	Internet of things
LTE	Long term evolution
MGF	Moment generating function
MRC	Maximal ratio combining
ML	Maximum likelihood

MIMO	Multiple input multiple output
NLOS	Non line of sight
NOMA	Non-orthogonal multiple access
OFDM	Orthogonal frequency division multiplexing
PEP	Pairwise error probability
PAPR	Peak-to-average power ratio
PAN	Personal area network
PDF	Probability density function
QOS	Quality of service
QPSK	Quadrature phase shift keying
RQAM	Rectangular quadrature amplitude modulation
SC	Selection combining
SIR	Signal to interference ratio
SIC	Successive interference cancellation
SISO	Single input single output
STBC	Space time block code
STCC	Space time convolutional code
STFC	Space time frequency code
STTC	Space time trellis code
SF	Space-frequency
ST	Space-time
STF	Space-time-frequency
SQAM	Spatial modulation
SM	Spatial multiplexing
SQAM	Square quadrature amplitude modulation
SNR	Signal to noise ratio
STO	Symbol timing offset
TDMA	Time division multiplexing access
TAS	Transmit antenna selection
TWDP	Two wave with diffuse power
WCDMA	Wideband code division multiplexing access
WER	Word error rate

Chapter 1

Introduction

Over the last two decades, an upsurge in the use of wireless communication technology as the prime mode of communication has been observed. The major goals of the present and upcoming communication systems are to achieve a better quality of service (QOS) along with high data-rates. In order to achieve these goals, it is quintessential for the system to be efficient as well as flexible while working within the limited available radio frequency (RF) spectrum. This efficiency is increased by utilizing multiple antennas at the transmitter and the receiver. Such systems are termed as multiple input multiple output (MIMO) systems. MIMO system when used along with the well-known orthogonal frequency division multiplexing (OFDM) is identified as a favorable technique in order to implement wireless communication [1].

This chapter gives the introduction about the evolution of wireless communication system and its recent scenarios in Section 1.1 and 1.2. In Section 1.3, the need of MIMO-OFDM systems is discussed. Thereafter, in Section 1.4, the classification of MIMO-OFDM system is given. Section 1.5 explains the MIMO-OFDM system model. The historical developments in MIMO-OFDM system are presented in Section 1.6. Section 1.7 gives the advantages and major problems associated with MIMO-OFDM systems. Section 1.8 presents the applications of MIMO-OFDM system. The organization of the thesis is presented in Section 1.9.

1.1 Evolution of Wireless Communication System

The term wireless communication refers to the transmission of data from one place to other through air without using wires. The ability to communicate with people on the move has evolved remarkably from the time when Guglielmo Marconi first established the continuous contact with ships sailing the English channel using radio in 1897 [2]. From then on, the wireless communication industry has developed significantly with the advancements in miniaturization technologies, improvements in digital and RF circuit fabrication and very large scale circuit integration [3]. In 1946, the first mobile telephone system for commercial use was set up in St. Louis by Bell telephone laboratories.

Thereafter, the cellular concept for commercial use was introduced by the works of Bell Laboratories in the 1960s and 1970s [2]. Some of the popular initial systems before 1970 named mobile radio telephone were push to talk, mobile telephone system, improved mobile telephone service and advanced mobile telephone system [4–6].

The promise of mobility, accessibility, and portability are the key driving forces behind wireless communication. Wired communication indubitably offers higher reliability, better performance, and more stability, yet there is always a restriction of the bounded environment to a certain location. Various radio communication standards have been developed in order to implement wireless communication. These standards are classified on the basis of generation wise development. The initial developments in wireless cellular communications were in the form of analog 1G systems deployed in the early 1980s. These systems provided only voice calling using frequency division multiplexing access (FDMA) [7]. Later on, in the early 1990s, time division multiplexing access (TDMA) based 2G systems were deployed by replacing the 1G systems. Circuit-switched data modems were used in 2G providing the maximum data-rate of about 230 Kb/s [6].

In 1995, international telecommunication union (ITU) initiated the program named international mobile telecommunications (IMT-2000) which resulted in the development of 3G mobile standard based on wideband code division multiplexing access (WCDMA). The WCDMA system was mainly developed to provide increased data-rates (up to 2 Mb/s) and to improve the system capacity [8].

1.2 Recent Scenarios in Wireless Communication

In order to fulfill the increasing demands of high data-rate applications, 4G standard was introduced by the ITU in 2008 under the international mobile telecommunications advanced (IMT-A) specifications. Consequently, several different diversity techniques like multicarrier (OFDM) and multi antenna (MIMO) techniques have become popular for 4G systems [9]. The future technologies for wireless communication come under 5G and are expected to be available by 2020. LTE-Advanced Pro (LTE-A pro) is the new marker approved by the 3GPP in October 2015 for 5G [9]. An impressive data-rate of 10 Gb/s and 100% coverage throughout the globe is to be provided in 5G technology using Millimeter wave wireless communications and massive MIMO systems [10]. The summary of all these mobile standards from 1G to 5G is given in Table 1.1.

The billions of connected internet of things (IoT) devices, vehicular communication for intelligent traffic systems (ITS) and public safety/critical communications impose the essential requirement to outperform the current wireless communication systems based on

Table 1.1: Comparison between different generations of cellular systems [3, 9, 11]

Type	**Year of introduction**	**Standards**	**Max data rate**	**Access technology**	**Channel bandwidth**	**Switching**
1G	1980's	AMPS TACS NMT-450 NMT-900 C-NETZ RTMS NTT	N.A.	FDMA	30 KHz	Circuit
2G	1990's	GSM CDMAONE GPRS EDGE CDMA2000	14.4 Kbps 14.4 Kbps 115 Kbps 135 Kbps 153.6 Kbps	TDMA,CDMA	200 KHz	Circuit
3G	1995	UMTS HSPVA EV-DO	384 Kbps 14.4 Mbps 2.4 Mbps	WCDMA GPRS EDGE HSDPA E-UTRA	1.25 MHz-5 MHz	Circuit/Packet
4G	2008	LTE LTE Advanced WiMAX	300 Mbps 3000 Mbps 25 Mbps	OFDM OFDMA SC-FDMA MIMO	1.4 MHz-20 MHz	Packet
5G	2020 (tentative)	LTE-A Pro Gigabit LTE	3-10 Gbps 1 Gbps	Massive MIMO MIMO-OFDM	60 GHz	Packet

LTE and LTE-Advanced (LTE-A) [12]. LTE and LTE-A provide high spectral efficiency even in hostile environments using techniques like MIMO-OFDM and multicarrier code division multiple access (MC-CDMA). As suggested in [9], the future wireless systems will work on the 3GPP Releases 13/14 [13] collectively known as LTE-A Pro. In release 10 of LTE in 2015, 2×2 and 8×8 MIMO systems employing carrier aggregation were proposed and it was discussed that the data-rate could further be increased using more spectrum and antennas. Multi-Gb/s data-rates are supposed to be achieved using the unlicensed 5 GHz band, full dimensional MIMO (FD-MIMO) and carrier aggregation [13].

Applications like high definition multimedia streaming, online gaming, wireless gigabit ethernet, machine to machine communication, online banking and real-time status monitoring through sensor networks etc. require high data-rate communication. The target of current and next-generation communication systems is to make these services accessible to the maximum number of users while keeping a keen eye on factors like coverage area, low latency and high spectral efficiency [14, 15].

On the other hand, communication systems are limited by mutipath propagation and shadowing. The multipath propagation causes fading of received signal and degrades the performance of system in terms of increased bit error rate (BER) or reduced capacity. Apart from this, due to the increase in number of users, the problems of interference from other users, intercarrier and symbol interferences also play a major role in degrading the QOS of the system. Therefore, achieving high data-rate transmission with consistent reliability over multipath fading channel is a major challenge for the current and next generation communication systems [13, 16].

To meet the challenges as discussed above, some conventional straight-forward techniques like increasing the transmit/receive power or bandwidth, and/or applying advanced error control coding (ECC) have been used in the past [17]. However, bandwidth and power prove to be very expensive and limited radio resources. On the other hand, ECC has a limit to which it can confront fading. This necessitates the adoption of other methods for performance enhancement in order to meet the future demands of wireless communication systems. For this purpose, different modulation and coding techniques like equalization, spread spectrum, MIMO, and multicarrier modulation systems have been proposed [1].

1.3 Need of MIMO-OFDM System

The need for MIMO-OFDM has emerged to resolve the problem of frequency selective multipath fading encountered by direct sequence CDMA (DS-CDMA) used in 2G systems

and WCDMA used in 3G systems. Due to this multipath fading, the performance of these systems degrades severely. It has been studied that the solution to this problem is to use narrowband signals which develops the concept of multi-carriers transmission using OFDM [8].

OFDM uses different carrier frequencies which are orthogonal to each other to carry information from the transmitter to receiver. Various Problems of OFDM systems like inter-carrier interference (ICI), inter-symbol interference (ISI) and high peak to average power ratio (PAPR) are studied by various researchers [18–21]. In order to further improve the performance, antenna diversity is used with OFDM systems to provide the diversity gain. The combination of MIMO and OFDM is known as MIMO-OFDM system and it provides the advantages of both multicarrier as well as antenna diversity in a single system. Therefore, OFDM and MIMO systems are two of the most enabling technologies for the present and future generation wireless systems [22].

1.4 Classification of MIMO-OFDM Systems

The choice of a particular coding technique for a communication system depends upon various parameters such as computational complexity, desirable performance, sensitivity of system to interferences and fading of channel. The complexity of system depends a lot on the design of transmitted signal. The process of designing these transmitted signal is explained in system model of upcoming chapters. A lot of research has been done on the design of suitable MIMO coding techniques. The classification of MIMO-OFDM systems is shown in Fig. 1.1 [23].

The distributed MIMO-OFDM systems take the aid of relay nodes which are scattered in the wireless network in order to maximize the total network channel capacity. Various relaying strategies such as decode & forward, amplify & forward, compress & forward etc. are employed in order to relay the information from the transmitter node to the receiver node [24].

Co-located MIMO-OFDM systems have multiples antennas located at both the transmitter as well as at the receiver side. The coding schemes for such MIMO-OFDM system can further be divided into two broad categories: spatial multiplexing (SM) and transmit diversity [23]. In SM, multiple unique data bits are sent from multiple antennas simultaneously. This provides gain in data-rate of the order of number of transmit antennas. But no diversity gain is achieved in this manner [25].

The other type of coding scheme is transmit diversity. It is used to improve the perfor-

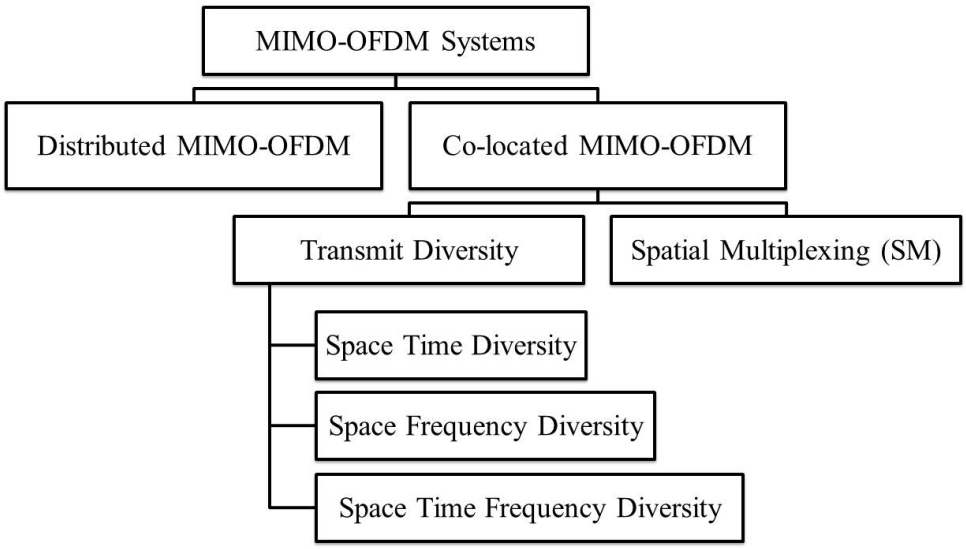

Figure 1.1: Classification of MIMO-OFDM system [23].

mance of system in hostile environments with the maximum possible coding gain, highest possible throughput and with the least decoding complexity [26]. This is done by exploiting the diversity in space, time and frequency domains illustrated in Fig. 1.2. The data is transmitted over space using multiple time slots in space time diversity whereas in space frequency diversity, multiple frequency slots are used along with space. It can be visualized from Fig. 1.2 that no additional resource is required in case of space time or space frequency diversities as compared to time diversity or frequency diversity [27].

Space time diversity is synthesized with space time coding (STC). In STC, the coded data is transmitted using multiple antennas over different subcarriers. STC adds another dimension of space into the MIMO-OFDM system. The principle behind STC is to generate redundancy by coding across the dimensions of both space and time simultaneously. The main motive of STC is to keep the data-rate of MIMO-OFDM system equivalent to the single input single output (SISO) system. It increases the robustness of the system by providing diversity gain. Whereas, SM is utilized for increasing the maximum data-rate of the system. Both of these techniques have different structures of transmitter and receivers and have different applications based on their advantages [23].

Space frequency diversity is implemented using space frequency coding (SFC). In SFC, data is sent through different antennas and OFDM sub-channels. Such coding has better performance than STC in fast fading environments. However, its performance degrades drastically in highly frequency selective channel conditions. To overcome the problems of both the STC and SFC, space-time-frequency coding is utilized which has advantages of both STC and SFC. In hostile environments affected by severe multipath fading, such

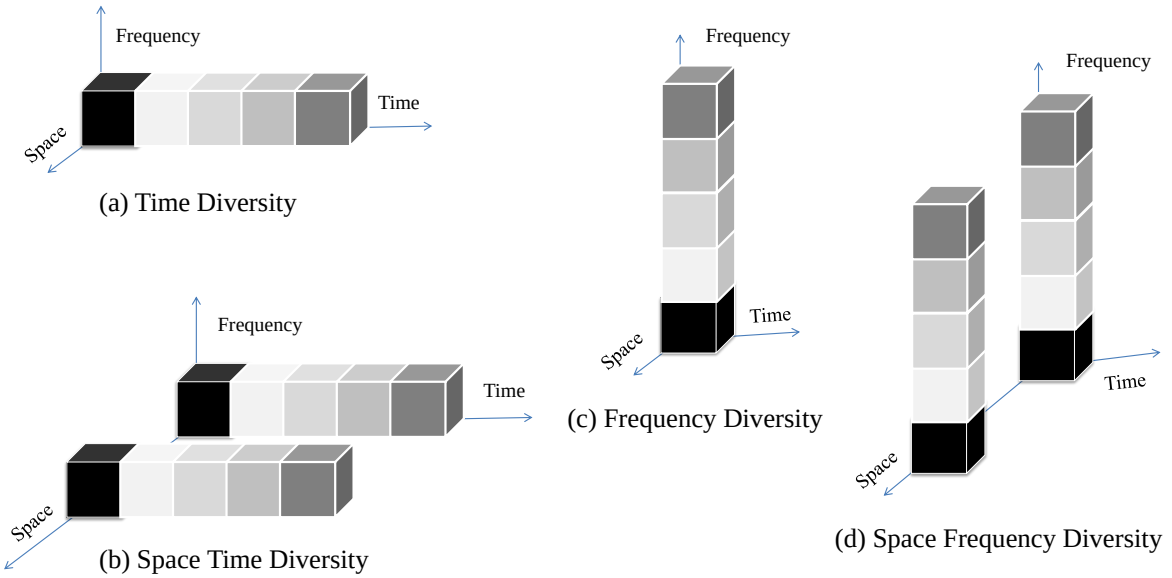

Figure 1.2: Time, frequency and space diversity techniques [27].

kind of coding techniques provide robustness to the communication system and helps to improve the ABER performance [28].

1.5 MIMO-OFDM System Model

The system model of MIMO-OFDM consists of three major blocks i.e. transmitter, channel and receiver. The block diagram of a MIMO-OFDM transmitter with T_x transmit antennas is given in Fig. 1.3. The analog message signal to be transmitted is first converted to digital bit stream using analog to digital (A/D) convertor. This is done to maintain the compatibility between the analog message and signal processing components of MIMO-OFDM system which operate on digital data. After that, this digital bit stream is modulated using symbol mapping. The Symbol mapping is applied by taking into consideration the detection scheme utilized in the system i.e. coherent, partially coherent and non-coherent detection. The symbol mapping block generates the symbol vector

$$\mathbf{x} = \{x[1], x[2], \cdots x[N_T - 1]\}.$$

This symbol vector is fed to MIMO encoder after applying serial to parallel conversion. The length of this vector (N_T) depends on the number of subcarriers in an OFDM symbol and code rate of MIMO encoder. If N is the number of subcarriers in an OFDM symbol and R_c is the code rate of MIMO encoder then $N_T = NR_c$. In this work, the matrices are represented by uppercase boldface letters, and lowercase boldface is used for vectors, whereas scalars are shown with un-boldface letters.

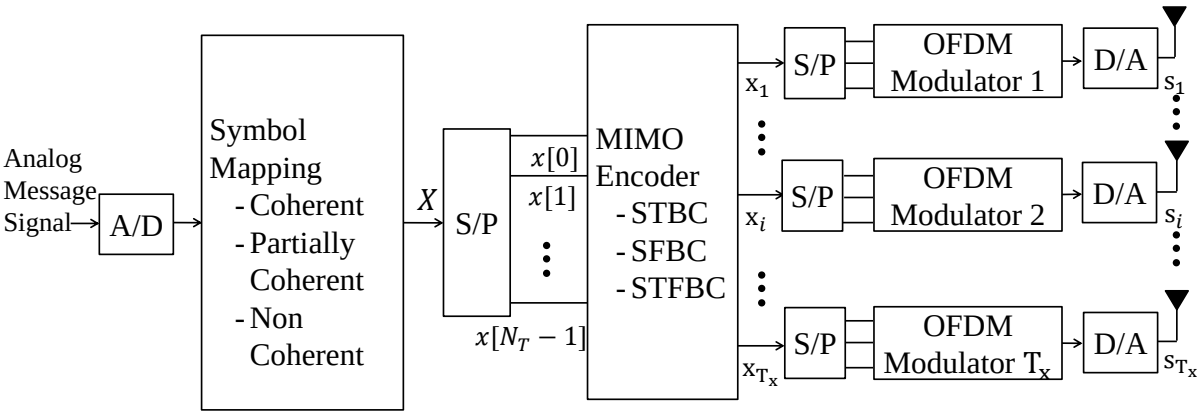

Figure 1.3: MIMO-OFDM transmitter.

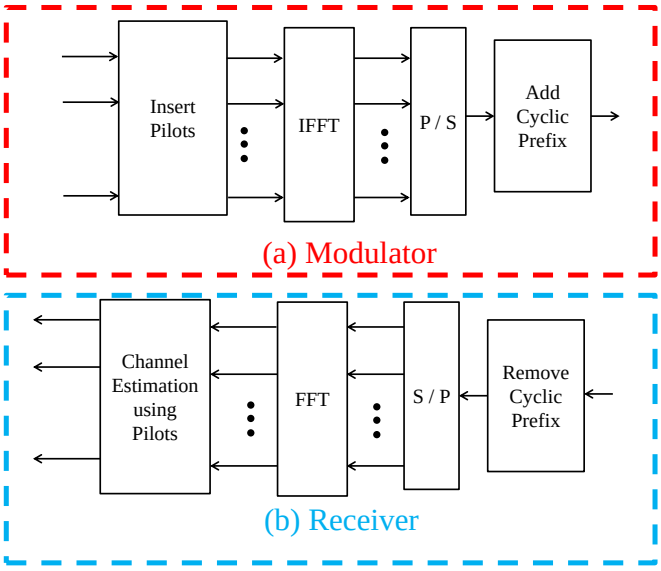

Figure 1.4: OFDM modulator and demodulator block diagram.

MIMO encoder generates T_x blocks each of length N for utilizing the diversity of OFDM in frequency domain. Thereafter, these blocks are fed to individual OFDM modulators. The block diagram of an OFDM modulator is given in Fig. 1.4 (a). In the first step, pilot carriers are inserted in MIMO encoded data symbols. These pilot carriers are used for the purpose of channel estimation at the receiver end. Next, inverse discrete Fourier transform (IDFT) is applied on the data using IFFT (inverse fast Fourier transform). After IFFT, cyclic prefix is added to the serial data symbols to avoid the problems of ICI and ISI. The outputs of these T_x OFDM modulators $(\mathbf{s}_1, \mathbf{s}_2, \cdots \mathbf{s}_i \cdots \mathbf{s}_{T_x})$ are transmitted from different transmit antennas simultaneously after digital to analog conversion.

The working of MIMO encoder is based on a coding matrix $\mathbb{G}$. The elements in matrix $\mathbb{G}$ are the complex conjugate combinations of the modulated symbols in $\mathbf{x}$. Each block of N symbols from $\mathbf{x}$ is encoded using a coding matrix of size $N \times T_x$ based on $\mathbb{G}$ [29]. The simplest of these encoders is based on Alamouti code defined for two transmit antennas.

Consider an example of two transmit ($T_x = 2$) and one receive antenna ($R_x = 1$) with code rate of one ($R_c = 1$). Let $\mathbf{x}$ contains two symbols $x[1]$ and $x[2]$. The coding matrix $\mathbb{G}$ in this case is defined as [30]

$$\mathbb{G} = \begin{bmatrix} x[1] & x[2] \\ -x[2]^* & x[1]^* \end{bmatrix}$$

Now, at the first time slot, the symbols $x[1]$ and $x[2]$ are transmitted from antenna one and two respectively. Then, the symbols $-x[2]^*$ and $x[1]^*$ are transmitted in the second time slot from antenna one and two.

Now, let us take another example when $\mathbf{x}$ contains four symbols $\{x[1],\ x[2],\ x[3]$ and $x[4]\}$. In this case, the signal transmitted from antenna one in four consecutive time slots is

$$\mathbf{x}_1 = \{x[1], -x^*[2], x[3], -x^*[4]\}.$$

Further, the signal transmitted from antenna two in four consecutive time slots is

$$\mathbf{x}_2 = \{x[2], x^*[1], x[4], x^*[3]\}.$$

The Alamouti code scheme is extended for more than two antennas using generalized real and complex orthogonal designs explained in [29]. Pseudo orthogonal block codes and quasi-orthogonal space time block codes (QOSTBC) can also be applied in MIMO encoder. Apart from time, these codes can also be applied in frequency domain re-

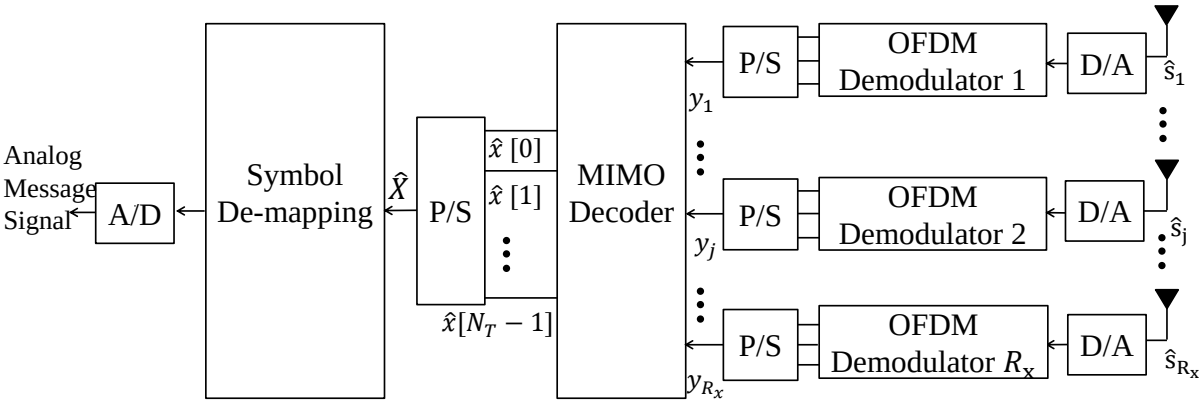

Figure 1.5: MIMO-OFDM receiver.

sulting in space frequency block codes (SFBC) and space time frequency block codes (STFBC).

At the receiver side, the sampled received signal after cyclic prefix removal can be written as

$$\mathbf{y}_n[k] = \sum_{m=1}^{T_x} \mathbf{H}_{m,n}[k]\mathbf{x}_m[k] + \mathbf{w}_n[k]; \quad k = 0, 1, \cdots, (N-1);\ 1 \leq n \leq R_x, \tag{1.1}$$

where $\mathbf{y}_n[k]$ is the received signal vector at the n^{th} receive antenna on k^{th} subcarrier, $\mathbf{x}_m[k]$ is the transmitted symbol from m^{th} antenna over k^{th} subcarrier, $\mathbf{H}_{m,n}[k]$ is the channel frequency response between m^{th} transmit and n^{th} receive antenna at the k^{th} subcarrier and $\mathbf{w}_n[k]$ is the complex additive white Gaussian noise (AWGN) vector.

The basic block diagram of a MIMO-OFDM receiver is given in Fig. 1.5. After passing through the MIMO channels, the received signals $\hat{\mathbf{s}}_1, \hat{\mathbf{s}}_2, \cdots, \hat{\mathbf{s}}_j, \cdots, \hat{\mathbf{s}}_{R_x}$ are first fed to the analog to digital conversion and then demodulated using R_x individual OFDM demodulators. The block diagram of an OFDM demodulator is shown in Fig. 1.4 (b). It consists of removal of cyclic prefix and fast Fourier transform (FFT) blocks. Channel estimation is done with the help of the pilot symbols inserted at the transmitter. After OFDM demodulation, these symbols are fed to MIMO decoder where linear combining is applied. The orthogonal property of block codes reduces the complexity of MIMO decoder. This is because only linear combining of the received signals is required for the perfect decoding into transmitted modulated symbols. Finally, the information bits are

extracted back from the modulated symbols using symbol demapper.

The MIMO encoder is classified into three types space time block codes (STBCs), SFBCs and STFBCs. This classification is based on the domain the data bits are encoded in space. The system model of these block codes is explained in the next chapters.

1.6 Historical Developments in MIMO-OFDM

The idea of orthogonal multiplexing to transmit the data bits simultaneously through a wireless transmission medium without inter-channel and inter-symbol interferences was coined by Chang [31] in 1966. Before this, the use of orthogonal time signals (sine and cosine functions) to transmit data was proposed by Harmuth in 1960 [32]. The US patent for OFDM was filed by Chang [33] in 1970. The use of OFDM in the field of communication was revolutionized by the application of Discrete Fourier transform (DFT) proposed by Weinstein et al. in 1971 [34]. Later on in 1985, Cimini [35] gave the idea of OFDM for mobile communications. In 1987, Alard et al. [36] paved the way for the application of OFDM for digital broadcasting. Further, the concept of multicarrier modulation was explained in the work of Bingham [37]. The performance of OFDM system has been analyzed under various effects like ICI, ISI, channel estimation errors and fading in the literature [19–21, 38–43].

The concept of transmit diversity in form of delay diversity scheme was given independently at the same time by Wittneben [44] and Seshadri [45] respectively in 1993. Another important work in this field was by DaSilva and Sousa [46] in which they proposed a fading resistant and bandwidth efficient method using L antennas at the base station. However, the research in this field grew enormously with the work of Alamouti [30]. A diversity technique for two transmit antennas was proposed in [30]. The diversity order of this technique was equal to MRC system employing two receive antenna.

In 1998, Tarokh et al. proposed space time trellis codes (STTCs) for achieving both diversity gain and coding gain [47]. These STTCs were introduced as an application of trellis coded modulation in transmit diversity. The concept of STTCs was further studied in the works of [48–52]. Thereafter, the idea of constructing orthogonal codes in shape of blocks called as space time block codes (STBCs) was proposed in 1999 [29]. STBCs were designed in order to attain maximum diversity order for a system. In STBC, linear maximum-likelihood (ML) decoding was used at the receiver [29].

The capacity analysis for STBC was given by Sandhu and Paulraj [53] in 2000 in which they argued about the lower capacity limits of STBCs. It was shown that the capacity of

STBC depends on the number of receive antennas, rank of channel and code rate. Further, in 2001, Ionescu et al. [54] proposed a novel STC for two transmit antennas achieving a data-rate of 2 b/s/Hz for 4-PSK modulation. In 2002, Blum in his work [55] provided the design process to optimize coding and diversity gain of space time convolutional codes (STCC). Orthogonal codes with square and rectangular matrix containing both real and imaginary values were analyzed in the work of Liang [48]. These codes were designed with the aim to achieve maximum rates. Later in 2004, Su et al. [56] proposed a design method for generating high rate STBC for any number of transmit antenna from complex orthogonal designs.

In order to improve the signal to noise ratio (SNR) or other performance criterions, diversity can also be applied at the receiver by using multiple antennas. Several combining techniques like maximum ratio combining (MRC), equal gain combining (EGC) and selection combining (SC) are proposed in literature for achieving receiver diversity. The analysis of these techniques was provided by Brennan [57] in 1959 in his landmark work. Later on in 1984, optimum signal combining for space diversity reception was studied by Winters [58] for cellular mobile radio systems which was further discussed for diversity antennas at the vehicular mobile by Voughan [59] in 1988.

1.7 Advantages and Major Problems of MIMO-OFDM System

As the MIMO-OFDM system is a combination of MIMO and OFDM systems, it provides the advantageous features of both of them. The major advantages of MIMO-OFDM system are as follows [35]:

- Robustness against frequency selective fading
- Spectral efficient due to the freedom of using overlapped subcarriers
- Provides both diversity as well as coding gain
- Highly effective against ISI due to the use of cyclic prefix
- Immune to narrowband interference
- Simple and efficient modulation/demodulation process

Apart from these advantages, the MIMO-OFDM system has problems of both MIMO and OFDM systems too. Some of the major problems of MIMO-OFDM system are as follows:

- Highly sensitive to orthogonality
- Inter carrier interference (ICI)
- High PAPR
- Sensitive towards channel state information and channel estimation errors
- Sub-channel correlation between transmit-receive antenna pairs
- Higher complexity of transmitter and receiver as compared with SISO systems.
- Sensitive to and synchronization errors (symbol timing offset (STO) and carrier frequency offset (CFO))
- Reduction in the spectral efficiency due to insertion of guard band.

1.8 Applications of MIMO-OFDM System

As explained in the previous sections that MIMO-OFDM system offers a lot of advantageous features when compared with its contemporary technical rivals. Due to this, MIMO-OFDM has emerged as a strong candidate to fulfill the needs of current and future communication systems and has been adopted by a lot of wireless communication standards like IEEE 802.11n, IEEE 802.16e, 3GPP long term evolution (LTE) and LTE-Advanced (LTE-A) [13].

1.9 Thesis Organization

The contents of this thesis are structured as follows.
The first chapter is devoted to introduce the reader with the wireless communication system and current advancements in the field. A complete introduction is given on MIMO-OFDM systems. The classification of MIMO-OFDM system is also provided along with its advantages and drawbacks.
Chapter 2 presents the comprehensive literature review of MIMO-OFDM system. The motivation for writing this thesis is also given in Chapter 2. The state of art work done by various researchers is acknowledged and presented in chronological order for MIMO-OFDM systems. The multipath channel models used in the study are explained. Thereafter, the gaps in presented study are pointed out and objectives achieved in this work are elaborated.
Chapter 3 gives the performance analysis of SFBC-OFDM system. The system model of SFBC-OFDM system is explained in detail. An MGF based generalized approach is

devised to calculate the ABER expressions for SFBC-OFDM system with AWGN case and under various fading scenarios. As an additional endeavor, very simple closed form approximate expressions for ABER based on a tight bounds are also derived for SFBC-OFDM system.

Chapter 4 presents the performance analysis of STBC-OFDM system under different fading scenarios. The system model of STBC-OFDM system is presented and explained. Exact expressions of ABER for MQAM modulated STBC-OFDM system are derived for the STBC-OFDM system under various fading scenarios.

The effect of impairments on the performance of MIMO-OFDM Systems is studied in Chapter 5. The effect of both carrier frequency offset and imperfect channel state information is taken into consideration while deriving the ABER expressions.

Finally, the main conclusions and the future work are outlined in Chapter 6.

Chapter 2

Literature Review

Literature survey of any research field or subject is required before contributing to the research of that field. The literature review gives a detailed study of published work in that research area. This chapter provides a comparative literature survey on MIMO-OFDM systems based on its developments over time and its performance analysis.

The motivation of thesis is presented in Section 2.1. In Section 2.2, a comprehensive review for performance analysis of MIMO-OFDM is presented. Subsequently, Section 2.3 presents a review of multipath channel models. In Section 2.4, the research gaps observed from the literature survey are given. The thesis objectives are summarized in Section 2.5 along with the scope of these objectives.

2.1 Motivation

According to Professor Elinor Ostrom, a Nobel Prize winner, the creation and usage of a general framework could help to identify the elements to be considered in a study or experiment. It also helps to understand the relationship of these elements to one another [60].

In the vast field of wireless communications, an analytical framework provides a platform for analysis and development of the system. This allows the researchers to work on a specific portion or part of the model while keeping the coherence intact. It also permits the hustle-free performance analysis of communication system which has been considered an important aspect among research fraternity. The rapid advancements in signal processing and VLSI technologies in the past few decades have prompted the communications systems to evolve quickly. These systems employ different modulation and coding schemes and their behavior/performance in fading environments is also unique. Therefore, in order to compare these systems, their performance needs to be evaluated [61].

Three different methods are proposed in the literature for performance evaluation of the communication systems: simulation, hardware prototyping and analytical methods. In the simulation method, the system is realized using software tools. As the number of

users communicating through wireless media are increasing day by day, the accurate modeling of wireless fading channels has become a necessary task. Channel impairments like attenuation, distortion, interference, fading, noise, and crosstalk etc. makes this task very difficult. The simulation of a communication system under fading and channel impairments becomes a cumbersome task for such complex systems.

On the other hand, in the hardware prototyping measurements are made using test benches of the system. This method is very accurate but comparatively time-consuming and less flexible in nature [62]. In analytical methods, formula based calculations are used for performance analysis. These methods are based on models and they provide an insight into the relationship between the system performance and design parameters. These methods are very useful and popular among research fraternity due to their simplicity and usefulness. Therefore, an analytical approach can be used in complex cases to derive closed-form accurate expressions for performance analysis. These approaches include calculation of the probability density function (PDF), or in some complicated cases, deriving the cumulative distribution function (CDF), the moment generating function (MGF) or the characteristic function (CF) of the same. The major advantage of these analytical approaches is their versatility, accuracy, ease to implementation, lower cost compared to simulation (software required) and prototyping (hardware required) [63].

2.2 Review of Performance Analysis

As discussed in Chapter 1, different methods have been utilized in calculating the performance of a wireless communication system. In this dissertation, we have focused our attention on the analytical methods for performance analysis. Various parameters have been proposed to measure the performance of practical communication systems, some of which are- average SNR, outage probability, ABER, amount of fading, average outage duration and capacity of the system [64].

This subsection provides the survey of some published works on the performance analysis of MIMO-OFDM system. To structure the survey in a more efficient manner, the survey has been classified into two classes. This classification is based on where the space diversity is being applied to i.e. either at the transmitter or at the receiver.

The performance of the concatenated STBC with outer codes has been studied in [65]. Both convolutional code (CC) and trellis-coded modulation (TCM) codes have been used in [65]. Novel full diversity STBC codes based on Hamiltonian constellations to achieve high diversity product were proposed by Niyomsataya et al. in 2006 [66]. In [67], a joint iterative detection has been introduced for orthogonal frequency and code division

multiplexing systems in which a closed-form expression for the optimal power allocation is derived. In the year 2010, Ropokis et al. [68] provided a unified framework in order to evaluate the ergodic capacity and SEP of OSTBC over generalized fading channels. Thereafter, in 2013, Jacobs and Moeneclaey [69] derived a closed-form approximation for the BER of QAM based STBC over correlated Rayleigh fading channels.

Subsequently, in 2015, a classification algorithm was developed by Marey and Dobre [70] for blind identification of the modulation format of the received signal. No subsequent information about block timing synchronization or channel coefficients was required in the algorithm of [70]. The performance analysis of 3GPP LTE SFBC system has been provided in [71] using both theoretical and simulation analyses. In this work by Heng and Jalloul [71], expressions to calculate the correlation between the channels and average SINR have also been derived. The performance of transmit antenna selection based STBC-MIMO system has been analyzed in the work of Guowei et al. [72] in which the PDF of channel gain coefficients is derived. The pairwise error probability (PEP) of Alamouti based STBC system with residual phase estimation error over Nakagami-m fading channel has been studied in [73]. The performance analysis of STBC combined with spatial modulation under imperfect CSI has been done in the work of Acar et al. [74]. An experimental MIMO-STBC scheme operating at 2.4-GHz frequency underground mine environment has been proposed by Boualleg et al. in [75]. Further, Hoojin Lee [76] has derived both the exact as well as asymptotic expression of ABER for binary phase shift keying (BPSK) modulated 2×2 full-rate linear-receiver STBCs over Rayleigh fading channel. The expressions for PEP of SM and space shift keying technique for MIMO wireless communication systems has been derived in the work of Badarneh et al. in [77].

An improved space time coding for MIMO-OFDM systems was presented by Blum et al. in 2001 [78]. In the same year, the performance of V-BLAST OFDM system was analyzed by Piechocki et al. [79]. Li [80] has worked on improving the performance of MIMO-OFDM by reducing the complexity of channel parameter estimation. Bolcskei et al. [81] have provided both the ergodic and outage capacities for MIMO-OFDM system in broadband fading. The capacity of dual-antenna-array systems was explored by Chuah et al. [82] in 2002 using both theoretical analysis and ray tracing simulations for correlated fading channels. In the same year, the effect of ICI in MIMO-OFDM was studied by Stamoulis et al. [83]. A novel channel estimation scheme for rapidly varying channels was proposed in [83].

A low density parity check code based ST-OFDM system for correlated fading channels was given by Lu et al. in 2002 [84]. Correlated fading channels were assumed in the anal-

ysis; outage probability and word error rate (WER) were calculated as the performance measure. In 2003, Gamal et al. presented the outage probability and frame error rate (FER) of BPSK and quadrature phase shift keying (QPSK) modulated STBC and SFBC-OFDM systems [85]. The performance of SF coded MIMO-OFDM system was studied by Bolcskei et al. in 2003 [86] using antenna spacing, Ricean K-factor and transmit-receive angle spread as parameters.

The PAPR of an STBC-OFDM system has been calculated by Lee et al. [87] using selective mapping approach. The research challenges in MIMO-OFDM system related to synchronization and channel estimation have been discussed in an excellent paper by Stuber et al. [88]. In another important paper, Paulraj et al. [89] have given the overview of MIMO-OFDM systems in terms of performance analysis, coding and channel models. Later on, in 2005, Su et al. [90] proposed a full-rate and full-diversity MIMO-OFDM system based on the general SF block code structure.

In 2005, the performance of ST coding with imperfect channel estimation was analyzed by Garg et al. [91]. In the same year, the issues of performance analysis and code design for MIMO-OFDM system were addressed by Su et al. [92]. The cases of spatial, temporal and frequency domain coding were taken in the study [92]. Tarighat and Sayed in [93] addressed the issue of IQ imbalances in MIMO-OFDM systems. A framework for combating IQ imbalances using digital signal processing was also provided in [93].

Various ST codes for OFDM systems were investigated by Liew and Hanzo in 2006 [94]. In a landmark paper by Jiang and Hanzo [95], the use of genetic algorithms (GAs) has been examined for MIMO-OFDM systems. The paper also provides a comprehensive study of existing MIMO-OFDM systems along with their limitations. Thereafter, the closed-form expressions of ABER were derived for an SFBC-OFDM system under Rayleigh fading by Torabi et al. in 2007 [96]. The analysis has been done for both MPSK and MQAM modulations and the effect of perfect and imperfect CSI has also been studied.

Subsequently, the SFBC-OFDM system under doubly selective fading channels has been analyzed in [97]. In 2010, the problem of estimating the nonlinear distortions in SFBC-OFDM system was solved by using a non-linear receiver [98]. Further, Kim et al. [99] have addressed the problem of ICI generated in SFBC-OFDM system and have proposed the use of a polynomial cancellation code. Correlative coding was used to suppress the effect of phase noise and ICI in SFBC-OFDM system by Kim et al. in 2011 [99].

Further, Jacobs et al. [100] gave the BER analysis of OSTBC for mismatched ML receiver in 2010. A widespread survey on the performance of successive interference cancellation (SIC) for MIMO-OFDM systems has been provided by Miridakis and Vergados in [101].

The ABER analysis for MIMO systems under spatially correlated Rayleigh fading channels has been presented in [69]. Thereafter, the use of ML decoding in SFBC-OFDM systems for the purpose of channel estimation was studied by Delestre et al. in 2014 [102]. In 2015, Al-Dweik et al. [22] proposed a technique to improve the robustness of SFBC-OFDM system in terms of BER by shaping the channel matrix.

The performance of SFBC-OFDM system in underwater acoustic channel was studied by Zorita et al. in 2015 [103]. Real data was collected in this study for the shallow water channel. In the same year, Heng et al. derived the closed-form expression of the SNR for an SFBC-OFDM system under frequency-selective fading [71]. The effect of imperfect channel estimation on SNR has also been studied in [71].

A novel pilot based channel estimator for MIMO systems and IQI coefficients has been analyzed in [104]. In [105], the impact of IQ imbalance on the performance of differential STBC-OFDM systems has been studied. A compensation algorithm has been introduced in [106] to mitigate the effect of IQ imbalance. A linear compensation algorithm to diminish the effect of IQI at the transmitter and receiver of STBC-OFDM systems has been proposed in [106]. The design of precoders for single-user MIMO channels for finite-alphabet signals has been discussed in [107]. A exhaustive literature survey of transmit diversity based MIMO-OFDM is given in Table 2.1 and Table 2.2. The parameters which are not defined in these works are denoted by N.D. in Table 2.1 and Table 2.2.

Another category of MIMO-OFDM systems is one in which the diversity is applied at the receiver in the form of different combining techniques. In 1984, optimum signal combining for space diversity reception was studied by Winters [58] for cellular mobile radio systems which were further discussed for diversity antennas at the vehicular mobile by Voughan [59] in 1988. The analytical expressions for outage probability of different combining techniques under generalized Nakagami fading have been derived in 1992 in the work of Abu-Dayya and Beaulieu [112]. Thereafter, the BER performance of MRC receiver under correlated Nakagami fading channel was analyzed by Aalo in 1995 [113] for frequency shift keying (FSK) and PSK modulations.

In a landmark study by Simon and Alouini in 1998, the performance of different combining techniques was analyzed with the aid of a unified approach [114]. The generalized fading channels were assumed in this study. An analysis on Shannon capacity of diversity combining techniques has been provided by Alouini and Goldsmith [115] over Rayleigh fading channel. The performance analysis of the generalized selection combining (GSC) over Rayleigh fading channels based on MGF approach has been given in [116]. Transmit antenna selection (TAS) and MRC systems were analyzed in the work of Chen et al. [117].

Table 2.1: Survey of transmit diversity based MIMO-OFDM systems

Year	**MIMO-OFDM Technique**	**Baseband Modulation**	**Fading Channel**	**Performance Parameter**
2000 [53]	STBC	N.D.	Rayleigh	channel capacity
2001 [54]	STTC	4-PSK	quasi-static Rayleigh	FEP
2001 [78]	STC	QPSK	quasi-static Jakes	WER
2001 [79]	VBLAST OFDM	QPSK	simulated/ measured channel data	ABER
2002 [55]	STCC	N.D.	quasi static slow Rayleigh	FEP
2002 [81]	OFDM based SM	N.D.	Rayleigh	ergodic/ outage capacity
2002 [82]	multiple element array	N.D.	Correlated Rayleigh	capacity
2002 [83]	STBC	N.D.	Rayleigh	SINR gain
2002 [84]	LDPC STC OFDM	N.D.	correlated selective Rayleigh	outage capacity
2003 [85]	STBC and SFBC	BPSK, QPSK	frequency selective Rayleigh	FER, outage probability
2003 [86]	SFBC	QPSK, MQAM	Ricean	block error rate, SER
2003 [87]	STBC	QPSK	Rayleigh	PAPR, ABER
2004 [88]	STBC	MQAM	AWGN	MSE, ABER, capacity
2004 [89]	STBC	4-QAM	Rayleigh	SER, outage & Ergodic capacity
2005 [90]	SFC	BPSK, QPSK	frequency selective Rayleigh	ABER
2005 [91]	STBC	BPSK	flat Rayleigh	PEP
2005 [92]	ST and SF coding	QPSK	flat Rayleigh	ABER
2005 [93]	STBC	64-QAM	AWGN	ABER
2006 [65]	CC and TCM	BPSK	Nakagami-m	ABER
2006 [94]	STT and STBC	MPSK, MQAM	Rayleigh	FER, BER, coding gain
2007 [95]	GA based MIMO-OFDM	MQAM, MPSK	Rayleigh	ABER
2007 [96]	SFBC	MPSK, MQAM	Rayleigh	ABER
2008 [67]	MIMO-OFCDM	QPSK	Parallel slow Rayleigh	Optimal power allocation
2009 [97]	SFBC	N.D.	doubly selective	ABER

Table 2.2: Survey of transmit diversity based MIMO-OFDM systems (contd.)

Year	**MIMO-OFDM Technique**	**Baseband Modulation**	**Fading Channel**	**Performance Parameter**
2010 [98]	SFBC	16 QAM, 64 QAM	Rayleigh	ABER
2010 [100]	Square OSTBC	MPAM, MQAM	Correlated Rayleigh	ABER
2010 [68]	MRC /OSTBC	MPSK, MPAM, MQAM	generalized fading channel	Ergodic capacity, ABER
2011 [108]	SFBC	QPSK, 16QAM	Time varying Rayleigh	Channel capacity, ABER
2011 [99]	SFBC	64 QAM	Rayleigh	CIR, ABER
2013 [101]	SIC based MIMO-OFDM	QPSK	Rayleigh	ABER
2013 [69]	OSTBC	MQAM	patially correlated Rayleigh	ABER
2014 [102]	SFBC	QPSK, 16QAM	frequency selective Rayleigh	ABER, MSE
2015 [70]	STBC	MPSK,MQAM	Frequency flat Rayleigh	probability of false alarm
2015 [71]	SFBC	MPSK,MQAM	Rayleigh	average SINR, ABER
2015 [22]	SFBC	MPSK, MQAM	Frequency selective Rayleigh	ABER
2015 [103]	SFBC	QPSK	shallow-water channel	ABER, MSE
2016 [109]	SFBC	MQAM, MPSK	TWDP	ABER
2016 [104]	MU-SIMO	N.D.	Rayleigh	MSE, spectral efficiency
2016 [105]	Differential STBC	QPSK, 8PSK	slow Rayleigh	ABER
2016 [72]	STBC	MPSK, MQAM	Rayleigh flat	ABER
2016 [73]	STBC	QPSK	Nakagami-m	ABER
2016 [74]	STBC and SM	MPSK, MQAM	time-varying Rayleigh	ABER
2016 [75]	STBC	MPSK	Underground MIMO Channels	ABER
2017 [76]	FRLR-STBC	BPSK	Rayleigh	ABER
2017 [77]	SM and SSK	4-QAM	α-μ and κ-μ	PEP
2018 [110]	SFBC-OFDM	MQAM and MPSK	Generalized fading	ABER
2018 [111]	SFBC-OFDM	MQAM and MPSK	Beaulieu-Xie fading	ABER

Subsequently, in 2009, the exact expression for average symbol error probability (ASEP) under η-μ channels was derived by Peppas et al. [118]. Different modulation techniques were considered in the analysis along with MRC. The ABER performance of MRC receiver over eta-mu and kappa-mu fading channels has been discussed by Dixit and Sahu in [119]. The analysis of M-PSK modulated MRC receiver in κ-μ fading environment has been presented in [120] for outdated CSI. The exact closed-form expression of ABER for SC based receiver employing rectangular QAM has been derived by CDF approach in [121].

Afterwards, the analysis of outage probability for MIMO-MRC system under Rician fading was given in the work of Wu et al. [122] in 2016. The SER expression for spatial modulation based MRC system was derived by Maleki et al. [123] in which the problem of constellation breakdown was explored for SM based MRC systems. The performance of a multi-antenna spectrum sensing system employing MRC and EGC diversity techniques has been analyzed in [124]. A closed-form expression of spectral efficiency (SE) for MRC based massive MIMO systems have been derived in [125]. A MIMO non-orthogonal multiple access based system has been analyzed in [126]. The ABER performance of free space optical (FSO) communication system with BPSK subcarrier intensity modulation employing MRC over Gamma-Gamma fading has been analyzed in the work of Liu et al. [127]. In [128], the tight expressions of index error probability (IEP) and BER have been derived for OFDM system based on MRC receiver. The effect of CSI uncertainty has been considered in this analysis. A complete literature survey of receiver diversity based MIMO-OFDM is given in Table 2.3.

2.3 Review of Multipath Channel Model

Accurate modeling of a wireless fading channel in a communication system plays a vital role in the performance evaluation of that system. The channel model used for this task must have flexible parameters in order to represent both specular and diffused scatter components. The specular components are the line of sight (LOS) components whose amplitude is assumed to be constant with a random phase. Whereas, the diffuse scatter components are the non-LOS (NLOS) components.

Most commonly used models to characterize fading channels are Rayleigh, Rician and Nakagami. The fading scenarios having only NLOS paths can be characterized by using Rayleigh fading. The Rician distribution has the ability to depict both LOS and NLOS components but it lacks flexibility in terms of characterizing practical LOS fading channels. The Nakagami-m model has more flexible parameters to characterize the

Table 2.3: Survey of receiver diversity based MIMO-OFDM systems

Year	**MIMO-OFDM Technique**	**Baseband Modulation**	**Fading Channel**	**Performance Parameter**
1992 [112]	MRC, EGC, SC	N.D.	generalized Nakagami	outage probability
1995 [113]	MRC	FSK, PSK	correlated Nakagami	ABER
1998 [114]	MRC and EGC	generalized modulation	generalized fading	ABER
1999 [115]	MRC, SC	N.D.	Rayleigh	Shannon capacity
2000 [116]	GSC	MPSK, MQAM	Rayleigh	average SNR, outage probability, ABER
2005 [117]	TAS and MRC	BPSK	flat Rayleigh	outage probability, ABER
2009 [118]	MRC	MPSK, MDPSK, MQAM	η- μ	ASEP
2012 [119]	MRC	MQAM	η- μ and κ-μ	ABER
2014 [120]	MRC	MPSK	κ-μ	ASER, diversity gain
2014 [121]	SC	MQAM	Nakagami-m	ASER
2016 [122]	MIMO-MRC	N.D.	double-correlated Rician	outage probability
2016 [123]	MRC	PSK	Rayleigh	ASER
2017 [124]	MRC and EGC	N.D.	Correlated Nakagami-m	detection probability
2017 [125]	MRC-MIMO	N.D.	Rayleigh fading	spectral efficiency (SE)
2018 [126]	MRC	QPSK	Rayleigh fading	ASINR
2018 [127]	MRC	BPSK	gamma-gamma fading	ABER
2018 [128]	MRC	MPSK	Rayleigh fading	IEP, ABER

fading severity of the signal. However, it has been proved in recent studies that the scenario containing both line of sight and non-line of sight paths cannot be effectively characterized by using the Nakagami-m model. This fact has also been proved by the field measurements for wireless sensor channels [129] and by curve-fitting performance comparison [130], [131].

Therefore, a lot of other more advanced and complex fading channels are introduced in the literature to model different fading scenarios. These fading channels are usually characterized by their PDFs of fading amplitude and instantaneous SNR. Now we present the PDF of instantaneous SNR and MGF expressions for some popular and useful fading channels.

2.3.1 Rayleigh Fading

Rayleigh is the most common distribution in the literature which is utilized to model the scenarios having only NLOS scattered paths. The instantaneous SNR γ of this fading has the PDF [4]

$$p_\gamma(\gamma) = \frac{1}{\bar{\gamma}} \exp\left(\frac{-\gamma}{\bar{\gamma}}\right), \tag{2.1}$$

where $\gamma = \alpha^2 \frac{E_S}{N_0}$ with α as the instantaneous power of received signal; $\bar{\gamma} = \bar{\alpha} E_S/N_0$ and $\bar{\alpha}$ is mean square value of α.

The MGF for a given PDF can be calculated as

$$\mathbb{M}_\gamma(s) = \int_0^\infty p_\gamma(\gamma) \exp(s\gamma) d\gamma. \tag{2.2}$$

Now, using (2.1) in (2.2), the MGF for Rayleigh fading can be calculated as [64]

$$\mathbb{M}_\gamma(s) = (1 - s\bar{\gamma})^{-1}. \tag{2.3}$$

2.3.2 Nakagami-q Fading

Nakagami-q fading is generated by using Gaussian distributed in-phase and quadrature signal components having 0 mean and arbitrary variance. The one-sided Gaussian and Rayleigh fading can be realized from Nakagami-q (Hyot) fading by substituting $q = 0$ and $q = 1$ respectively. This model was initially used to characterize the satellite links facing ionospheric scintillations but later on found its applications to model wireless communi-

cation channels. The PDF of Nakagami-q fading can be represented as [132]

$$p_\gamma(\gamma) = \frac{(1+q^2)}{2q\bar{\gamma}} \exp\left(\frac{-(1+q^2)^2\gamma}{4q^2\bar{\gamma}}\right) I_0\left(\frac{(1-q^4)\gamma}{4q^2\bar{\gamma}}\right), \tag{2.4}$$

where I_0 represents modified Bessel function of first kind with order 0 [133].

For Nakagami-q fading, the MGF can be represented as [64]

$$\mathbb{M}_\gamma(s) = \left(1 - 2s\bar{\gamma} + \frac{(2s\bar{\gamma})^2 q^2}{(1+q^2)^2}\right)^{-1/2}. \tag{2.5}$$

2.3.3 Nakagami-n Fading

The fading process consisting of single LOS and multiple NLOS components can be modelled by using Nakagami-n distribution with n as the fading parameter. The PDF of SNR for this fading can be represented as [64]

$$p_\gamma(\gamma) = \frac{(1+n^2)\exp -n^2}{\bar{\gamma}} \exp\left(\frac{-(1+n^2)\gamma}{\bar{\gamma}}\right) I_0\left(2n\frac{(1+n^2)\gamma}{\bar{\gamma}}\right). \tag{2.6}$$

Keeping $n = 0$, Rayleigh fading can be realized from Rice fading and it converges to the case of no fading for $n = \infty$. The MGF associated with Nakagami-n fading is given as [64]

$$\mathbb{M}_\gamma(s) = \frac{(1+n^2)}{(1+n^2) - s\overline{\gamma}} \exp\left(\frac{n^2 s\overline{\gamma}}{(1+n^2) - s\overline{\gamma}}\right). \tag{2.7}$$

Rice fading is another name for Nakagami-n fading.

2.3.4 Nakagami-m Fading

Nakagami-m is a generalized distribution including fading parameter $m = 1$ for Rayleigh, $m < 1$ for Hoyt, and $m > 1$ for Rician as its special cases. The PDF of Nakagami-m fading is [134]

$$p_\gamma(\gamma) = \frac{m^m \gamma^{m-1}}{\bar{\gamma}^m \Gamma(m)} \exp\left(\frac{-m\gamma}{\bar{\gamma}}\right), \tag{2.8}$$

The MGF of Nakagami-m fading is given as [64]

$$\mathbb{M}_\gamma(s) = \left(1 - \frac{s\overline{\gamma}}{m}\right)^{-m}. \tag{2.9}$$

2.3.5 Beckmann Fading

Beckmann fading is described by complex Gaussian process. It is often called as the generalized Rice or generalized Gaussian model. The exact expression for the PDF of SNR for Beckmann fading is not available. But the closed form expression of MGF for this fading is given as [64]

$$\mathbb{M}_{\gamma}(s) = \frac{(1+q^2)}{\sqrt{((1+q^2)(1+K)-2q^2\overline{\gamma}s)}} \times \frac{(1+K)}{\sqrt{((1+q^2)(1+K)-2\overline{\gamma}s)}} \times \exp\left(\frac{K(\frac{r^2}{1+r^2})(1+q^2)\overline{\gamma}s}{(1+q^2)(1+K)-2q^2\overline{\gamma}s} + \frac{K(\frac{1}{1+r^2})(1+q^2)\overline{\gamma}s}{(1+q^2)(1+K)-2\overline{\gamma}s}\right), \tag{2.10}$$

where K, q and r are channel parameters. The Beckmann model includes many fading channels as its special cases like one-sided Gaussian ($r^2 = 1$, $q^2 = 0$, $K = 0$), Rayleigh ($r^2 = 1$, $q^2 = 1$, $K = 0$), Rician ($r^2 = 1$, $q^2 = 1$, $K \neq 0$) and Nakagami-q ($r^2 = 1$, $q^2 \neq 1$, $K = 0$).

2.3.6 Generalized-K (K_G) Fading

The Generalized-K or K_G is a relatively new fading model. The K fading, Nakagami-m and Rayleigh-Lognormal (R-L) fading can be derived from Generalized-K model. The multipath fading plus shadowing scenario can be modelled using generalized-K (K_G) fading. Such scenario can otherwise be modeled using much complex lognormal based fading models. The PDF of instantaneous SNR for this channel is given as [135]

$$p_{\gamma}(\gamma) = \frac{2\Xi^{\frac{\widehat{\beta}+1}{2}}\gamma^{\frac{\widehat{\beta}-1}{2}}}{\Gamma(m)\Gamma(k)} K_{\widehat{\alpha}}(2(\Xi\gamma)^{1/2}), \tag{2.11}$$

where $\widehat{\alpha} = K - m$, K and m are channel parameters; $\Xi = \frac{Km}{\overline{\gamma}}$, $K_x(\cdot)$ is the modified Bessel function of order x, $\widehat{\beta} = K + m - 1$. For K_G fading, the expression of MGF is [135]

$$\mathbb{M}_{\gamma}(s) = \left(\frac{\Xi}{s}\right)^{\frac{\widehat{\beta}}{2}} \exp\left(\frac{\Xi}{2s}\right) W_{-\frac{\widehat{\beta}}{2},-\frac{\widehat{\alpha}}{2}}\left(\frac{\Xi}{s}\right), \tag{2.12}$$

where $W_{a,b}(\cdot)$ is the Whittaker function [133].

2.3.7 Generalized Two-Ray (GTR) Fading

The problem of Two Wave With Diffuse Power (TWDP) fading channel [136] was overcome by GTR fading model. Unlike TWDP, the MGF of GTR fading can be expressed

in closed form. This fading model is used to characterize the scenario with two LOS multipath waves and several NLOS diffused power waves. Several channels like TWDP, Rayleigh, Rician and two ray fading are the special cases of GTR fading. For GTR fading, the SNR PDF is defined as [137]

$$p_\gamma(\gamma) = \frac{1+K}{\overline{\gamma}} \exp\left(-\frac{\gamma(1+K)}{\overline{\gamma}}\right) \frac{1}{2\pi} \int_0^{2\pi} \exp\left(-\overline{K}(\alpha)\right) I_0\left(2\sqrt{\frac{\overline{K}(\alpha)(K+1)}{\overline{\gamma}}}\right) d\alpha, \tag{2.13}$$

where $\overline{K} = K(1+\Delta cos(\alpha))$, α represents the difference in phase of two LOS components; K, Δ are fading parameters. The exact MGF of TWDP fading is given in [137] as

$$\mathbb{M}_\gamma(s) = \frac{1+K}{1+K-s\overline{\gamma}} \exp\left(\frac{Ks\overline{\gamma}}{1+K-s\overline{\gamma}}\right) I_0\left(\frac{Ks\overline{\gamma}\Delta}{1+K-s\overline{\gamma}}\right). \tag{2.14}$$

2.3.8 $\eta - \lambda - \mu$ Fading

The η-μ and λ-μ distributions are combined in a single expression which results in η-λ-μ distribution [138]. The $\eta - \lambda - \mu$ fading includes a lot of other fading channels as its special cases. The MGF for η-λ-μ fading is given as [68]

$$M(s) = \left(\frac{4\eta(1-\lambda)^2\tilde{b}^2}{(\tilde{c}+s\overline{\gamma}_t)^2 - \tilde{d}^2}\right), \tag{2.15}$$

where η, λ, and μ are channel parameters with $\tilde{b}$, $\tilde{c}$, $\tilde{d}$ are the internal parameters defined as $\tilde{b} = \frac{\mu(1+\eta)}{2\eta(1-\lambda^2)}$; $\tilde{c} = \frac{\mu(1+\eta)^2}{2\eta(1-\lambda^2)}$ and $\tilde{d} = \tilde{b}\sqrt{(\eta-1)^2 + 4\eta\lambda^2}$. Fading channels like Rayleigh, η-μ fading, λ-μ fading, Nakagami-q, one-sided Gaussian and Rician can be derived from $\eta - \lambda - \mu$ fading by using different values of fading parameters.

2.3.9 Beaulieu-Xie Fading

Beaulieu-Xie fading model was introduced by Beaulieu and Xie in 2015 [131] to better represent both the LOS and NLOS components using a single distribution. This flexible fading model is derived from Rician distribution and is related to Nakagami-m distribution. In Beaulieu-Xie model, the fading amplitude consists of multiple specular and diffuse scatter components. This model has applications in modeling the fading channels of high speed vehicular applications and femtocells [139, 140].

In [131], Beaulieu and Xie derived the closed-form expression of PDF of the fading ampli-

tude, cumulative distribution function (CDF), moments, K-factor and symbol error rate of a 16-QAM system. Subsequently, Olutayo et al. have worked on this fading model in 2017 [141]. However, the expressions for the PDF of instantaneous SNR and MGF along with other key statistical parameters were not available in literature and were deduced by Singh and Joshi in [111].

The PDF of γ for Beaulieu-Xie fading is given in [111] as

$$p_\gamma(\gamma) = \left(\frac{\sqrt{2\gamma}}{\lambda}\right)^{m-1} \left(\sqrt{\frac{m}{\bar{\gamma}}}\right)^{m+1} \exp\left(-\left(\frac{\lambda^2}{2} + \frac{m\gamma}{\bar{\gamma}}\right)\right) I_{m-1}\left(\sqrt{\frac{2m\gamma}{\bar{\gamma}}}\lambda\right). \tag{2.16}$$

Fig. 2.1 demonstrates the effect of fading parameters on the shape of PDF. It can be visualized form Fig. 2.1 that if the fading parameter m is kept constant, the PDF height increases with increase in λ. On the other hand, changing m affects the spread of PDF when λ is kept constant.

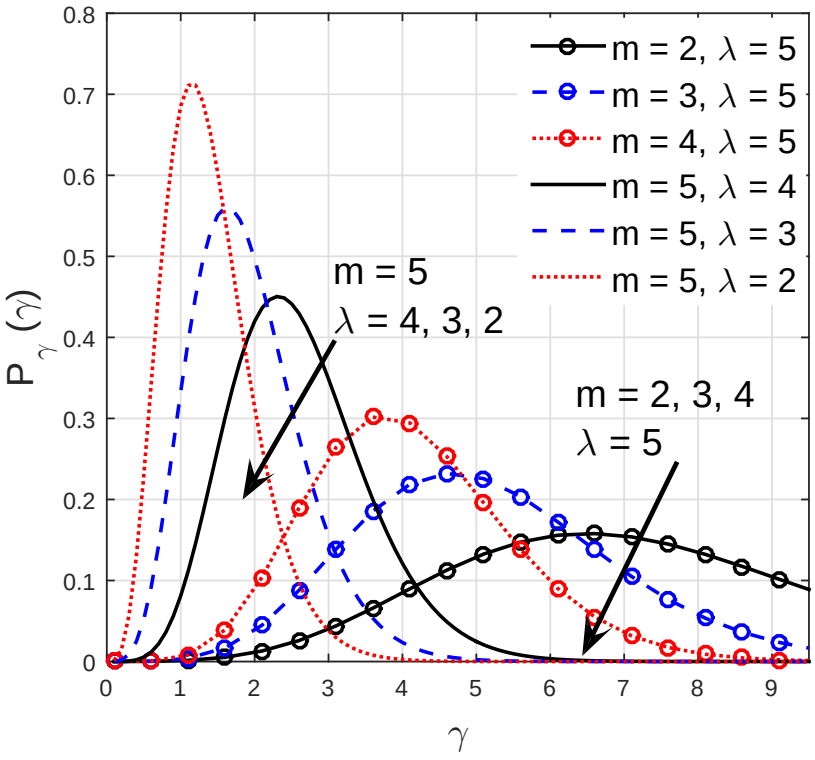

Figure 2.1: Beaulieu-Xie distribution with different values of the channel parameters.

For Beaulieu-Xie fading, the generalized MGF is calculated as [111]

$$\mathbb{M}_\gamma^{(n)}(s) = \left(\frac{m}{\bar{\gamma}}\right)^m \exp\left(-\frac{\lambda^2}{2}\right) \left(\frac{m}{\bar{\gamma}} - s\right)^{-m+n} \Gamma[m+n]_1F_{1R}\left[m+n, m, \frac{m\lambda^2}{2(m-s\bar{\gamma})}\right], \tag{2.17}$$

where $\Gamma[\cdot]$ and ${}_1F_{1R}[\cdot,\cdot,\cdot]$ represents the Euler gamma function and the regularized confluent hypergeometric function respectively [133, p. 650].

2.4 Research Gaps

The following gaps are observed from the literature study:
It has been identified through a comprehensive literature survey that significant research has been carried out on the performance analysis of MIMO-OFDM systems considering the conventional fading channels like Rayleigh, Rician and Nakagami [53–55, 67–72, 74, 76]. However, the performance of these systems is yet to be studied for some complex fading environments like TWDP fading [136, 142], α-μ [143], κ-μ [144]and η-μ [145] fading, Beaulieu-Xie fading model [131] etc. The real world fading scenarios comprising complex hostile environments can be better represented by these fading models. Therefore, an analytical framework is the need of the hour for MIMO-OFDM systems which can accommodate the large variety of fading scenarios.

It is also observed that most of the researches in the area of MIMO-OFDM focus on performance analysis of MIMO-OFDM system under idealistic conditions. These conditions are not met in many cases which lead to the need of a unified framework for performance analysis of MIMO-OFDM system while taking into account channel impairments.

2.5 Thesis Objectives and Scope

This dissertation aims to present an analytical framework for MIMO-OFDM systems, the principle purpose of which is to calculate the performance of MIMO-OFDM systems.
The main objectives of the research doctoral dissertation are:

- To propose an analytical framework for MIMO-OFDM system in multipath fading channel.
- To study the proposed system under the effect of channel impairments.
- To compare the analytical and simulated results for the proposed framework.

In this dissertation, we propose an analytical framework for MIMO-OFDM systems in fading environment. This framework includes the system model and the study of various sub-blocks of MIMO-OFDM communication system like transmitter, channel and receiver for different possible forms of MIMO-OFDM system.

The second objective is to study the proposed system under the effect of channel im-

pairments. Therefore, a unified approach is formulated for obtaining the BER of MIMO-OFDM system. Using the proposed unified approach, the ABER of MIMO-OFDM system can be calculated for any given fading conditions. The performance of MIMO-OFDM systems is also calculated to include the effect of channel impairments like carrier frequency offset and imperfect CSI on the ABER. Both SFBC-OFDM and STBC-OFDM systems are considered in this analysis.

The third objective is to compare the analytical and simulated results for the proposed framework. Extensive simulation results are provided to verify the results calculated from the derived analytical expressions. This proves the validity by providing a cross-check over the proposed framework of MIMO-OFDM. The results obtained by this unified approach are mostly in closed form and are very accurate. In some cases, numerical integration is required over finite limits which is very well implemented hustle-free with ignorable error using efficient tools like MATLAB and Mathematica.

Chapter 3

Bit Error Rate Analysis of SFBC-OFDM Systems

The performance of SFBC-OFDM system in terms of bit error rate is calculated using both exact and closed form analysis in this chapter. Generalized Fading scenario is assumed while deriving the exact error rate expressions which allow the calculation of ABER of SFBC-OFDM system for any family of fading PDF. A simple closed form bound of error rate is also provided along with the exact expressions. This analysis is done for both MPSK and MQAM modulation techniques.

Numerical simulation of derived expressions has been used for performance evaluation of different configurations of SFBC-OFDM system. Simulation results are provided along with numerical results which are found to be very close to numerical results. Alternatively, the results obtained using bounds provide good approximations in some cases with lesser complexity. The derived expressions of ABER can serve as a basis to calculate the error rate of SFBC-OFDM system with impairments as discussed in later chapters.

The system model of SFBC-OFDM is presented in Section 3.1. Thereafter, the error rate analysis over fading channel is given in Section 3.2. In Section 3.3, the illustrations of the derived ABER for different fading channels are given. The results obtained from numerical analysis and simulations are given in Section 3.4. Section 3.5 holds the summary of chapter.

3.1 SFBC-OFDM System Model

Consider a SFBC-OFDM system with T_x transmit and R_x receiving antenna. The block diagram of such a system is given in Fig. 3.1. A comparison can be made between the MIMO-OFDM system given in Fig. 1.3 and Fig. 3.1. A distinctive difference between the two is the generalized MIMO encoder is replaced here with the SFBC encoder. The orthogonal symbols generated by using the coding matrix $\mathbb{G}$ are complex conjugate combinations of the modulated symbols in vector $\mathbf{x}$. Subsequent subcarriers of the same OFDM symbol is utilized to transmit the symbols generated by using the coding matrix

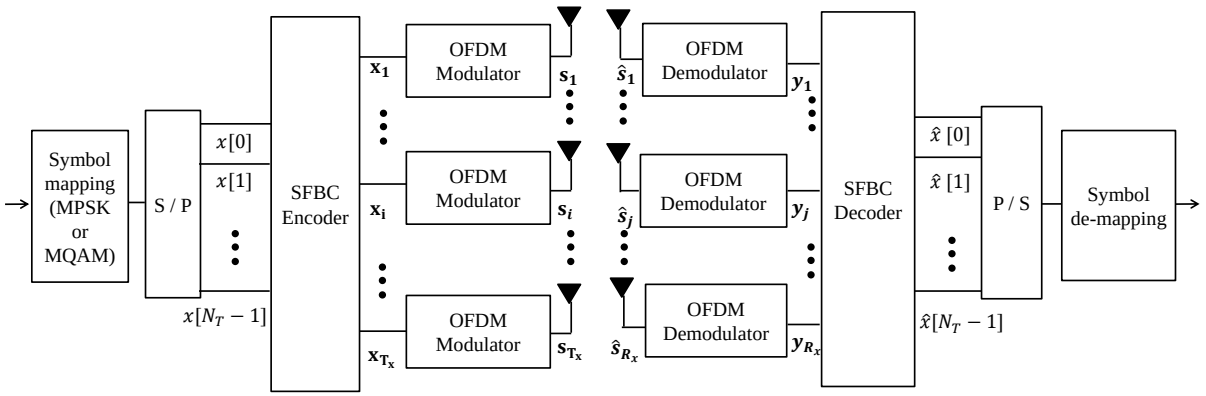

Figure 3.1: SFBC-OFDM system model [96].

$\mathbb{G}$. This kind of coding is very useful to ambush the conditions with fast channel variations. Also, it reduces the transmission delay as all the symbols required to decode the first two modulated symbols are available in first time instant only. On the other hand, the channel over N neighboring subcarriers should be constant for the error free working of SFBC-OFDM system. If the assumption of a constant channel over N subcarriers does not hold true, the performance of SFBC-OFDM degrades. This occurs in highly frequency selective fading. [146].

To illustrate the process of encoding used in SFBC-OFDM, let us take the simple case of two transmit antennas and an OFDM system with four subcarriers as given in Fig. 3.2. In this work, the matrices are represented by uppercase boldface letters, and lowercase boldface is used for vectors, whereas scalars are shown with un-boldface letters. Let the vector containing input symbols for SFBC encoder is

$$\mathbf{x} = \{x_0, x_1, x_2, x_3\}. \tag{3.1}$$

Now, according to Alamouti's scheme, the orthogonal symbols generated for transmit antenna one are [30]

$$\mathbf{x}_1 = \{x_0, -x_1^*, x_2, -x_3^*\}, \tag{3.2}$$

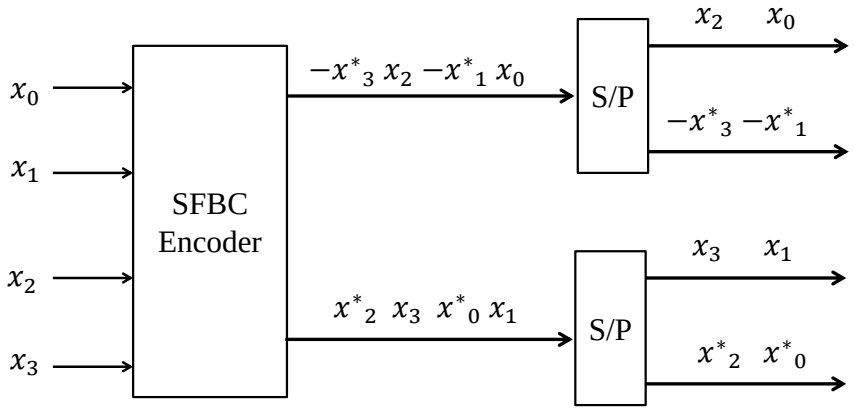

Figure 3.2: SFBC encoder for $T_x = 2$, $N = 2$.

and for transmit antenna two are

$$\mathbf{x}_2 = \{x_1, x_0^*, x_3, x_2^*\}. \tag{3.3}$$

These data streams are fed to two individual OFDM modulators after applying serial to parallel conversion. It can be clearly visualized that the first set of symbols at the input to OFDM modulators contain orthogonal design for x_0 and x_1 and are sufficient for their decoding [30].

Now, as all the subcarriers of one transmitting antenna are assumed to be affected by the same channel. Therefore, let us assume two independent and identically distributed (IID) l tap fading channels h_1 and h_2 for transmitting antenna one and two respectively. For single receiving antenna case, the signal received in the first time instant is given by [96]

$$\begin{bmatrix} y_{11} \\ y_{12} \end{bmatrix} = h_1 \begin{bmatrix} x_0 \\ -x_1^* \end{bmatrix} + h_2 \begin{bmatrix} x_1 \\ x_0^* \end{bmatrix}. \tag{3.4}$$

Further, taking the conjugate of second row in (3.4) results in

$$\begin{bmatrix} y_{11} \\ y_{12}^* \end{bmatrix} = \begin{bmatrix} h_1 & h_2 \\ h_2^* & -h_1^* \end{bmatrix} \begin{bmatrix} x_0 \\ x_1 \end{bmatrix}. \tag{3.5}$$

Similarly, the signal received at the second time instant is given as

$$\begin{bmatrix} y_{21} \\ y_{22} \end{bmatrix} = h_1 \begin{bmatrix} x_2 \\ -x_3^* \end{bmatrix} + h_2 \begin{bmatrix} x_3 \\ x_2^* \end{bmatrix}. \tag{3.6}$$

Again taking the conjugate of second row, the received signal at second time instant becomes

$$\begin{bmatrix} y_{21} \\ y_{22}^* \end{bmatrix} = \begin{bmatrix} h_1 & h_2 \\ h_2^* & -h_1^* \end{bmatrix} \begin{bmatrix} x_2 \\ x_3 \end{bmatrix}. \tag{3.7}$$

Finally, the decoded signals can be calculated by multiplying (3.6) and (3.7) with the hermitian of channel matrix. This hermitian is defined as

$$\mathbf{H} = \begin{bmatrix} h_1 & h_2 \\ h_2^* & -h_1^* \end{bmatrix}. \tag{3.8}$$

3.2 Error Rate Analysis of SFBC-OFDM Systems over Fading Channel

There are three major factors which affect the error rate performance of SFBC-OFDM system. These factors are modulation technique, fading channel and system impairments. The effect of modulation is visible on the conditional BER of the system. Generally, the average error rate for any communication system is calculated from the conditional BER by solving an integral from 0 to ∞ with the fading channel PDF. This conditional error rate is equivalent to the performance over AWGN channel which means that there is no fading available and the transmitted signal gets affected only by channel noise [6].

Here in this analysis, the conditional error rate ($p(e/\gamma)$) of the SISO-OFDM system is defined. Then, this conditional error rate is used to define the expression of conditional error rate ($p(e/\gamma_t)$) in AWGN channel for SFBC-OFDM system. A simple exponential bound for conditional error rate is also provided. Finally, the closed form expressions are derived for the ABER of SFBC-OFDM system over fading channel by using these conditional error rates.

Let us take the case of a SISO-OFDM system for which the conditional bit error rate is

given as [96]

$$p(e/\gamma) = \frac{1}{N}\sum_{k=0}^{N-1} p_{[k]}(e/\gamma), \tag{3.9}$$

where N is the number of subcarriers and $p_{[k]}(e/\gamma)$ represents the conditional probability of error on k^{th} sub-channel in OFDM block conditioned on the SNR (γ). There are two factors which affect $p_{[k]}(e/\gamma)$. These factors are the modulation scheme used and SNR of system. Therefore, first we have to derive the relation between the SNR of individual transmit-receive antenna pair and the overall SNR of SFBC-OFDM system. An assumption is made here that the error provided by all the N subchannels is equal. So the statistical averaging operation can be removed in (3.9).

Consider a SFBC-OFDM system employing T_x transmit and R_x receive antennas. At the receiver side, after removing the cyclic prefix and FFT, the resultant received signal vector at j^{th} receive antenna is represented as

$$\mathbf{y}_j = \sum_{i=1}^{T_x} \mathbf{H}_{j,i}\mathbf{x}_i + \mathbf{w}_j; \qquad 1 \leq j \leq R_x, \tag{3.10}$$

where $\mathbf{H}_{j,i}$ is defined as $\mathbf{H}_{j,i} = diag\{H_{j,i}[k]\}_{k=0}^{N-1}$. The elements of channel matrix $\mathbf{H}_{j,i}$ composed of DFT of independent fading channel from i^{th} transmit and j^{th} receive antenna and $\mathbf{w}_j$ is AWGN vector [96]. Both $\mathbf{H}_{j,i}$ and $\mathbf{w}_j$ are assumed to be ergodic and stationary.

It is assumed that the average energy of transmitted signal is $\frac{E_s}{T_x}$. Now, the received signal average power can be calculated for a single receive antenna as $\frac{E_s}{T_x}\sum_{i=1}^{T_x}\mathbb{E}\left[|\mathbf{H}_{j,i}|^2\right]$. Also, the SNR per receive antenna is given by $\frac{E_s}{N_0}$.

From the column orthogonal property of the SFBC coded matrix, the total average energy of a block (E_{tot}) can be written as [147]

$$E_{tot} = T_x N E_0, \tag{3.11}$$

where E_0 represents average energy in a constellation which is given as

$$E_0 = \frac{E_s}{T_x R_C}, \tag{3.12}$$

where R_C is the SFBC code rate. For the case when the channel is perfectly estimated

at the receiver, the condition of choosing $\hat{\mathbf{x}}_n$ for $\mathbf{x}_n$ is

$$\hat{\mathbf{x}}_n = \text{argmin} \left| \left(||\mathbf{H}||_F^2 \mathbf{x}_n + \mathbf{w}_n \right) - \left(||\mathbf{H}||_F^2 \mathbf{x}_n \right) \right|^2, \tag{3.13}$$

where $(||\mathbf{H}||_F^2 \mathbf{x}_n + \mathbf{w}_n)$ and $\mathbf{w}_n$ is the output of combiner and AWGN respectively. The squared Frobenius norm $||\mathbf{H}||_F^2$ can be represented as [133]

$$||\mathbf{H}||_F^2 = tr(\mathbf{H}\mathbf{H}^T) = \sum_{i=1}^{M_T} \sum_{j=1}^{M_R} |\mathbf{H}|^2. \tag{3.14}$$

The signal power (P_x) and the noise power (P_w) can be calculated using (3.12) and (3.13) as

$$\begin{aligned} P_x &= \mathbb{E}\left[||\mathbf{H}||_F^2 \mathbf{x} \right]^2 = ||\mathbf{H}||_F^4 \frac{E_s}{T_x R_C}, \\ P_w &= ||\mathbf{H}||_F^2 N_0. \end{aligned} \tag{3.15}$$

Now, using the definition of the Frobenius norm from (3.14) and using (3.15), the normalized instantaneous SNR for SFBC-OFDM system is given by the relation [110]

$$\gamma_t = \frac{1}{R_C T_x} \sum_{i=1}^{T_x} \sum_{j=1}^{R_x} \gamma_{i,j}, \tag{3.16}$$

where $\gamma_{i,j}$ represents the instantaneous SNR in-between i^{th} transmit and j^{th} receive antenna pair. The conditional BER for SFBC-OFDM system can be expressed by substituting the SFBC-OFDM SNR (γ_t) defined in (3.16) in place of SISO-OFDM SNR (γ).

In this analysis, two different modulation schemes are considered i.e. PSK and QAM. The modulated signal for M-PSK is given as [4]

$$\mathbf{a}_m(t) = \Re \left[\mathbf{a}(t) \exp\left(j \frac{2\pi(m-1)}{M} \right) \exp\left(j 2\pi f_c t \right) \right], \tag{3.17}$$

where $\Re[\cdot]$ represents the real part, $\mathbf{a}(t)$ is the amplitude of modulating signal. The modulated signal has M different phase values of the carrier. Fig. 3.3 shows the constellation diagrams of different M-PSK configurations. For M-PSK the SEP over the AWGN channel is given by several authors in different forms [148, 149]. A very simplified expression for conditional BER is given by Proakis [4] which is used further in this dissertation

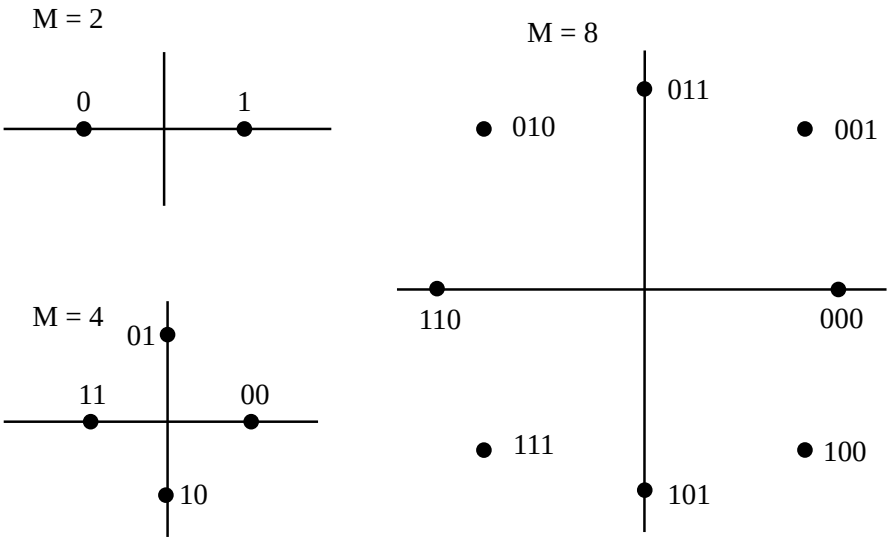

Figure 3.3: Constellation diagrams of MPSK for different modulation orders.

is

$$p(e/\gamma) = \frac{2}{\log_2 M} Q\left(\sqrt{2sin^2\left(\frac{\pi}{M}\right)\gamma_t}\right). \tag{3.18}$$

QAM is another modulation technique which is bandwidth efficient and is acquired by using two separate quadrature carriers $\cos 2\pi f_c t$ and $\sin 2\pi f_c t$ for two k-bit symbols. The signal waveform for M-QAM can be expressed as [4]

$$\mathbf{a}_m(t) = \Re\left[\left(\mathbf{a}_{m_i} + j\mathbf{a}_{m_q}\right)\mathbf{g}(t)\exp\left(j2\pi f_c t\right)\right], \tag{3.19}$$

where $\mathbf{a}_{m_i}$ and $\mathbf{a}_{m_q}$ are the amplitudes of the inphase and quadrature phase carrier signals, $\mathbf{g}(t)$ represents the modulating signal which independently range over the equiprobable values $\mathbf{a}_{m_i} = (2\mathbf{x} - 1 - \sqrt{M})$ with $\mathbf{x} = 1, 2, \cdots \sqrt{M}$ and $\mathbf{a}_{m_q} = (2\mathbf{y} - 1 - \sqrt{M})$ with $\mathbf{y} = 1, 2, \cdots \sqrt{M}$. The constellation diagrams of M-QAM for M = 4, 16 and 32 are shown in Fig. 3.4. The expression for BER of M-QAM under AWGN channel is presented as [4]

$$p(e/\gamma) = \frac{4}{log_2 M}\left(1 - \frac{1}{\sqrt{M}}\right) Q\left(\frac{\sqrt{3\gamma_t}}{M-1}\right). \tag{3.20}$$

Multipath and shadowing effects degrade the performance of a communication system. This results in fading of the transmitted signal. Fading can be characterized by using different statistical models. In this study the performance analysis of SFBC-OFDM system is performed under several different fading channels using MGF approach.

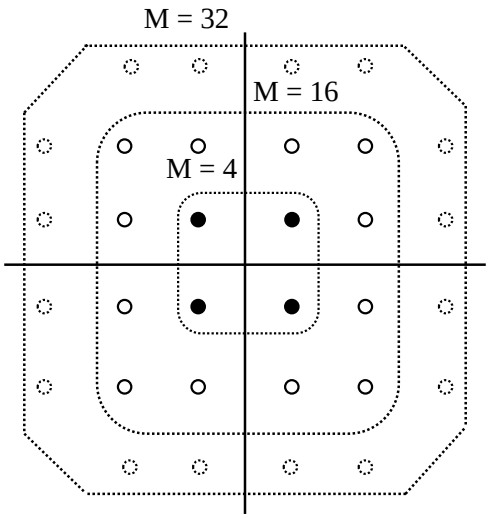

Figure 3.4: Constellation diagrams of MQAM for different modulation orders.

After careful observation of (3.18) and (3.20) and to support the unified approach, both (3.18) and (3.20) are combined into a generalized expression of conditional BER of SFBC-OFDM system valid for both MQAM and MPSK as

$$P(e/\gamma_t) = \alpha\, Q\left(\sqrt{\beta\, \gamma_t}\right), \tag{3.21}$$

where

$$\alpha = \begin{cases} \frac{2}{\log_2 M} & \text{for MPSK} \\ 4\left(1 - \frac{1}{\sqrt{M}}\right)\frac{1}{\log_2 M} & \text{for MQAM} \end{cases},$$

and

$$\beta = \begin{cases} 2\sin^2\left(\frac{\pi}{M}\right) & \text{for MPSK} \\ \frac{3}{(M-1)^2} & \text{for MQAM} \end{cases}.$$

Now, the ABER for SFBC-OFDM system over fading channel is calculated as [110]

$$ABER = \int_0^\infty \int_0^\infty \cdots \int_0^\infty P(e/\gamma_t) p_\gamma(\gamma_{1,1}) p_\gamma(\gamma_{1,2}) \cdots p_\gamma(\gamma_{T_x,R_x}) d\gamma_{1,1} d\gamma_{1,2} \cdots d\gamma_{T_x,R_x}, \tag{3.22}$$

where $P(e/\gamma_t)$ represents the conditional probability of error and $p_\gamma(\gamma_{i,j})$ represents the PDF of fading channel between i^{th} transmit and j^{th} receive antenna. Unlike most of

the traditional studies, this analysis is not restricted to only one class of fading PDF. Generalized fading scenario is assumed in this study.

Two different approaches can be used to solve the integral in (3.22). The alternate definition for Q function is used in the first approach for deriving exact expression of ABER. Whereas, in the second approach, an exponential bound on the conditional BER is utilized. Both these approaches are given in subsections below.

3.2.1 Using Exact Analysis

In order to find the exact expression of ABER for a SFBC-OFDM system over generalized fading channel, the alternate definition of Q function is used [64]. After substituting (3.21) in (3.22), the exact ABER can be written as

$$\begin{aligned} ABER_{exact} = \int_0^\infty \int_0^\infty \cdots \int_0^\infty \alpha \quad Q\left(\sqrt{\beta\gamma_t}\right) p_\gamma(\gamma_{1,1}) p_\gamma(\gamma_{1,2}) \cdots \times \\ p_\gamma(\gamma_{T_x,R_x}) d\gamma_{1,1} d\gamma_{1,2} \cdots d\gamma_{T_x,R_x}. \end{aligned} \tag{3.23}$$

The integral in (3.23) can be solved by using the alternate definition for Q function given in [64, Eqn. 4.2] as

$$Q(z) = \frac{1}{\pi} \int_0^{\frac{\pi}{2}} \exp\left(-\frac{z^2}{2\sin^2\phi}\right) d\phi. \tag{3.24}$$

Now, using (3.16) and (3.24) in (3.23) and interchanging the order of integrals, (3.23) can be written as

$$\begin{aligned} ABER_{exact} = & \frac{\alpha}{\pi} \int_0^{\frac{\pi}{2}} \Bigg[\int_0^\infty \int_0^\infty \cdots \int_0^\infty \exp\left(-\frac{\beta \sum_{i=1}^{T_x} \sum_{j=1}^{R_x} \gamma_{i,j}}{2C_R T_x \sin^2\phi}\right) \times \\ & p_\gamma(\gamma_{1,1}) p_\gamma(\gamma_{1,2}) \cdots p_\gamma(\gamma_{T_x,R_x}) \times \\ & d\gamma_{1,1} d\gamma_{1,2} \cdots d\gamma_{T_x,R_x} \Bigg] d\phi. \end{aligned} \tag{3.25}$$

For an arbitrary number of T_x and R_x and with different fading distributions, the solution of double integral in (3.25) is very difficult to find. This difficulty increases further if the PDF of channel involves infinite series. Therefore, in order to solve the integral in (3.25), MGF based approach is utilized. This approach eliminates the need of calculating double integral by expressing (3.25) in terms of MGF of channel.

In order to apply MGF approach, the integral in (3.25) can be represented as

$$ABER_{exact} = \frac{\alpha}{\pi} \int_0^{\frac{\pi}{2}} \left(I_{1,1} I_{1,2} \cdots I_{T_x,R_x}\right) d\phi, \tag{3.26}$$

where $I_{x,y}$ is calculated as

$$I_{x,y} = \int_0^{\infty} \exp\left(-\frac{\beta\, \gamma_{x,y}}{2C_R T_x \sin^2\phi}\right) p_\gamma(\gamma_{x,y}) d\gamma_{x,y}. \tag{3.27}$$

By using the definition of MGF as $M_x(A) = \int_0^{\infty} \exp\left(A.x\right) p_x(x) dx$, (3.27) can be written as

$$I_{x,y} = M_{\gamma_{x,y}}\left(-\frac{\beta}{2C_R T_x \sin^2\phi}\right). \tag{3.28}$$

Now, (3.26) can be further simplified by using (3.28) as

$$ABER_{exact} = \frac{\alpha}{\pi} \int_0^{\frac{\pi}{2}} \left[M_{\gamma_{1,1}}\left(-\frac{\beta}{2C_R T_x \sin^2\phi}\right) M_{\gamma_{1,2}}\left(-\frac{\beta}{2C_R T_x \sin^2\phi}\right) \cdots \times M_{\gamma_{T_X,R_X}}\left(-\frac{\beta}{2C_R T_x \sin^2\phi}\right)\right] d\phi. \tag{3.29}$$

For independent and non-identical fading paths, (3.29) can be written as

$$ABER_{exact} = \frac{\alpha}{\pi} \int_0^{\frac{\pi}{2}} \left[\prod_{i=1}^{T_x} \prod_{j=1}^{R_x} M_{\gamma_{i,j}}\left(-\frac{\beta}{2C_R T_x \sin^2\phi}\right)\right] d\phi. \tag{3.30}$$

For the case of independent and identically distributed fading paths, (3.30) can be further simplified to form the exact expression of ABER for SFBC-OFDM system as

$$ABER_{exact} = \frac{\alpha}{\pi} \int_0^{\frac{\pi}{2}} \left[M_{\gamma_t}\left(-\frac{\beta}{2C_R T_x \sin^2\phi}\right)\right]^{T_x R_x} d\phi. \tag{3.31}$$

Using the MGF of a given fading channel in (3.31), the ABER under generalized fading can be calculated. Numerical methods are used to finally solve this expression for the exact ABER of SFBC-OFDM system in any given fading environment.

3.2.2 Using Exponential Bound

A simple approximate solution for the ABER of SFBC-OFDM under generalized fading channels can be calculated by utilizing a well-known exponential bound on the conditional BER [150]. This approximation simplifies the process of calculating ABER and results

in a simple yet effective expression of ABER. Utilizing the tight bound given in [150], the conditional BER of SFBC-OFDM system given in (3.21) can now be defined as

$$P\left(e/\gamma_t\right) \approx 0.2 \exp\left(\zeta \gamma_t\right), \tag{3.32}$$

where ζ depends on modulation technique and for MQAM, $\zeta = \frac{-1.6}{M-1}$ and for MPSK, $\zeta = \frac{-7}{\left(2^{(1.9 \log_2 M)}+1\right)}$. Now, the ABER of SFBC-OFDM can be derived by substituting (3.32) in (3.22) as

$$\begin{aligned} ABER \approx \int_0^\infty \int_0^\infty \cdots \int_0^\infty 0.2 \exp\left(\zeta \gamma_t\right) p_\gamma(\gamma_{1,1}) p_\gamma(\gamma_{1,2}) \cdots \times \\ p_\gamma(\gamma_{T_x,R_x}) d\gamma_{1,1} d\gamma_{1,2} \cdots d\gamma_{T_x,R_x}. \end{aligned} \tag{3.33}$$

After substituting the value of γ_t from (3.16) in (3.33), the ABER can be expressed as

$$\begin{aligned} ABER \approx 0.2 \int_0^\infty \int_0^\infty \cdots \int_0^\infty \exp\left(\frac{\zeta}{C_R T_x} \sum_{i=1}^{T_x} \sum_{j=1}^{R_x} \gamma_{i,j}\right) p_\gamma(\gamma_{1,1}) p_\gamma(\gamma_{1,2}) \cdots \times \\ p_\gamma(\gamma_{T_x,R_x}) d\gamma_{1,1} d\gamma_{1,2} \cdots d\gamma_{T_x,R_x}. \end{aligned} \tag{3.34}$$

After some algebraic manipulations, (3.34) can be further simplified into

$$\begin{aligned} ABER \approx 0.2 \int_0^\infty \exp\left(\frac{\zeta}{C_R T_x} \gamma_{1,1}\right) p_\gamma(\gamma_{1,1}) d\gamma_{1,1} \times \\ \int_0^\infty \exp\left(\frac{\zeta}{C_R T_x} \gamma_{1,2}\right) p_\gamma(\gamma_{1,2}) d\gamma_{1,2} \cdots \times \\ \int_0^\infty \exp\left(\frac{\zeta}{C_R T_x} \gamma_{T_x,R_x}\right) p_\gamma(\gamma_{T_x,R_x}) d\gamma_{T_x,R_x}. \end{aligned} \tag{3.35}$$

Now, a closed form expression of ABER using exponential bound is derived by using the MGF approach as discussed in (3.28)-(3.31) and substituting $\xi = \frac{\zeta}{C_R T_x}$ as

$$ABER \approx 0.2 \left[M_{\gamma_t}\left(\xi\right)\right]^{T_x R_x}. \tag{3.36}$$

The MGF for most of the fading channels are well defined and discussed in literature. Hence, by using (3.36), the ABER of a SFBC-OFDM system for any fading channel with a valid MGF is calculated easily and effectively. The derived closed form expressions (3.31) and (3.36) are very helpful in evaluating the ABER performance in real-time for a SFBC-OFDM system employing adaptive modulation technique over different fading channels.

3.3 Illustration of Derived ABER for Different Fading Channels

In the following subsections, the expressions of ABER are derived for different fading channels which are considered in this study. It is important to mention here that our analysis is not limited to these fading channels only and can be readily applied to any given case.

3.3.1 Rayleigh Fading

Using the MGF from (2.3) in (3.31), the exact ABER for SFBC-OFDM system in Rayleigh fading channel can be derived as

$$ABER_{exact} = \frac{\alpha}{\pi} \int_0^{\frac{\pi}{2}} \left[1 + \frac{\beta \overline{\gamma}_t}{2C_R T_x \sin^2 \phi}\right]^{T_x R_x} d\phi. \tag{3.37}$$

Similarly, by using the MGF from (2.3) in (3.36), the ABER for SFBC-OFDM system in Rayleigh fading channel using exponential bound can be derived as

$$ABER \approx 0.2 \left(1 - \xi \overline{\gamma}_t\right)^{-T_x R_x}. \tag{3.38}$$

Upon substituting the value of α, β and ξ into (3.38), our result in (3.38) reduces to the ABER expression given in [96].

3.3.2 Nakagami-q Fading

The ABER for SFBC-OFDM system using exponential bound under Nakagami-q fading is derived using (2.3) in (3.36) as

$$ABER \approx 0.2 \left(1 - 2\xi \overline{\gamma}_t + \frac{(2\xi \overline{\gamma}_t)^2 q^2}{(1+q^2)^2}\right)^{-\frac{T_x R_x}{2}}. \tag{3.39}$$

Equation (3.39) can easily be simplified to match the ABER results of [96] if we let $q = 1$.

3.3.3 Nakagami-n (Rice) Fading

For the case of Nakagami-n fading, the ABER using exponential bound can be derived by using (2.7) in (3.36) as

$$ABER \approx 0.2\left(\frac{(1+n^2)}{(1+n^2)-\xi\overline{\gamma}_t}\exp\left(\frac{n^2\xi\overline{\gamma}_t}{(1+n^2)-\xi\overline{\gamma}_t}\right)\right)^{T_xR_x}. \tag{3.40}$$

Now, (3.40) reduces to (3.38) for $n = 0$ and results of Rayleigh fading can be verified.

3.3.4 Nakagami-m Fading

The ABER of a SFBC-OFDM system using exponential bound under Nakagami-m fading is derived using (2.9) in (3.36) as

$$ABER \approx 0.2\left(1-\frac{\xi\overline{\gamma}_t}{m}\right)^{-mT_xR_x}. \tag{3.41}$$

Nakagami-m distribution transforms into one sided Gaussian fading and nonfading AWGN for the values of fading parameter $m = 0.5$ and ∞ respectively whereas, it reduces to (3.38) for $m = 1$.

3.3.5 GTR Fading

The ABER for SFBC-OFDM system using exponential bound in GTR fading can be derived using (2.14) in (3.36) as

$$ABER \approx 0.2\left(\frac{1+K}{1+K-\xi\overline{\gamma}_t}\exp\left(\frac{K\xi\overline{\gamma}_t}{1+K-\xi\overline{\gamma}_t}\right)I_0\left(\frac{K\xi\overline{\gamma}_t\Delta}{1+K-\xi\overline{\gamma}_t}\right)\right)^{T_xR_x}. \tag{3.42}$$

The results of Rayleigh and Rician fading can be verified by using $K = 0$, $\Delta = 0$ and $K > 0$, $\Delta = 0$ respectively.

3.3.6 Beckmann Fading

Using (2.10) in (3.36), the ABER for SFBC-OFDM system using exponential bound in Beckmann fading can be derived as

$$\begin{aligned}ABER \approx 0.2\Bigg[&\frac{(1+q^2)}{\sqrt{((1+q^2)(1+K)-2q^2\overline{\gamma}_t\xi)}}\times\frac{(1+K)}{\sqrt{((1+q^2)(1+K)-2\overline{\gamma}_t\xi)}}\times\\ &\exp\left(\frac{K(\frac{r^2}{1+r^2})(1+q^2)\overline{\gamma}_t\xi}{(1+q^2)(1+K)-2q^2\overline{\gamma}_t\xi}+\frac{K(\frac{1}{1+r^2})(1+q^2)\overline{\gamma}_t\xi}{(1+q^2)(1+K)-2\overline{\gamma}_t\xi}\right)\Bigg]^{T_xR_x}.\end{aligned} \tag{3.43}$$

Results of (3.38) and (3.39) can be verified from (3.43) using appropriate values of K, q and r. The Beckmann model includes many fading channels as its special cases like Rayleigh ($r^2 = 1$, $q^2 = 1$, $K = 0$), Rician ($r^2 = 1$, $q^2 = 1$, $K \neq 0$) and Hoyt ($r^2 = 1$, $q^2 \neq 1$, $K = 0$).

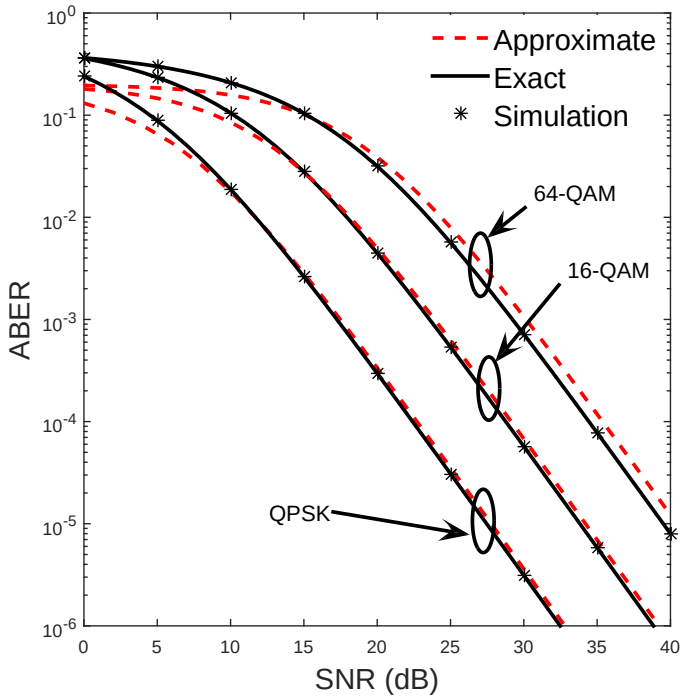

Figure 3.5: ABER results using exact and exponential bound (approximate) for SFBC-OFDM with $T_x = 2$, $R_x = 1$, and $C_R = 1$ under Rayleigh fading.

3.3.7 Generalized-K (K_G) Fading

Using the MGF of Generalized-K (K_G) fading from (2.12) in (3.36), the ABER for SFBC-OFDM system using exponential bound can be derived as

$$ABER \approx 0.2 \left[\left(\frac{\Xi}{\xi} \right)^{\frac{\widehat{\beta}}{2}} \exp\left(\frac{\Xi}{2\xi} \right) W_{-\frac{\widehat{\beta}}{2},-\frac{\widehat{\alpha}}{2}} \left(\frac{\Xi}{\xi} \right) \right]^{T_x R_x}. \tag{3.44}$$

Nakagam-m and K-distribution can be generated as a special case of generalized-K fading by using $K \to \infty$ and $m = 1$ respectively. On the other hand, for $m \to \infty$ and $K \to \infty$, it approaches the AWGN channel.

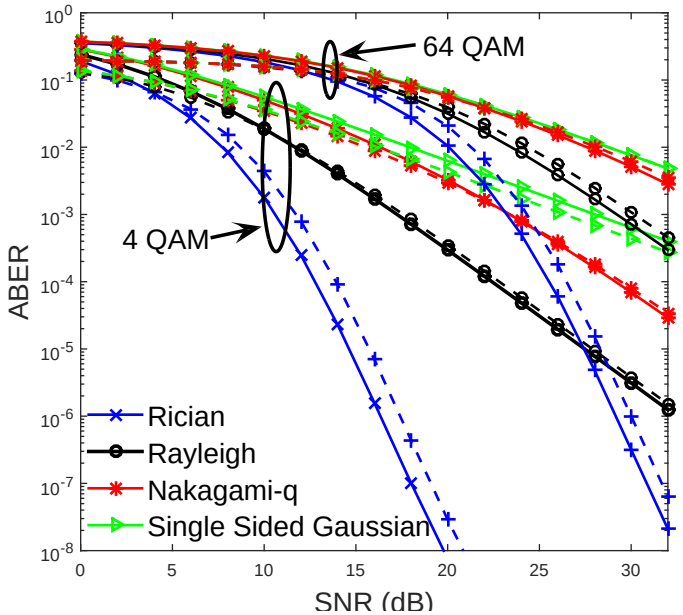

Figure 3.6: ABER results for 4-QAM and 64-QAM-SFBC-OFDM with $T_x = 2$, $R_x = 1$, and $C_R = 1$ under Beckmann fading. Rayleigh ($q = 1$, $K = 0$, $r = 1$), Rician ($q = 1$, $K = 10$, $r = 1$), Nakagami- q ($q = 10$, $K = 0$, $r = 1$), and single-sided Gaussian ($q = 0$, $K = 0$, $r = 1$) are special cases of Beckmann fading.

3.3.8 $\eta - \lambda - \mu$ Fading

Using the MGF from (2.15) in (3.36), the ABER for SFBC-OFDM system in η-λ-μ fading using exponential bound can be derived as

$$ABER \approx 0.2 \left(\frac{4\eta(1-\lambda)^2 \tilde{b}^2}{(\tilde{c} + \xi\overline{\gamma}_t)^2 - \tilde{d}^2} \right)^{T_x R_x}. \tag{3.45}$$

The ABER for η-μ fading channel can be generated as a special case of (3.45) for $\lambda \to 0$ and $\mu = \mu'$. Also, the results of λ-μ and Hyot fading can be verified by setting $\eta \to 1$, $\mu = \mu'$ and $\lambda \to 0$, $\mu = 1/2$ respectively.

3.3.9 Beaulieu-Xie Fading

The generalized MGF for Beaulieu-Xie fading was recently derived by Singh and Joshi in [111]. The ABER of SFBC-OFDM system using exponential bound under Beaulieu-Xie

fading can be derived using (2.17) with n=0 in (3.36) as

$$ABER \approx 0.2 \left(\left(\frac{m}{\overline{\gamma}_t} \right)^m \exp\left(-\frac{\lambda^2}{2} \right) \left(\frac{m}{\overline{\gamma}_t} - \xi \right)^{-m} \Gamma[m+n]_1 F_{1R} \left[m, m, \frac{m\lambda^2}{2(m-\xi\overline{\gamma}_t)} \right] \right)^{T_x R_x}. \tag{3.46}$$

In the comparison of ABER of Beaulieu-Xie fading with Nakagami- m fading, it is observed that for equivalent fading conditions, the performance of former is better. This is because of the presence of LOS channel in Beaulieu-Xie fading which has better performance than NLOS channel if the power at the receiver is kept constant [111]. By setting $m = 1$, the results of Rician distribution can be verified from (3.46).

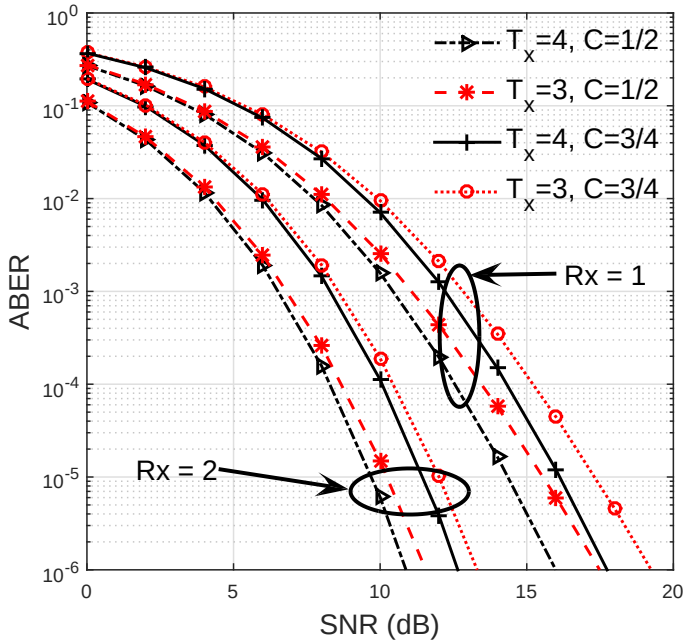

Figure 3.7: ABER curves of MPSK-SFBC-OFDM with $M = 2$, $T_x = 3$, 4; $R_x = 1$, 2; $C_R = 1/2$, 3/4; $m = 2$ and $\lambda = 1$ under Beaulieu-Xie fading model.

3.4 Results and Discussion

The ABER expressions (3.31) and (3.36) derived in this chapter are numerically evaluated to calculate the performance of SFBC-OFDM system. Along with this, Monte-Carlo simulations are given for the verification purpose. It can be visualized from (3.31) and (3.36) that the ABER of SFBC-OFDM system depends on SFBC parameters like T_x, R_x, normalized instantaneous SNR of SFBC-OFDM system, code rate and fading channel

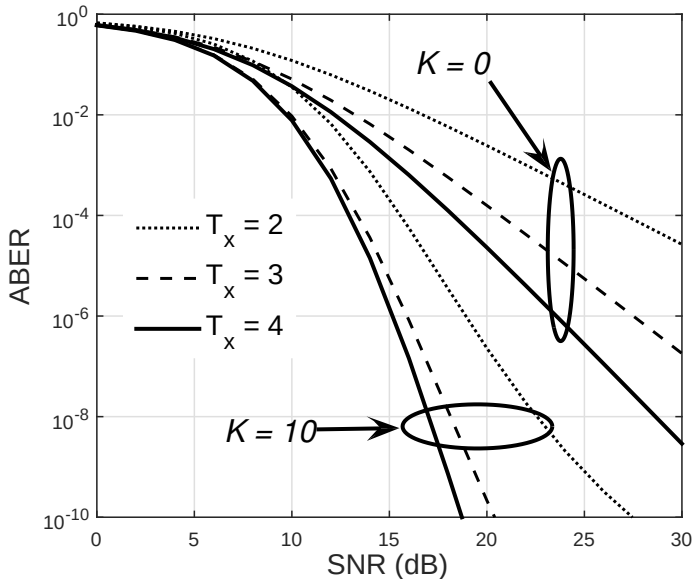

Figure 3.8: ABER v/s SNR for 8-PSK-SFBC-OFDM system for $K = 0$, 10, $\Delta = 0$, $T_x = 2$, 3, 4 and $R_x = 1$ under GTR fading.

parameters of a particular channel. Therefore, results are shown for different fading channels, and system parameters.

For simulation of system, the value of $N = 512$ is taken along with the cyclic prefix of $N/4$. A 4 tap fading channel is assumed in this analysis. The numerical results obtained using exponential bound (3.36) are referred to as Approximate results and are shown using dotted lines, whereas the exact results obtained from (3.31) are shown with solid lines.

Figure 3.5 shows the results using exact analysis and exponential bound for a 2 transmitter 1 receiver SFBC-OFDM system with code rate unity (code G2). ABER curves are for M=4, 16, 64 and the difference between the exact and approximate results are 0.0321, 0.0851, and 0.1091 respectively for a constant SNR = 5 dB. These values are calculated by using the relation $|ABER_{exact} - ABER|$. It can also be visualized from Figure 3.5 that this difference in ABER reduces to 1.0763×10^{-4}, 0.0016, and 0.0115 at SNR = 20 dB. This difference in results is due to the exactness of our derived results as compared to the similar approximate results for Rayleigh fading in the work of Torabi et al [96].

The ABER performance under Beckmann fading is observed in Figure 3.6 for 4-QAM and 64-QAM modulated SFBC-OFDM system with $T_x = 2$, $R_x = 1$, and $C_R = 1$. Results are plotted for Rayleigh ($q = 1$, $K = 0$, $r = 1$), single-sided Gaussian ($q = 0$, $K = 0$, $r = 1$), Rician ($q = 1$, $K = 10$, $r = 1$) and Nakagami- q ($q = 10$, $K = 0$, $r = 1$) as special case. The effect of change in modulation order is also observed from Figure 3.6 as the ABER

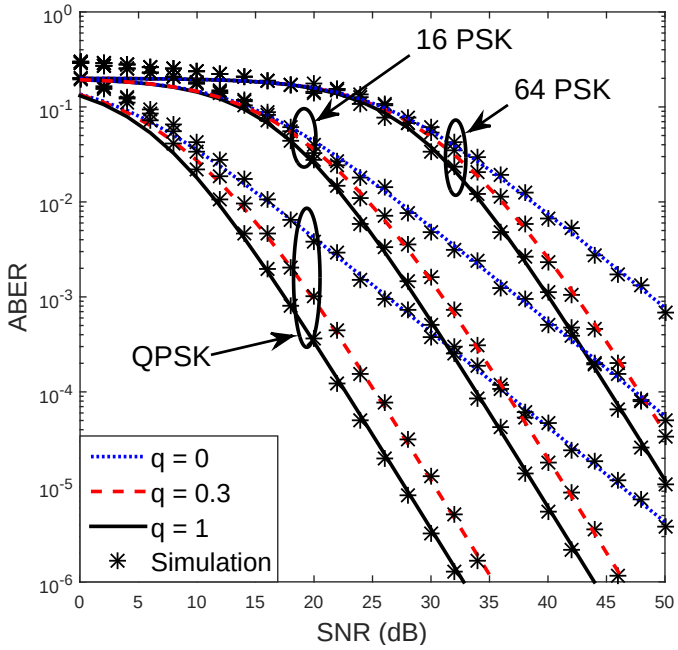

Figure 3.9: ABER vs SNR plot of MPSK-SFBC-OFDM with 2 transmitter and one receiver antennas in Nakagami-q channel with different values of q.

performance of 4-QAM is better than 64-QAM under similar fading conditions.

Fig. 3.7 shows the ABER vs. SNR plots for MPSK-SFBC-OFDM system with $M = 2$, $T_x = 3$, 4; $R_x = 1$, 2; $C_R = 1/2$, 3/4; under Beaulieu-Xie fading model with parameters $m = 2$ and $\lambda = 1$. Code rate $C_R = 1/2$ is achieved by using $G3$ and $G4$ codes and $C_R = 3/4$ is attained by $H3$ and $H4$ codes. These codes are explained in great detail in a book by Hamid Jafarkhani [27]. It is evident from Fig. 3.7 that for a given transmit-receive antenna pair, the ABER performance degrades with increase in C_R as expected. For example, at SNR = 10 dB, the ABER increases from 1.579×10^{-3} to 7.078×10^{-3} for a SFBC-OFDM system employing $T_x = 4$, $R_x = 1$ as C_R changes from 1/2 to 3/4. Another interesting observation is that with the increase in T_x, the ABER performance improves due to the increase in diversity order of system. Similar trend can be visualized when R_x is increased from 1 to 2.

The effect of increasing transmitting antennas is shown in Fig. 3.8 with the plot of ABER v/s SNR for 8-PSK-SFBC-OFDM system for $K = 0$, 10, $\Delta = 0$, $T_x = 2$, 3, 4 and $R_x = 1$ under GTR fading. It is evident that for constant R_x and channel parameters, the ABER performance improves when T_x is increased. The reason behind this is that the probability of all fading channels going to deep fade at the same time decreases with an increase in T_x. Another interesting observation is that with the change in the value of

K, the ABER performance improves in the same fashion for every set of transmit-receive antenna pairs.

Fig. 3.9 shows the ABER results for MPSK-SFBC-OFDM system with $T_x = 2$, $R_x = 1$ (code G2 [27]) for various values of Nakagami parameter q. With $q = 1$, the results for Rayleigh fading can be verified from Nakagami-q fading as reported in [96, 110]. The ABER performance degrades as q decreases to 0 which corresponds to one sided Gaussian case. The effect of varying modulation order ($M = 4$, 16, 64) is also observed from Fig. 3.9. As expected, the ABER performance degrades as M increases.

The ABER vs SNR results for different fading channel are shown in Figures 3.5 to 3.9. Apart from the effect of channel parameters, the effect of varying transmitting antennas, modulation technique (MPSK and MQAM), modulation order and code rate is also shown in the results. As the number of transmitting antenna increase, there is a significant improvement in the performance os system which is due to the increase in diversity order. With higher values of T_x, the probability that the system goes into deep fading is also reduced. With the change in modulation order, the ABER of SFBC-OFDM system changes as expected. It is also observed that as M increases, the ABER performance degrades.

3.5 Summary

The performance of SFBC-OFDM system under generalized fading scenario has been explored in this chapter for MPSK and MQAM modulations. Both exact as well as approximate ABER expressions are derived. The derived analytical expressions have been numerically evaluated and crosschecked with Monte-Carlo simulations.

Chapter 4

Bit Error Rate Analysis of STBC-OFDM Systems

In recent years, the STBC based OFDM systems have received considerable attention both in academics and research due to its several advantageous features. Several STBC techniques have been reported in the literature to implement the MIMO-OFDM system for exploiting both the spatial and temporal diversities. It is evident from the literature review that the STBC-OFDM system is more suited for highly frequency selective scenario, however, its performance degrades in high mobility conditions [85].

The exact expressions of error rate for STBC-OFDM system are derived in this chapter. The generalized fading channels are assumed in this analysis for supporting the proposed framework of MIMO-OFDM system. Illustrations of the derived expression for some popular fading channels are given. The remainder of this chapter is organized as: Section 4.1 presents the system model of STBC-OFDM system. The exact expressions of ABER performance for STBC-OFDM system are derived in Section 4.2. Section 4.3 illustrates the ABER expressions for different fading channels. In Section 4.4, the numerical results of the derived expressions along with the Monte-Carlo simulations are given. Section 4.5 gives the chapter summary.

4.1 STBC-OFDM System Model

Consider an STBC-OFDM system as shown in Fig. 4.1. The STBC encoder generates orthogonal symbols using the coding matrix $\mathbb{G}$ similar to SFBC encoder discussed in Section 3.1. These symbols are complex conjugate combinations of the modulated symbols. Same subcarriers are used to transmit the symbols of orthogonal design on subsequent OFDM symbols. Due to this reason, STBC is a more suitable candidate in order to survive the frequency selective fading scenario when it is compared with SFBC systems. But its performance degrades if there are fast channel variations in time. It is because STBC assumes that the channel does not change during one STBC matrix [72].

Like SFBC-OFDM, let us take the simple case of two transmit antennas and an OFDM

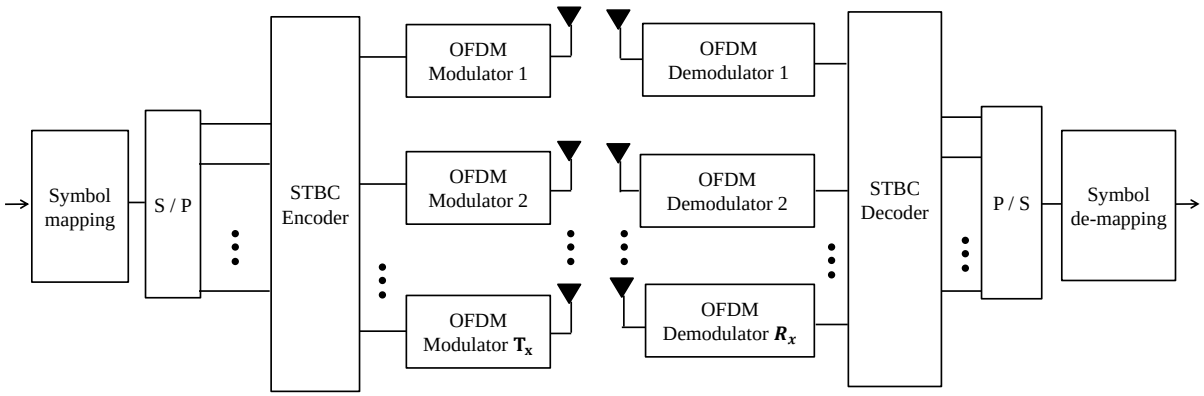

Figure 4.1: STBC-OFDM system model [106].

system with four subcarriers. The symbols $\{x_0, x_1, x_2, x_3\}$ are taken as input to STBC encoder. Again, Alamouti's scheme is applied to generate orthogonal symbols for first and second transmit antennas as [27]

$$\boldsymbol{x}_1 = \{x_0, -x_1^*, x_2, -x_3^*\}, \tag{4.1}$$

and

$$\boldsymbol{x}_2 = \{x_1, x_0^*, x_3, x_2^*\}. \tag{4.2}$$

respectively. These two data streams are fed to two individual OFDM modulators after applying serial to parallel conversion as shown in Fig. 4.2. The signals from first and second antennas are transmitted through two IID l tap fading channels h_1 and h_2, respectively. Here, the matrices are represented by uppercase boldface letters, and lowercase boldface is used for vectors, whereas scalars are shown with un-boldface letters. For single receiving antenna case, the received signal for the first time instant is given as [27]

$$\begin{bmatrix} y_{11} \\ y_{12} \end{bmatrix} = h_1 \begin{bmatrix} x_0 \\ x_2 \end{bmatrix} + h_2 \begin{bmatrix} x_1 \\ x_3 \end{bmatrix}. \tag{4.3}$$

An interesting observation here is that unlike SFBC-OFDM, it is not possible to decode the first two symbols x_0 and x_1 using only the data from first time instant. It is because the received data contains all the four data symbols x_0, x_1, x_2 and x_3. In order to decode

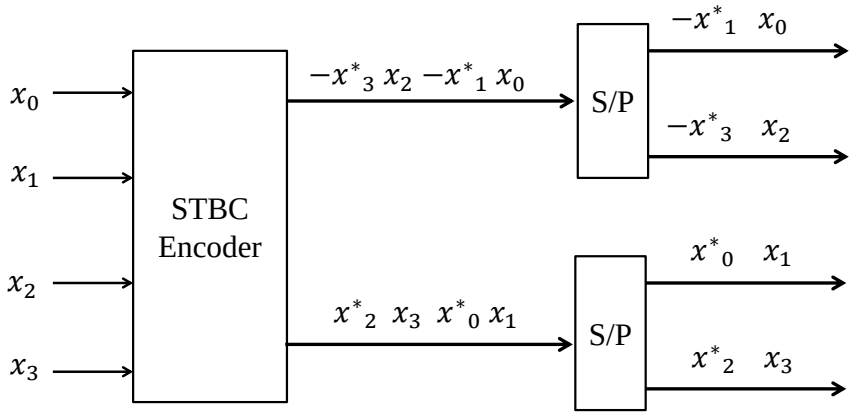

Figure 4.2: STBC encoder for $T_x = 2$, $N = 2$.

all the four data symbols simultaneously, it is required to get the data from the second time instant. This means that there is a fundamental time delay of T_x instants in case of STBC-OFDM which was absent in the case of SFBC-OFDM.

At the second time instant, the received signal can be represented as

$$\begin{bmatrix} y_{21} \\ y_{22} \end{bmatrix} = h_1 \begin{bmatrix} -x_1^* \\ -x_3^* \end{bmatrix} + h_2 \begin{bmatrix} x_0^* \\ x_2^* \end{bmatrix}. \tag{4.4}$$

To decode the signals transmitted from the two antennas, the matrices obtained in (4.3) and (4.4) are multiplied with hermitian of channel matrix (**H**) which is defined as [27]

$$\mathbf{H} = \begin{bmatrix} h_1 & h_2^* \\ h_2 & -h_1^* \end{bmatrix}. \tag{4.5}$$

4.2 Error Rate Analysis of STBC-OFDM Systems over Fading Channel

A STBC-OFDM system with T_x transmitting and a single receiving antenna is assumed in this analysis. At the receiver, the resultant received signal vector after cyclic prefix

removal and FFT can be represented as [106]

$$\mathbf{y} = \sum_{i=1}^{T_x} \mathbf{h}_{i,1}\mathbf{x}_i + \mathbf{z}, \tag{4.6}$$

where $\mathbf{h}_{i,1}$ is a vector composed of DFT of independent fading channel response from the i^{th} transmit antenna and $\mathbf{z}$ is AWGN. In order to calculate the average error rate for any communication system, the conditional error rate is to be averaged across the fading channel PDF. This conditional error rate is equivalent to the performance over AWGN channel where the transmitted signal is only affected by AWGN and does not undergo fading [6].

Let us consider a M-QAM modulated STBC-OFDM system. The conditional bit error rate of this MQAM-STBC-OFDM system is given by [151]

$$\begin{aligned} p_{e|\alpha} = {} & 2A_I Q\left(\sqrt{\frac{\left(\sum_{i=1}^{T_x}\alpha_i^2\right)d_I^2}{\sigma_z^2}}\right) + 2A_Q Q\left(\sqrt{\frac{\left(\sum_{i=1}^{T_x}\alpha_i^2\right)d_Q^2}{\sigma_z^2}}\right) \\ & - 4A_I A_Q Q\left(\sqrt{\frac{\left(\sum_{i=1}^{T_x}\alpha_i^2\right)d_I^2}{\sigma_z^2}}\right) Q\left(\sqrt{\frac{\left(\sum_{i=1}^{T_x}\alpha_i^2\right)d_Q^2}{\sigma_z^2}}\right), \end{aligned} \tag{4.7}$$

where $A_I = \left(1 - \frac{1}{M_I}\right)$, $A_Q = \left(1 - \frac{1}{M_Q}\right)$; d_Q and d_I are the quadrature-phase and in-phase decision distances, α_i is the magnitude of the channel $H_{i,1}$, $M = M_I \times M_Q$. Subsequently, the unconditional probability of error which is the ABER is derived as [109]

$$ABER = \int_0^\infty \int_0^\infty \cdots \int_0^\infty P_{e|\alpha}\ p(\alpha_1)p(\alpha_2)\cdots p(\alpha_{T_x})d(\alpha_1)d(\alpha_2)\cdots d(\alpha_{T_x}), \tag{4.8}$$

where $p(\alpha_i)$ is the PDF of α_i.

Now, substituting (4.7) in (4.8) the ABER can be further simplified and expressed as a sum of three terms F_1, F_2 and F_3. Now, F_1 is defined as

$$\begin{aligned} F_1 = {} & \int_0^\infty \int_0^\infty \cdots \int_0^\infty 2A_I Q\left(\sqrt{\frac{\left(\sum_{i=1}^{T_x}\alpha_i^2\right)d_I^2}{\sigma_z^2}}\right) \times \\ & p(\alpha_1)p(\alpha_2)\cdots p(\alpha_{T_x})d(\alpha_1)d(\alpha_2)\cdots d(\alpha_{T_x}), \end{aligned} \tag{4.9}$$

Further, (4.9) can be simplified using the identity [64, (4.2)] as

$$F_1 = \int_0^{\infty}\int_0^{\infty}\cdots\int_0^{\infty}\int_0^{\frac{\pi}{2}} \frac{2}{\pi} A_I \exp\left(\frac{-\left(\sum_{i=1}^{T_x}\alpha_i^2\right) d_I^2}{2\sigma_z^2 \sin^2\theta}\right) d\theta \times$$
$$p(\alpha_1)p(\alpha_2)\cdots p(\alpha_{T_x})d(\alpha_1)d(\alpha_2)\cdots d(\alpha_{T_x}). \tag{4.10}$$

As $\alpha_1, \alpha_2 \cdots \alpha_{T_x}$ are assumed to be IID, (4.10) can further be simplified into

$$F_1 = \int_0^{\frac{\pi}{2}} \frac{2}{\pi} A_I \int_0^{\infty} \exp\left(\frac{-\left(\alpha_1^2\right) d_I^2}{2\sigma_z^2 \sin^2\theta}\right) p(\alpha_1)d(\alpha_1) \times$$
$$\int_0^{\infty} \exp\left(\frac{-\left(\alpha_2^2\right) d_I^2}{2\sigma_z^2 \sin^2\theta}\right) p(\alpha_2)d(\alpha_2)\cdots \times$$
$$\int_0^{\infty} \exp\left(\frac{-\left(\alpha_{T_x}^2\right) d_I^2}{2\sigma_z^2 \sin^2\theta}\right) p(\alpha_{T_x})d(\alpha_{T_x})d\theta. \tag{4.11}$$

By using the definition of MGF, (4.11) becomes

$$F_1 = \int_0^{\frac{\pi}{2}} \frac{2}{\pi} A_I \mathbb{M}\left(\frac{-d_I^2}{2\sigma_z^2 \sin^2\theta}\right) \mathbb{M}\left(\frac{-d_I^2}{2\sigma_z^2 \sin^2\theta}\right) \cdots \mathbb{M}\left(\frac{-d_I^2}{2\sigma_z^2 \sin^2\theta}\right). \tag{4.12}$$

After some algebraic manipulations, (4.12) becomes

$$F_1 = \int_0^{\frac{\pi}{2}} \frac{2}{\pi} A_I \left[\mathbb{M}\left(\frac{-d_I^2}{2\sigma_z^2 \sin^2\theta}\right)\right]^{T_x} d\theta. \tag{4.13}$$

Similarly, the expression for F_2 can be calculated as

$$F_2 = \int_0^{\frac{\pi}{2}} \frac{2}{\pi} A_Q \left[\mathbb{M}\left(\frac{-d_Q^2}{2\sigma_z^2 \sin^2\theta}\right)\right]^{T_x} d\theta. \tag{4.14}$$

Now, F_3 can be represented as

$$F_3 = \int_0^{\infty}\int_0^{\infty}\cdots\int_0^{\infty} 4A_I A_Q Q\left(\sqrt{\frac{\left(\sum_{i=1}^{T_x}\alpha_i^2\right) d_I^2}{\sigma_z^2}}\right) Q\left(\sqrt{\frac{\left(\sum_{i=1}^{T_x}\alpha_i^2\right) d_Q^2}{\sigma_z^2}}\right) \times$$
$$p(\alpha_1)p(\alpha_2)\cdots p(\alpha_{T_x})d(\alpha_1)d(\alpha_2)\cdots d(\alpha_{T_x}). \tag{4.15}$$

Using [64, (4.8)], (4.15) can be simplified as

$$\begin{aligned}F_3 =&4A_IA_Q\int_0^{\frac{\pi}{2}-\tan^{-1}\left(\frac{d_I^2}{d_Q^2}\right)}\int_0^{\infty}\int_0^{\infty}\cdots\int_0^{\infty}\exp\left(\frac{-\left(\sum_{i=1}^{T_x}\alpha_i^2\right)d_I^2}{2\sigma_z^2\sin^2\theta}\right)\times\\ &p(\alpha_1)p(\alpha_2)\cdots p(\alpha_{T_x})d(\alpha_1)d(\alpha_2)\cdots d(\alpha_{T_x})d\theta\times\\ &+4A_IA_Q\int_0^{\tan^{-1}\left(\frac{d_I^2}{d_Q^2}\right)}\int_0^{\infty}\int_0^{\infty}\cdots\int_0^{\infty}\exp\left(\frac{-\left(\sum_{i=1}^{T_x}\alpha_i^2\right)d_Q^2}{2\sigma_z^2\sin^2\theta}\right)\times\\ &p(\alpha_1)p(\alpha_2)\cdots p(\alpha_{T_x})d(\alpha_1)d(\alpha_2)\cdots d(\alpha_{T_x})d\theta. \end{aligned}\tag{4.16}$$

Equation (4.16) can be further simplified using the definition of MGF as

$$\begin{aligned}F_3 =&\frac{2}{\pi}A_IA_Q\int_0^{\frac{\pi}{2}-\tan^{-1}\left(\frac{d_I^2}{d_Q^2}\right)}\left[\mathbb{M}\left(\frac{-d_I^2}{2\sigma_z^2\sin^2\theta}\right)\right]^{T_x}d\theta\times\\ &+\frac{2}{\pi}A_IA_Q\int_0^{\tan^{-1}\left(\frac{d_I^2}{d_Q^2}\right)}\left[\mathbb{M}\left(\frac{-d_Q^2}{2\sigma_z^2\sin^2\theta}\right)\right]^{T_x}d\theta. \end{aligned}\tag{4.17}$$

The final expression of ABER can be written by using (4.13), (4.14) and (4.17) as

$$\begin{aligned}ABER_{exact} =&\frac{2}{\pi}\Bigg\{\int_0^{\frac{\pi}{2}}\Bigg(A_I\left[\mathbb{M}\left(\frac{-d_I^2}{2\sigma_z^2\sin^2\theta}\right)\right]^{T_x}\\ &+A_Q\left[\mathbb{M}\left(\frac{-d_Q^2}{2\sigma_z^2\sin^2\theta}\right)\right]^{T_x}\Bigg)d\theta\\ &-\int_0^{\frac{\pi}{2}-\tan^{-1}\left(\frac{d_I^2}{d_Q^2}\right)}A_IA_Q\left[\mathbb{M}\left(\frac{-d_I^2}{2\sigma_z^2\sin^2\theta}\right)\right]^{T_x}d\theta\\ &-\int_0^{\tan^{-1}\left(\frac{d_I^2}{d_Q^2}\right)}A_IA_Q\left[\mathbb{M}\left(\frac{-d_Q^2}{2\sigma_z^2\sin^2\theta}\right)\right]^{T_x}d\theta\Bigg\}. \end{aligned}\tag{4.18}$$

Now, we can generate several special cases from the derived expression. The BER of rectangular QAM valid for equal in-phase and quadrature phase decision distances can be calculated with the substitution $d_Q = d_I = d$ and using the relation between distance and energy for MQAM as $\frac{d^2}{\sigma_z^2} = \frac{6}{M_IM_Q-1}$, as

$$\begin{aligned}ABER_{exact} =&\frac{2}{\pi}\left[A_I+A_Q\right]\int_0^{\frac{\pi}{2}}\left[\mathbb{M}\left(\frac{-3}{(M_IM_Q-1)\sin^2\theta}\right)\right]^{T_x}d\theta\\ &-\frac{2}{\pi}\left[A_IA_Q\right]\int_0^{\frac{\pi}{4}}\left[\mathbb{M}\left(\frac{-3}{(M_IM_Q-1)\sin^2\theta}\right)\right]^{T_x}d\theta. \end{aligned}\tag{4.19}$$

For M-ary square QAM (SQAM), the ABER is calculated from (4.19) by substituting $M_I = M_Q = \sqrt{M}$ and $d_Q = d_I = d$.

$$\begin{aligned} ABER_{exact} =& \frac{4}{\pi}\left(1-\frac{1}{\sqrt{M}}\right)\int_0^{\frac{\pi}{2}}\left[\mathbb{M}\left(\frac{-3}{(M^2-1)\sin^2\theta}\right)\right]^{T_x} d\theta \\ & -\frac{2}{\pi}\left(1-\frac{1}{\sqrt{M}}\right)^2\int_0^{\frac{\pi}{4}}\left[\mathbb{M}\left(\frac{-3}{(M^2-1)\sin^2\theta}\right)\right]^{T_x} d\theta. \end{aligned} \tag{4.20}$$

4.3 Illustration of Derived ABER for Different Fading Channels

In the following subsections, the ABER expressions of STBC-OFDM system are derived for different fading channels. It is important to mention here that our analysis is not limited to these fading channels only and can be readily applied to any given case.

4.3.1 Rayleigh Fading

The ABER of RQAM-STBC-OFDM under Rayleigh fading can be calculated by using the MGF from (2.3) in (4.19) as

$$ABER_{exact} = \alpha_{stbc1}\int_0^{\frac{\pi}{2}}\left(1-\beta_{stbc1}(\theta)\overline{\gamma}_t\right)^{-T_x} d\theta - \alpha_{stbc2}\int_0^{\frac{\pi}{4}}\left(1-\beta_{stbc1}(\theta)\overline{\gamma}_t\right)^{-T_x} d\theta, \tag{4.21}$$

where $\alpha_{stbc1} = \frac{2}{\pi}\left[A_I + A_Q\right]$, $\alpha_{stbc2} = \frac{2}{\pi}\left[A_I A_Q\right]$ and $\beta_{stbc1}(\theta) = \left(\frac{-3}{\left(M_I M_Q - 1\right)\sin^2\theta}\right)$. Similarly, for SQAM, the ABER under Rayleigh fading can be calculated by using (2.3) in (4.20) as

$$\begin{aligned} ABER_{exact} =& \frac{4}{\pi}\left(1-\frac{1}{\sqrt{M}}\right)\int_0^{\frac{\pi}{2}}\left(1+\frac{3\bar{\gamma}_T}{(M^2-1)\sin^2\theta}\right)^{-T_x} d\theta \\ & -\frac{2}{\pi}\left(1-\frac{1}{\sqrt{M}}\right)^2\int_0^{\frac{\pi}{4}}\left(1+\frac{3\bar{\gamma}_T}{(M^2-1)\sin^2\theta}\right)^{-T_x} d\theta. \end{aligned} \tag{4.22}$$

The ABER expression in (4.22) can written as a difference of two integrals as

$$ABER_{exact} = I_1 - I_2, \tag{4.23}$$

where

$$I_1 = \frac{4}{\pi}\left(1 - \frac{1}{\sqrt{M}}\right)\int_0^{\frac{\pi}{2}} \left(1 + \frac{3\bar{\gamma}_T}{(M^2-1)\sin^2\theta}\right)^{-T_x} d\theta, \tag{4.24}$$

and

$$I_2 = \frac{2}{\pi}\left(1 - \frac{1}{\sqrt{M}}\right)^2\int_0^{\frac{\pi}{4}} \left(1 + \frac{3\bar{\gamma}_T}{(M^2-1)\sin^2\theta}\right)^{-T_x} d\theta. \tag{4.25}$$

After some algebraic manipulations, (4.24) can be rewritten as

$$I_1 = \frac{4}{\pi}\left(1 - \frac{1}{\sqrt{M}}\right)\int_0^{\frac{\pi}{2}} \left[\left(\frac{\sin^2\theta}{\frac{3\bar{\gamma}_T}{(M^2-1)} + \sin^2\theta}\right)\right]^{T_x} d\theta. \tag{4.26}$$

The closed form expression for I_1 is calculated by making its equivalence with another definite integral given in literature.

Using [152, App. (A8)], the closed form expression of (4.26) can be calculated as

$$I_1 = 2\left(1 - \frac{1}{\sqrt{M}}\right)\left[1 - \mu(A)\sum_{k=0}^{T_x-1}\binom{2k}{k}\left(\frac{1-\mu^2(A)}{4}\right)^k\right], \tag{4.27}$$

where $\mu(A) = \sqrt{\frac{A}{1+A}}$ with $A = \frac{3\bar{\gamma}_T}{(M^2-1)}$.

The integral in (4.25) can be solved by using [153, (18)] as

$$\begin{aligned} I_2 =& \frac{1}{2}\left(1 - \frac{1}{\sqrt{M}}\right)^2 - \frac{2}{\pi}\left(1 - \frac{1}{\sqrt{M}}\right)^2\sqrt{\frac{A}{1+A}}\Bigg[\left(\frac{\pi}{2} - \tan^{-1}\sqrt{\frac{A}{1+A}}\right)\times \\ & \sum_{k=0}^{T_x-1}\binom{2k}{k}\frac{1}{(4(1+A))^k} - \sin(\tan^{-1}\sqrt{\frac{A}{1+A}})\sum_{k=1}^{T_x-1}\sum_{i=1}^{k}\frac{T_{ik}}{(1+A)^k}\times \\ & \left(\cos(\tan^{-1}\sqrt{\frac{A}{1+A}})\right)^{2(k-i)+1}\Bigg], \end{aligned} \tag{4.28}$$

where $\binom{\cdot}{\cdot}$ represents the binomial expansion and $T_{i,k} = \frac{\binom{2k}{k}}{\binom{2(k-i)}{k-i}4^i(2(k-i)+1)}$.

Finally, substituting (4.27) and (4.28) into (4.23) gives the exact closed form expression

of ABER for STBC-OFDM system under Rayleigh fading channel as

$$\begin{aligned} ABER_{exact} =& 2\left(1-\frac{1}{\sqrt{M}}\right)\left[1-\mu(A)\sum_{k=0}^{T_x-1}\binom{2k}{k}\left(\frac{1-\mu^2(A)}{4}\right)^k\right] \\ & -\frac{1}{2}\left(1-\frac{1}{\sqrt{M}}\right)^2+\frac{2}{\pi}\left(1-\frac{1}{\sqrt{M}}\right)^2\sqrt{\frac{A}{1+A}}\Bigg[\left(\frac{\pi}{2}-\tan^{-1}\sqrt{\frac{A}{1+A}}\right)\times \\ & \sum_{k=0}^{T_x-1}\binom{2k}{k}\frac{1}{(4(1+A))^k}-\sin\left(\tan^{-1}\sqrt{\frac{A}{1+A}}\right)\times \\ & \sum_{k=1}^{T_x-1}\sum_{i=1}^{k}\frac{T_{ik}}{(1+A)^k}\left(\cos\left(\tan^{-1}\sqrt{\frac{A}{1+A}}\right)\right)^{2(k-i)+1}\Bigg]. \end{aligned} \tag{4.29}$$

The results presented in [154] can be obtained as a special case of (4.29) by substituting T_x =2.

4.3.2 Nakagami-q Fading

The ABER for RQAM-STBC-OFDM system under Nakagami-q fading is derived using (2.5) in (4.19) as

$$\begin{aligned} ABER_{exact} =& \alpha_{stbc1}\int_0^{\frac{\pi}{2}}\left(\left(1-2\beta_{stbc1}\bar{\gamma}+\frac{(2\beta_{stbc1}\bar{\gamma})^2q^2}{(1+q^2)^2}\right)\right)^{-T_x/2}d\theta \\ & -\alpha_{stbc2}\int_0^{\frac{\pi}{4}}\left(\left(1-2\beta_{stbc1}\bar{\gamma}+\frac{(2\beta_{stbc1}\bar{\gamma})^2q^2}{(1+q^2)^2}\right)\right)^{-T_x/2}d\theta, \end{aligned} \tag{4.30}$$

The ABER for SQAM-STBC-OFDM under Nakagami-q fading can be calculated by using (2.5) in (4.20) as

$$\begin{aligned} ABER_{exact} =& \frac{4}{\pi}\alpha_{stbc3}\int_0^{\frac{\pi}{2}}\left(\left(1-2\beta_{stbc1}\bar{\gamma}+\frac{(2\beta_{stbc2}\bar{\gamma})^2q^2}{(1+q^2)^2}\right)\right)^{-T_x/2}d\theta \\ & -\frac{2}{\pi}\left(\alpha_{stbc3}\right)^2\int_0^{\frac{\pi}{4}}\left(\left(1-2\beta_{stbc1}\bar{\gamma}+\frac{(2\beta_{stbc2}\bar{\gamma})^2q^2}{(1+q^2)^2}\right)\right)^{-T_x/2}d\theta. \end{aligned} \tag{4.31}$$

The ABER results of Rayleigh fading can be verified from (4.30) and (4.31) if we let q = 1. Further, the results of one-sided Gaussian fading can be verified for (4.30) and (4.31) by substituting q = 0.

4.3.3 Nakagami-n (Rice) Fading

The ABER for RQAM-STBC-OFDM in Nakagami-n fading can be derived by using (2.7) in (4.19) as

$$\begin{aligned} ABER_{exact} =& \alpha_{stbc1} \int_0^{\frac{\pi}{2}} \left(\frac{(1+n^2)}{(1+n^2)-\beta_{stbc1}\overline{\gamma}_t} \exp\left(\frac{n^2\beta_{stbc1}\overline{\gamma}_t}{(1+n^2)-\beta_{stbc1}\overline{\gamma}_t} \right) \right)^{T_x} d\theta \\ & - \alpha_{stbc2} \int_0^{\frac{\pi}{4}} \left(\frac{(1+n^2)}{(1+n^2)-\beta_{stbc1}\overline{\gamma}_t} \exp\left(\frac{n^2\beta_{stbc1}\overline{\gamma}_t}{(1+n^2)-\beta_{stbc1}\overline{\gamma}_t} \right) \right)^{T_x} d\theta. \end{aligned} \quad (4.32)$$

Now, for SQAM-STBC-OFDM case, the ABER can be calculated by using (2.7) in (4.20) as

$$\begin{aligned} ABER_{exact} =& \frac{4}{\pi}\alpha_{stbc3} \int_0^{\frac{\pi}{2}} \left(\frac{(1+n^2)}{(1+n^2)-\beta_{stbc2}\overline{\gamma}_t} \exp\left(\frac{n^2\beta_{stbc2}\overline{\gamma}_t}{(1+n^2)-\beta_{stbc2}\overline{\gamma}_t} \right) \right)^{T_x} d\theta \\ & - \frac{2}{\pi}\left(\alpha_{stbc3}\right)^2 \int_0^{\frac{\pi}{4}} \left(\frac{(1+n^2)}{(1+n^2)-\beta_{stbc2}\overline{\gamma}_t} \exp\left(\frac{n^2\beta_{stbc2}\overline{\gamma}_t}{(1+n^2)-\beta_{stbc2}\overline{\gamma}_t} \right) \right)^{T_x} d\theta. \end{aligned} \quad (4.33)$$

It can be observed that (4.32) and (4.33) reduces to (4.21) and (4.22) respectively for $n = 0$ and results of Rayleigh fading can be verified.

4.3.4 Nakagami-m Fading

The ABER of a RQAM-STBC-OFDM system under Nakagami-m fading is derived using (2.9) in (4.19) as

$$\begin{aligned} ABER_{exact} =& \alpha_{stbc1} \int_0^{\frac{\pi}{2}} \left(1 - \frac{\beta_{stbc1}\overline{\gamma}_t}{m} \right)^{-mT_x} d\theta \\ & - \alpha_{stbc2} \int_0^{\frac{\pi}{4}} \left(1 - \frac{\beta_{stbc1}\overline{\gamma}_t}{m} \right)^{-mT_x} d\theta. \end{aligned} \quad (4.34)$$

Now, for SQAM-STBC-OFDM case, the ABER can be calculated by using (2.9) in (4.20) as

$$\begin{aligned} ABER_{exact} =& \frac{4}{\pi}\left(1 - \frac{1}{\sqrt{M}}\right) \int_0^{\frac{\pi}{2}} \left(1 + \frac{3\bar{\gamma}_T}{m\left(M^2-1\right)\sin^2\theta} \right)^{-mT_x} d\theta \\ & - \frac{2}{\pi}\left(1 - \frac{1}{\sqrt{M}}\right)^2 \int_0^{\frac{\pi}{4}} \left(1 + \frac{3\bar{\gamma}_T}{m\left(M^2-1\right)\sin^2\theta} \right)^{-mT_x} d\theta. \end{aligned} \quad (4.35)$$

The one sided Gaussian fading is realized from (4.35) by substituting $m = 0.5$. On the other hand, the results of nonfading AWGN are obtained by using $m = \infty$ whereas, it

reduces to (4.22) for $m = 1$.

Now, a closed form expression for Nakagami-m fading can be derived for STBC-OFDM system using the similar approach as used in the case of Rayleigh fading (4.29). The integral I_1 in this case can be derived using (4.35) as

$$I_1 = \frac{4}{\pi}\left(1 - \frac{1}{\sqrt{M}}\right)\int_0^{\frac{\pi}{2}}\left[\left(\frac{\sin^2\theta}{\frac{3\bar{\gamma}_T}{m(M^2-1)} + \sin^2\theta}\right)\right]^{mT_x} d\theta. \tag{4.36}$$

Due to the presence of fading channel parameter m, the term mT_x in this case can take both integer as well as non-integer values. Now, (4.36) can be further simplified by using [152, App. (A8)] as

$$I_1 = \frac{4}{\pi}\left(1 - \frac{1}{\sqrt{M}}\right)\frac{\sqrt{A/\pi}}{2(1+A)^{mT_x+0.5}}\frac{\Gamma(mT_x+0.5)}{\Gamma(mT_x+1)}{}_2F_1\left(1, mT_x+0.5; mT_x+1; \frac{1}{1+A}\right), \tag{4.37}$$

where $\Gamma(\cdot)$ is the Gamma function, $A = \frac{3\bar{\gamma}_T}{m(M^2-1)}$, ${}_2F_1(\cdot,\cdot;\cdot;\cdot)$ represents the Gaussian hypergeometric function. Further, in (4.28), the integral given for I_2, is valid for both the integer as well as non-integer values of mT_x. Therefore, for Nakagami-m fading channel, the exact closed form expression of ABER for MQAM-STBC-OFDM can be calculated by using (4.28) and (4.37) into (4.35) as

$$\begin{aligned} ABER_{exact} =& \frac{4}{\pi}\left(1 - \frac{1}{\sqrt{M}}\right)\frac{\sqrt{A/\pi}}{2(1+A)^{mT_x+0.5}}\frac{\Gamma(mT_x+0.5)}{\Gamma(mT_x+1)}\times \\ & {}_2F_1\left(1, mT_x+0.5; mT_x+1; \frac{1}{1+A}\right) - \frac{1}{2}\left(1 - \frac{1}{\sqrt{M}}\right)^2 + \frac{2}{\pi}\left(1 - \frac{1}{\sqrt{M}}\right)^2 \times \\ & \sqrt{\frac{A}{1+A}}\Bigg[\left(\frac{\pi}{2} - \tan^{-1}\sqrt{\frac{A}{1+A}}\right)\sum_{k=0}^{T_x-1}\binom{2k}{k}\frac{1}{(4(1+A))^k} \\ & - \sin\left(\tan^{-1}\sqrt{\frac{A}{1+A}}\right)\sum_{k=1}^{T_x-1}\sum_{i=1}^{k}\frac{T_{ik}}{(1+A)^k}\left(\cos(\tan^{-1}\sqrt{\frac{A}{1+A}})\right)^{2(k-i)+1}\Bigg]. \end{aligned} \tag{4.38}$$

The ABER expression (4.38) for Nakagami-m fading is exact and in closed form. This means that no finite integral is required to be solved in this case.

The results obtained by Rayleigh fading in (4.29) can be obtained from (4.38) if we let $m = 1$. Further, the results of Hoyt and Rician fading can be derived from Nakagami-m for the cases of $m < 1$ for $m > 1$.

4.3.5 GTR Fading

For the GTR fading, the ABER expression of RQAM-STBC-OFDM system can be derived using (2.14) in (4.19) as

$$\begin{aligned} ABER_{exact} =&\alpha_{stbc1}\int_0^{\frac{\pi}{2}}\left(\frac{1+K}{1+K-\beta_{stbc1}\overline{\gamma}_t}\exp\left(\frac{K\beta_{stbc1}\overline{\gamma}_t}{1+K-\beta_{stbc1}\overline{\gamma}_t}\right)\times\right.\\ &\left.I_0\left(\frac{K\beta_{stbc1}\overline{\gamma}_t\Delta}{1+K-\beta_{stbc1}\overline{\gamma}_t}\right)\right)^{T_x}d\theta-\alpha_{stbc2}\int_0^{\frac{\pi}{4}}\left(\frac{1+K}{1+K-\beta_{stbc1}\overline{\gamma}_t}\times\right.\\ &\left.\exp\left(\frac{K\beta_{stbc1}\overline{\gamma}_t}{1+K-\beta_{stbc1}\overline{\gamma}_t}\right)I_0\left(\frac{K\beta_{stbc1}\overline{\gamma}_t\Delta}{1+K-\beta_{stbc1}\overline{\gamma}_t}\right)\right)^{T_x}d\theta. \end{aligned} \tag{4.39}$$

The ABER of SQAM-STBC-OFDM can be calculated by using (2.14) in (4.20) as

$$\begin{aligned} ABER_{exact} =&\frac{4}{\pi}\alpha_{stbc3}\int_0^{\frac{\pi}{2}}\left(\frac{1+K}{1+K-\beta_{stbc2}\overline{\gamma}_t}\exp\left(\frac{K\beta_{stbc1}\overline{\gamma}_t}{1+K-\beta_{stbc2}\overline{\gamma}_t}\right)\times\right.\\ &\left.I_0\left(\frac{K\beta_{stbc2}\overline{\gamma}_t\Delta}{1+K-\beta_{stbc2}\overline{\gamma}_t}\right)\right)^{T_x}d\theta-\frac{2}{\pi}\left(\alpha_{stbc3}\right)^2\int_0^{\frac{\pi}{4}}\left(\frac{1+K}{1+K-\beta_{stbc2}\overline{\gamma}_t}\times\right.\\ &\left.\exp\left(\frac{K\beta_{stbc1}\overline{\gamma}_t}{1+K-\beta_{stbc2}\overline{\gamma}_t}\right)I_0\left(\frac{K\beta_{stbc2}\overline{\gamma}_t\Delta}{1+K-\beta_{stbc2}\overline{\gamma}_t}\right)\right)^{T_x}d\theta. \end{aligned} \tag{4.40}$$

GTR fading reduces to Rayleigh fading for $K = 0$ and $\Delta = 0$. Whereas, the ABER results of Rician fading can be verified by substituting $K > 0$ and $\Delta = 0$.

4.3.6 Beckmann Fading

Using (2.10) in (4.19), the ABER of RQAM-STBC-OFDM system in Beckmann fading can be derived as

$$\begin{aligned} ABER_{exact} =&\alpha_{stbc1}\int_0^{\frac{\pi}{2}}\left[\frac{(1+q^2)}{\sqrt{((1+q^2)(1+K)-2q^2\overline{\gamma}_t\beta_{stbc1})}}\times\right.\\ &\frac{(1+K)}{\sqrt{((1+q^2)(1+K)-2\overline{\gamma}_t\beta_{stbc1})}}\exp\left(\frac{K(\frac{r^2}{1+r^2})(1+q^2)\overline{\gamma}_t\beta_{stbc1}}{(1+q^2)(1+K)-2q^2\overline{\gamma}_t\beta_{stbc1}}\right.\\ &\left.\left.+\frac{K(\frac{1}{1+r^2})(1+q^2)\overline{\gamma}_t\beta_{stbc1}}{(1+q^2)(1+K)-2\overline{\gamma}_t\beta_{stbc1}}\right)\right]^{T_x}d\theta\\ &-\alpha_{stbc2}\int_0^{\frac{\pi}{4}}\left[\frac{(1+q^2)}{\sqrt{((1+q^2)(1+K)-2q^2\overline{\gamma}_t\beta_{stbc1})}}\times\frac{(1+K)}{\sqrt{((1+q^2)(1+K)-2\overline{\gamma}_t\beta_{stbc1})}}\times\right.\\ &\left.\exp\left(\frac{K(\frac{r^2}{1+r^2})(1+q^2)\overline{\gamma}_t\beta_{stbc1}}{(1+q^2)(1+K)-2q^2\overline{\gamma}_t\beta_{stbc1}}+\frac{K(\frac{1}{1+r^2})(1+q^2)\overline{\gamma}_t\beta_{stbc1}}{(1+q^2)(1+K)-2\overline{\gamma}_t\beta_{stbc1}}\right)\right]^{T_x}d\theta. \end{aligned} \tag{4.41}$$

Now, the ABER of SQAM-STBC-OFDM can be calculated by using (2.10) in (4.20) as

$$\begin{aligned}
ABER_{exact} =& \frac{4}{\pi}\alpha_{stbc3}\int_0^{\frac{\pi}{2}}\left[\frac{(1+q^2)}{\sqrt{((1+q^2)(1+K)-2q^2\overline{\gamma}_t\beta_{stbc2})}}\times\right. \\
& \left.\frac{(1+K)}{\sqrt{((1+q^2)(1+K)-2\overline{\gamma}_t\beta_{stbc2})}}\times\right. \\
& \left.\exp\left(\frac{K(\frac{r^2}{1+r^2})(1+q^2)\overline{\gamma}_t\beta_{stbc2}}{(1+q^2)(1+K)-2q^2\overline{\gamma}_t\beta_{stbc2}}+\frac{K(\frac{1}{1+r^2})(1+q^2)\overline{\gamma}_t\beta_{stbc2}}{(1+q^2)(1+K)-2\overline{\gamma}_t\beta_{stbc2}}\right)\right]^{T_x}d\theta \\
& -\frac{2}{\pi}\left(\alpha_{stbc3}\right)^2\int_0^{\frac{\pi}{4}}\left[\frac{(1+q^2)}{\sqrt{((1+q^2)(1+K)-2q^2\overline{\gamma}_t\beta_{stbc2})}}\times\right. \\
& \left.\frac{(1+K)}{\sqrt{((1+q^2)(1+K)-2\overline{\gamma}_t\beta_{stbc2})}}\times\right. \\
& \left.\exp\left(\frac{K(\frac{r^2}{1+r^2})(1+q^2)\overline{\gamma}_t\beta_{stbc2}}{(1+q^2)(1+K)-2q^2\overline{\gamma}_t\beta_{stbc2}}+\frac{K(\frac{1}{1+r^2})(1+q^2)\overline{\gamma}_t\beta_{stbc2}}{(1+q^2)(1+K)-2\overline{\gamma}_t\beta_{stbc2}}\right)\right]^{T_x}d\theta.
\end{aligned} \tag{4.42}$$

Results of (4.21), (4.22), (4.30) and (4.31) can be verified from (4.41) and (4.42) by using appropriate values of K, q and r. The results of Rayleigh fading can be verified using ($r^2 = 1$, $q^2 = 1$, $K = 0$), for Rician ($r^2 = 1$, $q^2 = 1$, $K \neq 0$), for Hoyt ($r^2 = 1$, $q^2 \neq 1$, $K = 0$), and finally, one-sided Gaussian fading can be verified using ($r^2 = 1$, $q^2 = 0$, $K = 0$).

4.3.7 Generalized-K (K_G) Fading

For RQAM-STBC-OFDM system under generalized-K (K_G) fading channel, the ABER expression can be derived using (2.12) in (4.19) as

$$\begin{aligned}
ABER_{exact} =& \alpha_{stbc1}\int_0^{\frac{\pi}{2}}\left[\left(\frac{\Xi}{\beta_{stbc1}}\right)^{\frac{\widehat{\beta}}{2}}\exp\left(\frac{\Xi}{2\beta_{stbc1}}\right)W_{-\frac{\widehat{\beta}}{2},-\frac{\widehat{\alpha}}{2}}\left(\frac{\Xi}{\beta_{stbc1}}\right)\right]^{T_x}d\theta \\
& -\alpha_{stbc2}\int_0^{\frac{\pi}{4}}\left[\left(\frac{\Xi}{\beta_{stbc1}}\right)^{\frac{\widehat{\beta}}{2}}\exp\left(\frac{\Xi}{2\beta_{stbc1}}\right)W_{-\frac{\widehat{\beta}}{2},-\frac{\widehat{\alpha}}{2}}\left(\frac{\Xi}{\beta_{stbc1}}\right)\right]^{T_x}d\theta,
\end{aligned} \tag{4.43}$$

where $\widehat{\alpha} = K - m$, $K_\alpha(\cdot)$ is the modified Bessel function with order α [133], $\Xi = \frac{Km}{\overline{\gamma}}$ and $\widehat{\beta} = K + m - 1$.

The results of K-distribution can be calculated by substituting $m = 1$ whereas, for Nakagami-m fading channel the substitution $K \to \infty$ is required in (4.43) and (4.44).

For the case of $m \to \infty$ and $K \to \infty$, the AWGN channel can be realized from (4.43) and (4.44).

Now, the ABER of SQAM-STBC-OFDM can be calculated by using (2.10) in (4.20) as

$$\begin{aligned} ABER_{exact} =& \frac{4}{\pi}\alpha_{stbc3}\int_0^{\frac{\pi}{2}}\left[\left(\frac{\Xi}{\beta_{stbc2}}\right)^{\frac{\widehat{\beta}}{2}}\exp\left(\frac{\Xi}{2\beta_{stbc2}}\right)W_{-\frac{\widehat{\beta}}{2},-\frac{\widehat{\alpha}}{2}}\left(\frac{\Xi}{\beta_{stbc2}}\right)\right]^{T_x}d\theta \\ &-\frac{2}{\pi}\left(\alpha_{stbc3}\right)^2\int_0^{\frac{\pi}{4}}\left[\left(\frac{\Xi}{\beta_{stbc2}}\right)^{\frac{\widehat{\beta}}{2}}exp\left(\frac{\Xi}{2\beta_{stbc2}}\right)W_{-\frac{\widehat{\beta}}{2},-\frac{\widehat{\alpha}}{2}}\left(\frac{\Xi}{\beta_{stbc2}}\right)\right]^{T_x}d\theta. \quad (4.44) \end{aligned}$$

4.3.8 $\eta-\lambda-\mu$ Fading

In the case of $\eta-\lambda-\mu$ fading, the ABER of RQAM-STBC-OFDM system can be derived by substituting (2.15) in (4.19) as

$$\begin{aligned} ABER_{exact} =& \alpha_{stbc1}\int_0^{\frac{\pi}{2}}\left(\frac{4\eta(1-\lambda)^2\tilde{b}^2}{(\tilde{c}+\beta_{stbc1}\overline{\gamma}_t)^2-\tilde{d}^2}\right)^{T_x}d\theta \\ &-\alpha_{stbc2}\int_0^{\frac{\pi}{4}}\left(\frac{4\eta(1-\lambda)^2\tilde{b}^2}{(\tilde{c}+\beta_{stbc1}\overline{\gamma}_t)^2-\tilde{d}^2}\right)^{T_x}d\theta. \quad (4.45) \end{aligned}$$

Now, the ABER of SQAM-STBC-OFDM can be calculated by using (2.15) in (4.20) as

$$\begin{aligned} ABER_{exact} =& \frac{4}{\pi}\alpha_{stbc3}\int_0^{\frac{\pi}{2}}\left(\frac{4\eta(1-\lambda)^2\tilde{b}^2}{(\tilde{c}+\beta_{stbc2}\overline{\gamma}_t)^2-\tilde{d}^2}\right)^{T_x}d\theta \\ &-\frac{2}{\pi}\left(\alpha_{stbc3}\right)^2\int_0^{\frac{\pi}{4}}\left(\frac{4\eta(1-\lambda)^2\tilde{b}^2}{(\tilde{c}+\beta_{stbc2}\overline{\gamma}_t)^2-\tilde{d}^2}\right)^{T_x}d\theta. \quad (4.46) \end{aligned}$$

The ABER for η-μ fading channel can be generated as a special case of (4.45) and (4.46) for $\lambda \to 0$ and $\mu = \mu'$. Similarly, the results of λ-μ and Hyot fading can be verified by setting $\eta \to 1$, $\mu = \mu'$ and $\lambda \to 0$, $\mu = 1/2$ respectively.

4.3.9 Beaulieu-Xie Fading

The ABER of RQAM-STBC-OFDM system under Beaulieu-Xie fading can be derived using (2.17) in (4.19) as

$$\begin{aligned} ABER_{exact} =& \alpha_{stbc1} \int_0^{\frac{\pi}{2}} \left(\left(\frac{m}{\overline{\gamma}_t} \right)^m \exp\left(-\frac{\lambda^2}{2} \right) \left(\frac{m}{\overline{\gamma}_t} - \beta_{stbc1} \right)^{-m} \Gamma[m+n] \times \right. \\ & \left. {}_1F_{1R}\left[m, m, \frac{m\lambda^2}{2(m - \beta_{stbc1}\overline{\gamma}_t)} \right] \right)^{T_x} d\theta \\ & - \alpha_{stbc2} \int_0^{\frac{\pi}{4}} \left(\left(\frac{m}{\overline{\gamma}_t} \right)^m \exp\left(-\frac{\lambda^2}{2} \right) \left(\frac{m}{\overline{\gamma}_t} - \beta_{stbc1} \right)^{-m} \Gamma[m+n] \times \right. \\ & \left. {}_1F_{1R}\left[m, m, \frac{m\lambda^2}{2(m - \beta_{stbc1}\overline{\gamma}_t)} \right] \right)^{T_x} d\theta. \end{aligned} \tag{4.47}$$

The ABER of SQAM-STBC-OFDM can be calculated by using (2.17) in (4.20) as

$$\begin{aligned} ABER_{exact} =& \frac{4}{\pi} \alpha_{stbc3} \int_0^{\frac{\pi}{2}} \left(\left(\frac{m}{\overline{\gamma}_t} \right)^m \exp\left(-\frac{\lambda^2}{2} \right) \left(\frac{m}{\overline{\gamma}_t} - \beta_{stbc2} \right)^{-m} \Gamma[m+n] \times \right. \\ & \left. {}_1F_{1R}\left[m, m, \frac{m\lambda^2}{2(m - \beta_{stbc2}\overline{\gamma}_t)} \right] \right)^{T_x} d\theta \\ & - \frac{2}{\pi} \left(\alpha_{stbc3} \right)^2 \int_0^{\frac{\pi}{4}} \left(\left(\frac{m}{\overline{\gamma}_t} \right)^m \exp\left(-\frac{\lambda^2}{2} \right) \left(\frac{m}{\overline{\gamma}_t} - \beta_{stbc2} \right)^{-m} \Gamma[m+n] \times \right. \\ & \left. {}_1F_{1R}\left[m, m, \frac{m\lambda^2}{2(m - \beta_{stbc2}\overline{\gamma}_t)} \right] \right)^{T_x} d\theta. \end{aligned} \tag{4.48}$$

The results of Rician distribution for RQAM and SQAM can be verified from (4.47) and (4.48) respectively by setting $m = 1$.

4.4 Results and Discussion

The ABER expressions derived in this chapter are numerically evaluated to calculate the performance of MQAM-STBC-OFDM system. Different antenna configurations are used in the analysis over generalized fading channels. Without the loss of generality, all the fading channels are assumed to have unity mean and zero variance.

Fig. 4.3 shows the plot of ABER v/s SNR for $T_x = 2, 4$, $R_x = 1$ for 16-SQAM-STBC-OFDM system. The effect of varying K on the ABER performance can be visualized from Fig. 4.3. Benchmark results of Rayleigh and Rician fading channels for STBC-OFDM can be verified form Fig. 4.3.

The results of 4×2-RQAM-STBC-OFDM system for $T_x = 2,4$; $R_x = 1$, $K = 5,10$ and Δ

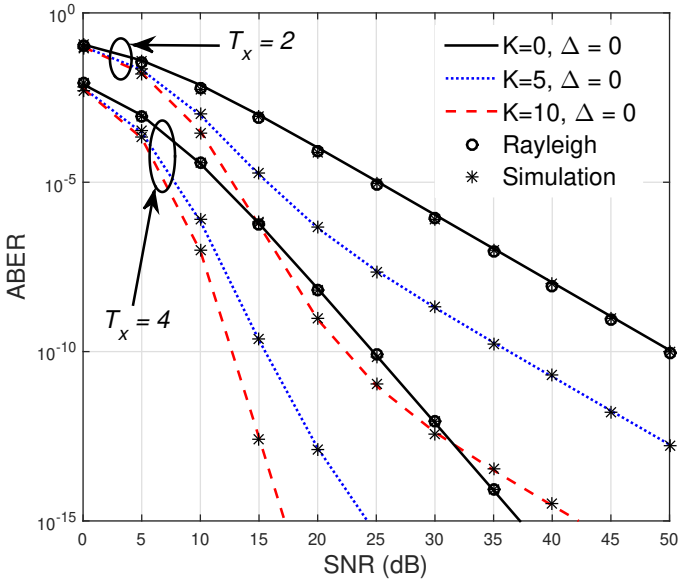

Figure 4.3: ABER v/s SNR for 16-SQAM-STBC-OFDM system with T_x = 2,4, R_x = 1, K= 0, 5, 10 and Δ = 0 in Rayleigh and GTR channel.

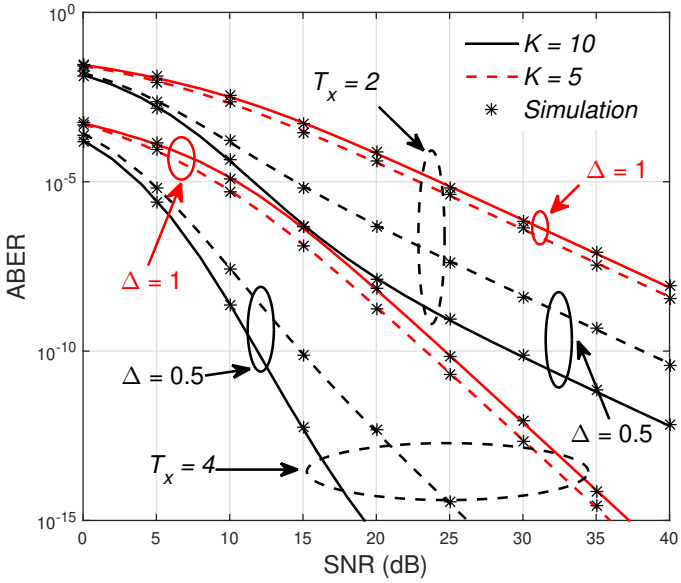

Figure 4.4: ABER plot of 4×2-RQAM-STBC-OFDM system under GTR fading channel for K = 5,10 and Δ = 0.5, 1.

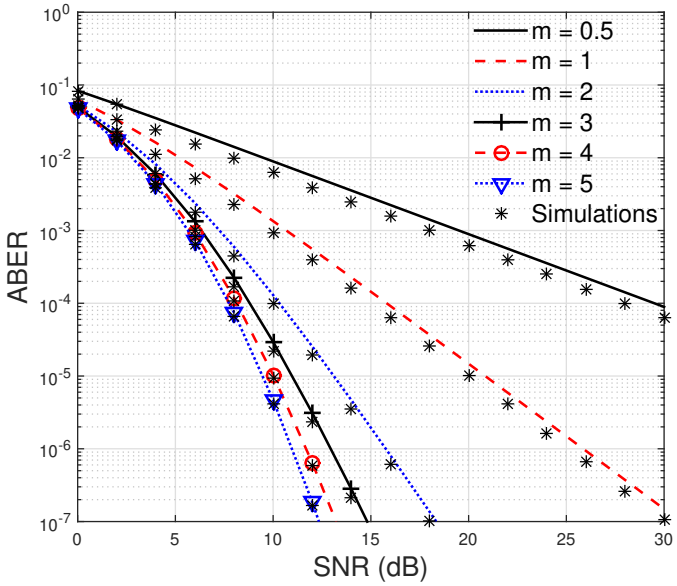

Figure 4.5: ABER of 4-SQAM-STBC-OFDM system for $T_x = 2$; $R_x = 1$ under Beaulieu-Xie fading channel for $\lambda = 1$ and different values of m.

= 0.5,1 are shown in Fig. 4.4. It can be visualized from Fig. 4.4 that as Δ increases, the performance of system degrades. Hence more severe fading than conventional Rayleigh can be modeled by using $\Delta > 0$.

Fig. 4.5 shows the ABER vs. SNR plots for 4 QAM-STBC-OFDM system for $T_x = 2$; $R_x = 1$ under Beaulieu-Xie fading channel for $\lambda = 1$ and $m = 0.5$, 1, 2, 3, 4 and 5. It can be visualized from the results that the ABER performance improves with the increase in fading parameter m from 0.5 to 5. For example, at SNR = 10 dB, the ABER takes values 8.773×10^{-3}, 1.245×10^{-3}, 9.649×10^{-5}, 1.733×10^{-5}, 4.868×10^{-6}, 1.809×10^{-6} for $m = 0.5$, 1, 2, 3, 4, 5 respectively.

4.5 Summary

The exact expressions of ABER are derived in this chapter for STBC-OFDM systems. SQAM-STBC-OFDM is found to be a special case of RQAM-STBC-OFDM (using $M_I = M_Q = M$ and $d_Q = d_I = d$). Numerical results have been verified using simulations. The derived results are obtained under generalized fading scenario.

Chapter 5

Effect of Impairments on Performance of MIMO-OFDM Systems

Despite its several advantages, MIMO-OFDM poses a lot of technical challenges in its implementation such as high sensitivity to frequency offsets, phase noise, requirement of perfect channel state information over all transmit-receive antenna pairs and high PAPR etc. The orthogonality between the subcarriers of OFDM is lost by frequency offset or phase noise. This also affects the block coded MIMO symbols and therefore the overall ABER of MIMO-OFDM system gets deteriorated by the ICI.

Apart from this, if the perfect CSI is not available at the receiver, the system performance degrades significantly. For MIMO-OFDM system containing a lot of transmits and receive antenna, the perfect estimation of CSI is not achievable all the time. Whereas, the CSI is an essential factor while correctly decoding the symbols at the receiver. A substantial amount of work has already been done to calculate the ABER of MIMO-OFDM system with ICI and imperfect CSI independently over different fading channels. However, most of these studies assume the fading process to be related with only a single family of PDF like Rayleigh, Rician or Nakagami fading. Therefore, in this chapter, the expressions are derived for the ABER of MIMO-OFDM system with both CFO and imperfect CSI under generalized fading scenarios. The effect of CFO on ABER is calculated by ICI coefficients and imperfect CSI is calculated by quality of channel estimation.

In Section 5.1, the relationship between the ICI coefficients and instantaneous SNR of MIMO-OFDM system is presented. Thereafter, in Section 5.2, the relation between quality of channel estimation and SNR is presented. Further, in Section 5.3 the closed form results for ABER are derived for MIMO-OFDM with channel impairments. Section 5.4 gives the numerical and simulation results based on derived expressions in this chapter. Section 5.5 holds the summary of chapter.

5.1 Effect of Carrier Frequency Offset on Instantaneous SNR

An MIMO-OFDM system employing T_x transmit antennas and N subcarriers is assumed in this analysis. For single receiving antenna case, the p^{th} sample of received signal including the effect of CFO (Δf) after removing the cyclic prefix and applying FFT can be represented as

$$\mathbf{r}(k) = \frac{1}{\sqrt{T_x}} \sum_{i=1}^{T_x} \left[s_0 \mathbf{H}_i(p)\mathbf{t}_i(p) + \sum_{l=0, l\neq p}^{N-1} \mathbf{s}_{l-p}\mathbf{H}_i(l)\mathbf{t}_i(l) \right] + \mathbf{z}(p); \quad 0 \leq p \leq (N-1), \quad (5.1)$$

where $\mathbf{H}_i(p)$ represents the channel frequency response, $\mathbf{t}_i(p)$ is the transmitted signal from i^{th} transmit antenna and $\mathbf{z}(p)$ is AWGN with variance σ_z^2. The term $\mathbf{s}_p$ represents the ICI coefficients and is represented as

$$\mathbf{s}_p = \frac{\sin(\pi(p+\epsilon))}{N \sin(\frac{\pi}{N}(p+\epsilon))} \exp\left(j\pi \left(1 - \frac{1}{N}(p+\epsilon) \right) \right), \quad (5.2)$$

where $\epsilon (= \Delta f T_u)$ is the normalized frequency offset and T_u represents the useful time period of one OFDM symbol. In this analysis, it is assumed that the channel for a specific subcarrier at time t is constant for at-least T_x consecutive symbols.

After equalization, the decision variable $\hat{\mathbf{t}}(p)$ is represented as

$$\hat{\mathbf{t}}(p) = \frac{1}{\sqrt{T_x}} \sum_{i=1}^{T_x} \left[|s_0|^2 |\mathbf{H}_i(p)|^2 \mathbf{t}_i(p) + s_0^* \mathbf{H}_i^*(p) \sum_{l=0, l\neq p}^{N-1} \mathbf{s}_{l-p}\mathbf{H}_i(l)\mathbf{t}_i(l) \right] + \mathbf{s}_0^* \mathbf{H}_i^*(p)\mathbf{z}(p). \quad (5.3)$$

Now, the signal power P_t can be calculated as

$$P_t = \frac{1}{T_x} |s_0|^4 \left[\sum_{i=1}^{T_x} |\mathbf{H}_i(p)|^2 \right]^2 \sigma_t^2. \quad (5.4)$$

Also, the interference power P_{in} due to ICI can be calculated as

$$P_{in} = |s_0|^2 \left[\sum_{i=1}^{T_x} |\mathbf{H}_i(p)|^2 \right] \left(1 - |s_0|^2 \right) \sigma_H^2 \sigma_t^2. \quad (5.5)$$

In (5.5), the term σ_H^2 which represents the channel power is assumed to be unity. Now,

the signal-to-interference ratio (SIR) is calculated by using (5.4) and ((5.5)) as

$$\gamma_I = \frac{|s_0|^2 \left[\sum_{i=1}^{T_x} |\mathbf{H}_i(p)|^2\right]}{T_x \left(1 - |s_0|^2\right)}. \tag{5.6}$$

The noise power P_z due to channel AWGN can be written as

$$P_z = |s_0|^2 \left[\sum_{i=1}^{T_x} |\mathbf{H}_i(p)|^2\right] \sigma_z^2. \tag{5.7}$$

Using (5.6) and ((5.7)), the signal to interference and noise ratio (SINR) is calculated as

$$\gamma_{IN} = \frac{|s_0|^2 \left[\sum_{i=1}^{T_x} |\mathbf{H}_i(p)|^2\right]}{T_x \left(1 - |s_0|^2 + \bar{\gamma}^{-1}\right)}, \tag{5.8}$$

where $\bar{\gamma} = \frac{\sigma_t^2}{\sigma_z^2}$ represents the average SNR.

5.2 Effect of Imperfect CSI on Instantaneous SNR

Perfect estimation of channel is required at the receiver for correctly decoding the transmitted signal. This is possible only when perfect CSI is available. However, in most of the cases, only partial information of channel is available at the receiver which is known as imperfect CSI. Due to this imperfect CSI, an error is induced in channel estimation. Let the error in estimating the channel at the receiver be δ. This error is represented as

$$\delta = \mathbf{H} - \hat{\mathbf{H}}, \tag{5.9}$$

where $\hat{\mathbf{H}}$ and $\mathbf{H}$ are the estimated and actual channel response respectively. It is assumed here that $\hat{\mathbf{H}}$ and δ are uncorrelated and values in δ belong to zero-mean circularly symmetric complex Gaussian distribution. The variance of δ can be calculated by using the minimum mean-squared error channel estimate on (5.9) as

$$\sigma_\delta^2 = \mathbb{E}[|\mathbf{H}|^2] - \mathbb{E}[|\hat{\mathbf{H}}|^2]. \tag{5.10}$$

The variance of estimation error σ_δ^2 is assumed to be known at both transmitter and receiver. The channel estimation quality is demonstrated by using σ_δ^2.

Now, to study the effect of the quality of channel estimation on ABER, first, the relation

between the quality of channel estimation and instantaneous SNR is to be defined. Under imperfect CSI, the instantaneous SNR between i^{th} transmit and j^{th} receive antenna pair depends on the variance of estimation error and can be written as [155]

$$\gamma_{i,j} = \frac{\gamma_{IN}}{1 + \sigma_{\delta}^2 \gamma_{IN}}. \tag{5.11}$$

The normalized instantaneous SNR for MIMO-OFDM system is given by the relation [96]

$$\gamma_T = \sum_{i=1}^{T_x} \sum_{j=1}^{R_x} \gamma_{i,j}. \tag{5.12}$$

5.3 ABER of MIMO-OFDM with Impairments

Now once we have derived the relationship between the instantaneous SNR of MIMO-OFDM system with ICI coefficients and quality of channel estimation, the procedure of calculating ABER expressions is quite straight-forward. The expressions of ABER for perfect conditions (no ICI and perfect CSI) were derived in Section 3.2 of Chapter 3 for SFBC-OFDM and in Section 4.2 of Chapter 4 for STBC-OFDM. Now, the ABER of these systems with channel impairments can be derived by substituting the perfect condition SNR by γ_T derived in (5.12).

- SFBC-OFDM
  Let us take the case of SFBC-OFDM, the ABER in this case by using exact analysis with channel impairments of ICI and imperfect CSI can be derived by substituting (5.12) in (3.31) as

$$ABER_{exact} = \frac{\alpha}{\pi} \int_0^{\frac{\pi}{2}} \left[M_{\gamma_T} \left(-\frac{\beta}{2C_R T_x \sin^2 \phi} \right) \right]^{T_x R_x} d\phi. \tag{5.13}$$

  Similarly, the closed form expression of ABER using exponential bound is derived by using (5.12) in (3.36) as

$$ABER \approx 0.2 \left[M_{\gamma_T} (\xi) \right]^{T_x R_x}. \tag{5.14}$$

- STBC-OFDM
  Further, the ABER for RQAM-STBC-OFDM with channel impairments of ICI and

imperfect CSI can be derived by substituting (5.12) in (4.17) as

$$ABER_{exact} = \frac{2}{\pi}\left[A_I + A_Q\right]\int_0^{\frac{\pi}{2}}\left[\mathbb{M}_{\gamma_T}\left(\frac{-3}{(M_I M_Q - 1)\sin^2\theta}\right)\right]^{T_x} d\theta - \frac{2}{\pi}\left[A_I A_Q\right]\int_0^{\frac{\pi}{4}}\left[\mathbb{M}_{\gamma_T}\left(\frac{-3}{(M_I M_Q - 1)\sin^2\theta}\right)\right]^{T_x} d\theta. \quad (5.15)$$

Now, for SQAM-STBC-OFDM, the ABER is calculated by substituting (5.12) in (4.18) as

$$ABER_{exact} = \frac{4}{\pi}\left(1 - \frac{1}{\sqrt{M}}\right)\int_0^{\frac{\pi}{2}}\left[\mathbb{M}_{\gamma_T}\left(\frac{-3}{(M^2 - 1)\sin^2\theta}\right)\right]^{T_x} d\theta - \frac{2}{\pi}\left(1 - \frac{1}{\sqrt{M}}\right)^2\int_0^{\frac{\pi}{4}}\left[\mathbb{M}_{\gamma_T}\left(\frac{-3}{(M^2 - 1)\sin^2\theta}\right)\right]^{T_x} d\theta. \quad (5.16)$$

The closed form expressions of ABER for RQAM-STBC-OFDM and SQAM-STBC-OFDM with channel impalements can be derived from (5.15) and (5.16) respectively for Rayleigh and Nakagami-m fading channels using similar approach as given in Section 4.3 of Chapter 4. However, for other fading channels, the closed form expression of ABER is not possible. Therefore, numerical methods are used to calculate ABER for these cases.

5.4 Results and Discussion

The ABER results of STBC-OFDM are presented with imperfect CSI and CFO over generalized fading channels. The derived expressions are valid for any family of fading PDF. For the purpose of validation of derived expressions through results, we have taken the case of some fading channels.

The plot of ABER v/s average SNR for $T_x = 2$, $R_x = 1$ for square 16 QAM-STBC-OFDM system over GTR fading channel is given in Fig. 5.1. The value of GTR fading parameters used are $\Delta = 0$ and $K = 0$, 5, 10. Fig. 5.1 is used to study the effect of varying K and ϵ on the ABER. Results are verified by changing GTR fading to Rayleigh ($K = 0, \Delta = 0$) and Rician ($K \neq 0, \Delta = 0$) fading cases. Without the loss of generality, the mean and variance of all the GTR fading channels are assumed to be 0 and 1 respectively. An interesting observation from Fig. 5.1 is that the ABER degrades with the increase in ϵ and improves when the value of fading parameter K is increased.

The ABER results of 4×2 QAM-STBC-OFDM system for $T_x = 1$ and 2, $R_x = 1$ under Beaulieu-Xie fading channel are shown in Fig. 5.2. The fading parameters $m = 0.5$, 1, 3

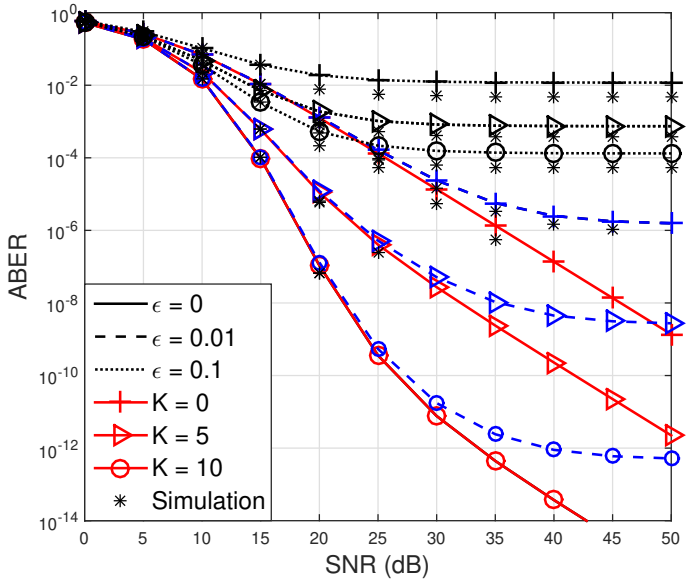

Figure 5.1: ABER v/s SNR for $T_x = 2$, $R_x = 1$, 16-SQAM-STBC-OFDM system with $K = 0$, 5, 10 (shown with $+$, $\triangle$, $\bigcirc$ markers) and $\Delta = 0$, $\epsilon = 0, 0.01, 0.1$ (shown with solid, dashed and dotted lines) in Rayleigh and GTR fading channel.

and $\lambda = 1$ are taken and the effect of imperfect CSI is observed in this figure. It can be visualized from Fig. 5.2 that as m increases, the ABER performance of system improves. On the other hand, the ABER performance degrades when the value of σ_δ^2 is increased. The effect of diversity gain can also be visualized from Fig. 5.2 as T_x increases from 1 to 2.

The ABER results of 8PSK-SFBC-OFDM system with four transmit antenna and code receive antenna, code rate $= \frac{3}{4}$ (code H_4 [27]) are given in Fig. 5.3 under Nakagami-n fading with $\sigma_\delta^2 = 0$, 0.02 and 0.05. The results obtained from exact expression are shown with solid lines whereas, the approximate results obtained from tight bound on ABER are shown with dotted lines in Fig. 5.3. The results of Rayleigh and Rician fading can be verified from Nakagami-n fading by substituting $n = 0$ and $n^2 = K$ respectively as shown in Fig. 5.3. The parameter K represents the Rician K factor. Fig. 5.4 shows the ABER vs SNR results for Nakagami-n fading channel with channel parameter $n = 5$. The system parameters are kept the same as Fig. 5.3 for comparison between two results. With the increase in channel estimation error in Fig. 5.4, the ABER performance degrades. Another observation from Fig. 5.3 and Fig. 5.4 is the improvement in ABER performance when the channel parameter n is increased from 0 to 5 for constant values of system parameters T_x, R_x, C_R and σ_δ^2.

The ABER v/s SNR results for 16-QAM-SFBC-OFDM with $T_x = 3$, $R_x = 1$ (code G_3

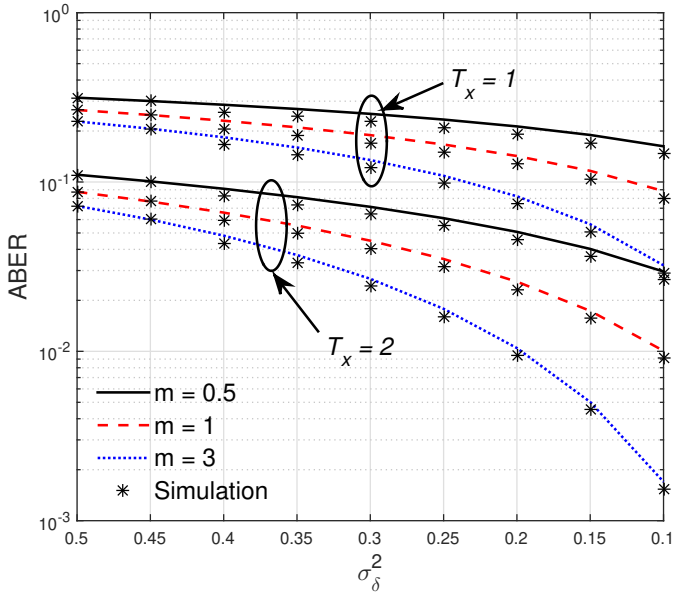

Figure 5.2: ABER v/s σ_δ^2 for $T_x = 1, 2$, $R_x = 1$, 4×2-RQAM-STBC-OFDM system with $m = 0.5$, 1, 3 and $\lambda = 1$ in Beaulieu-Xie fading channel.

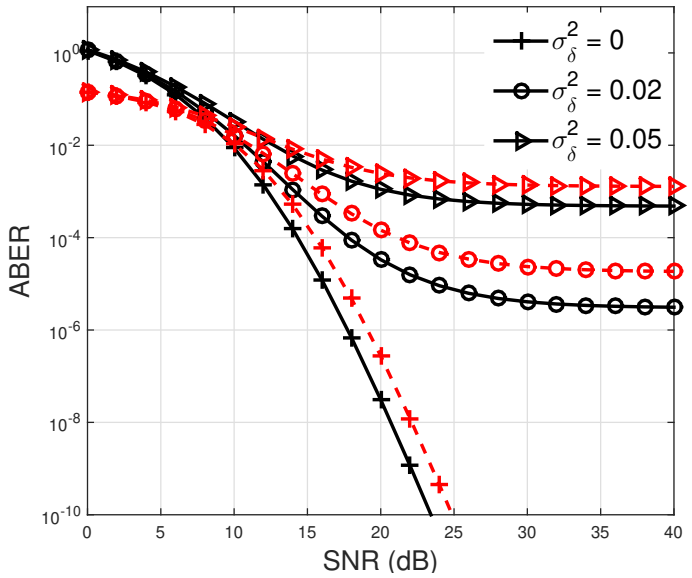

Figure 5.3: ABER v/s SNR plot for 8-PSK-SFBC-OFDM with $T_x = 4$, $R_x = 2$, $C_R = 3/4$ under Nakagami-n fading with $n = 0$ and channel estimation error $\sigma_\delta^2 = 0$, 0.02, 0.05, (Exact results - solid black lines, results exponential bound - dashed red lines).

[27]) are presented in Fig. 5.5. For this analysis, the Nakagami-q fading channel is considered and results are provided for various values of σ_δ^2. It can be visualized from the plot that with the increase in channel estimation error parameter, the ABER performance deteriorates. The channel parameter q also affects ABER performance. The results of

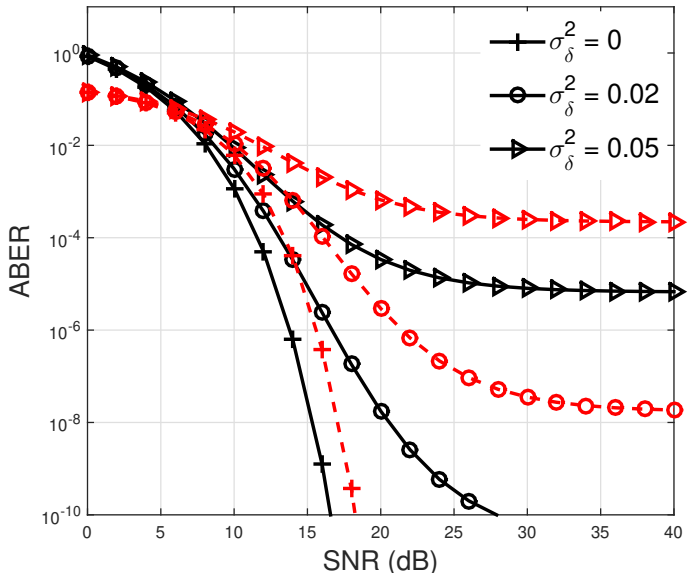

Figure 5.4: ABER v/s SNR plot for 8-PSK-SFBC-OFDM with $T_x = 4$, $R_x = 2$, $C_R = 3/4$ under Nakagami-n fading with $n = 5$ and channel estimation error $\sigma_\delta^2 = 0$, 0.02, 0.05, (Exact results - solid black lines, results exponential bound - dashed red lines).

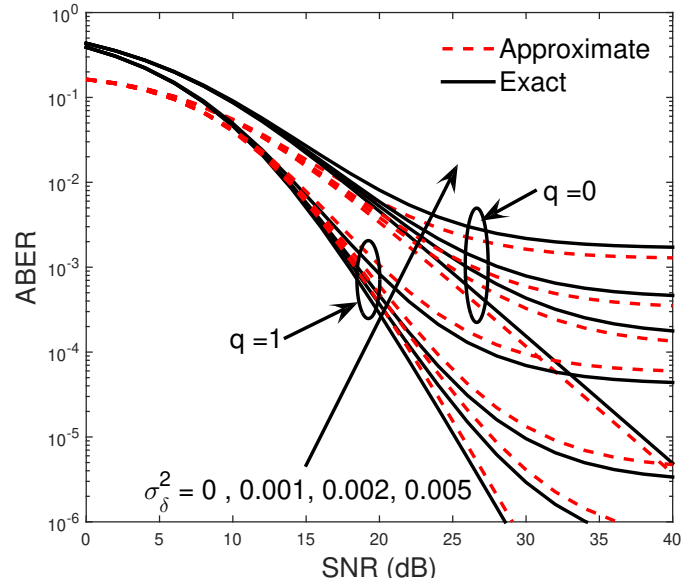

Figure 5.5: ABER results for 16-QAM-SFBC-OFDM with $T_x = 3$, $R_x = 1$ and $C_R = 1/2$ under Nakagami-q fading and channel estimation error $\sigma_\delta^2 = 0$, 0.001, 0.002, 0.005.

Rayleigh fading presented in [96, 110] can be verified from Nakagami-q fading for $q = 0$ whereas, the Nakagami-q fading converges to one-sided Gaussian fading if $q = 1$. The one-sided Gaussian fading channel gives better performance in terms of ABER as compared to Rayleigh fading channel.

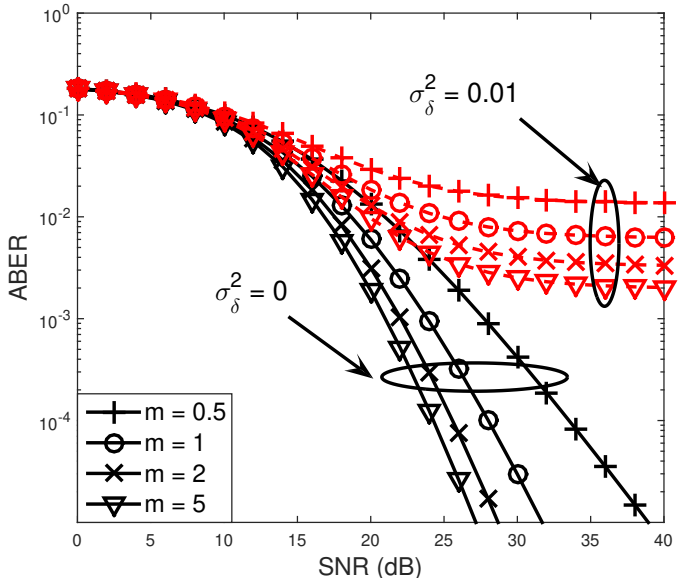

Figure 5.6: ABER v/s SNR plot for 32-QAM-SFBC-OFDM using exponential bound with $T_x = 2$, $R_x = 2$, $C_R = 1$, $\sigma_\delta^2 = 0$ and 0.01 under Generalized-K (K_G) fading with fading parameters $m = 0.5$, 1, 2, 5 and $K = 1$.

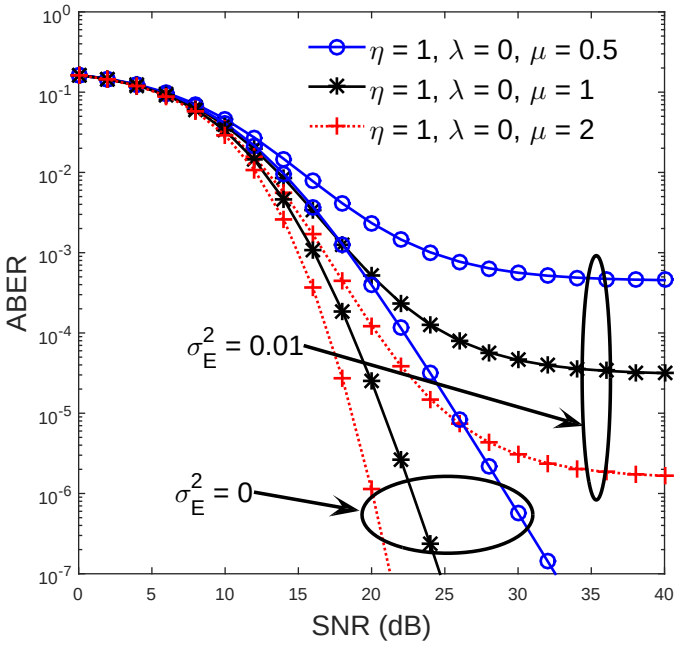

Figure 5.7: ABER plot for 16-QAM-SFBC-OFDM system with three transmit and one receive antenna using exponential bound under η-λ-μ fading ($\eta = 1$, $\lambda = 0$ and $\mu = 0.5$, 1 and 2).

Fig. 5.6 presents the ABER results using exponential bound for 32 QAM modulated SFBC-OFDM system having two transmit and two receive antennas. The code rate is

taken to be unity. Generalized-K (K_G) fading channel is taken in this results with $\sigma_\delta^2 = 0$ and 0.01. The results are provided by taking channel parameters $K = 1$ while m is varied from 0.5, 1, 2 and 5. The Generalized-K fading is considered as a very flexible model for the accurate modeling of both short term and long term fading conditions. Rayleigh fading channel can be obtained as a special case of Generalized-K (K_G) fading channel if $K = 1$ and $m = 2$ and the results can be verified from [96]. Another observation from Fig. 5.6 is that with the increase in fading parameter m from 0.5 to 5, the ABER also improves.

The ABER v/s SNR plot of 16 QAM modulated SFBC-OFDM system with $T_x = 3$, $R_x = 1$, $C_R = 1/2$ and $\sigma_\delta^2 = 0$, 0.01 is shown in Fig. 5.7. These results are calculated using the exponential bound under η-λ-μ fading. The results of different fading scenarios like Nakagami-q, Rayleigh, λ-μ, Gamma, exponential, η-μ, One-Sided Gaussian and Nakagami-m distribution can be obtained using different combinations of fading variables η, λ and μ. For a constant value of η and λ, there is an improvement in ABER as μ is increased from 0.5 to 2.

5.5 Summary

The effect of channel impairments has been studied on MIMO-OFDM systems. Expressions have been derived to examine the effect of CFO and imperfect CSI on instantaneous SNR and ABER of system. The results calculated by using the numerical evaluation of derived expressions are verified using Monte-Carlo simulations.

Chapter 6

Conclusions and Future Works

This chapter includes the conclusions drawn from the analytical and simulation studies made in this dissertation. This research was focused on exploring the performance of diversity based MIMO-OFDM systems under multipath fading as well as different channel impairments. For this purpose, an analytical framework for MIMO-OFDM systems has been developed and presented in this dissertation.

6.1 Conclusions

In Chapter 1, a brief introduction of the MIMO-OFDM system has been presented. The chapter focuses upon the need, classification and system model of MIMO-OFDM. The advantages, drawbacks and applications of MIMO-OFDM system have also been discussed. In Chapter 2, a comprehensive survey containing the state of art work done by various researchers in the field of MIMO-OFDM has been presented.

The performance of SFBC-OFDM system has been analyzed in Chapter 3 using BER as the performance measure. An MGF based approach has been devised to generalize the analysis for different sets of modulation schemes and fading channels. The ABER expressions derived for SFBC-OFDM system have been calculated in generalized fading scenarios. Simple closed-form approximate expressions for ABER based on a tight bound have also been derived for SFBC-OFDM system.

In Chapter 4, the exact error rate analysis of STBC-OFDM systems has been presented. Again an MGF based generalized approach has been utilized. The analysis has been done for many fading scenarios having a valid expression of MGF. Thereafter, the performance of MIMO-OFDM system under the influence of impairments has been studied in Chapter 5. For this analysis, two major impairments i.e. CFO and imperfect CSI have been taken into account. It was observed that the results of conventional SISO-OFDM system can be obtained as a special case of the derived expressions.

The main contributions of this dissertation are summarized as:

- Development of an analytical framework for MIMO-OFDM systems

  - STBC-OFDM system
  - SFBC-OFDM system
- BER performance of SFBC-OFDM systems
- BER performance of STBC-OFDM systems
- Effect of impairments on performance of MIMO-OFDM systems
  - Effect of CFO on instantaneous SNR and ABER
  - Effect of imperfect CSI on instantaneous SNR and ABER
- Comparison of simulations and analytical results

6.2 Future Works

The work in this dissertation has focused on the development of an analytical framework and performance analysis of MIMO-OFDM systems in fading environments and channel impairments. The increasing demands in terms of data-rates and quality of service have resulted in rapid advancements in current wireless communication technology. Despite the comprehensive nature of the study undertaken in this dissertation, the scope for further research on this topic is always present. So here are some issues that require further study:

- Study of the effect of other channel impairments like symbol timing offset, co-channel interference, multiuser interference.
- Effect of correlated and non-independent MIMO channels.
- The analysis can be further extended for generalized frequency division multiplexing (GFDM).
- Effect of massive MIMO scenarios.

References

[1] Y. S. Cho, J. Kim, W. Y. Yang, and C. G. Kang, *MIMO-OFDM wireless communications with MATLAB*. John Wiley & Sons, 2010.

[2] T. S. Rappaport *et al.*, *Wireless Communications: Principles and Practice*. Prentice Hall PTR New Jersey, 1996, vol. 2.

[3] A. Goldsmith, *Wireless communications*. Cambridge University Press, 2005.

[4] J. G. Proakis, *Digital Communications Fourth Edition, 2001*. McGraw-Hill Companies, Inc., New York, NY, 1998.

[5] B. P. Lathi, *Modern Digital and Analog Communication Systems 3e Osece*. Oxford University Press, 1998.

[6] W. C. Lee, *Wireless and cellular communications*. McGraw-Hill Professional, 2005.

[7] R. Steele and L. Hanzo, *Mobile Radio Communications: Second and Third Generation Cellular and WATM Systems: 2nd*. IEEE Press-John Wiley, 1999.

[8] R. V. Nee and R. Prasad, *OFDM for wireless multimedia communications*. Artech House, Inc., 2000.

[9] Nokia Networks., *LTE-Advanced Pro: Pushing LTE Capabilities Towards 5G. [Online]*. Available: https://onestore.nokia.com/asset/200176/Nokia LTE-Advanced Pro White Paper EN.pdf

[10] A. Gupta and R. K. Jha, "A Survey of 5G Network: Architecture And Emerging Technologies," *IEEE Access*, vol. 3, pp. 1206-1232, 2015.

[11] R. S. Campos, "Evolution of Positioning Techniques in Cellular Networks, from 2G to 4G," *Wireless Communications and Mobile Computing*, vol. 2017, Article ID 2315036, 17 pages, 2017.

[12] A. Bishnu and V. Bhatia, "Receiver for IEEE 802.11 ah in Interference Limited Environments," *IEEE Internet Things J.*, vol. 5, no. 5, pp. 4109-4118, 2018.

[13] J. Lee, Y. Kim, Y. Kwak, J. Zhang, A. Papasakellariou, T. Novlan, C. Sun, and Y. Li, "LTE-Advanced in 3GPP Rel-13/14: An Evolution Toward 5G," *IEEE Commun. Mag.*, vol. 54, no. 3, pp. 36-42, 2016.

[14] A. F. Demir, M. Elkourdi, M. Ibrahim, and H. Arslan, "Waveform Design for 5G and Beyond," *arXiv preprint arXiv:1902.05999*, 2019.

[15] E. G. Larsson, O. Edfors, F. Tufvesson, and T. L. Marzetta, "Massive MIMO for Next Generation Wireless Systems," *IEEE Commun. Mag.*, vol. 52, no. 2, pp. 186-195, 2014.

[16] D. Mattera, M. Tanda, and M. Bellanger, "New Multicarrier Modulations for 5G," in *5G Mobile Communications*. Springer, 2017, pp. 165-202.

[17] W. C. Jakes and D. C. Cox, *Microwave mobile communications*. Wiley-IEEE Press, 1994.

[18] N. Y. Ermolova, "Analysis of OFDM Error Rates over Nonlinear Fading Radio Channels," *IEEE Trans. Wireless Commun.*, vol. 9, no. 6, 2010.

[19] P. Dharmawansa, N. Rajatheva, and H. Minn, "An Exact Error Probability Analysis of OFDM Systems with Frequency Offset," *IEEE Trans. Commun.*, vol. 57, no. 1, pp. 26-31, 2009.

[20] A. M. Hamza and J. W. Mark, "Closed Form SER Expressions for QPSK OFDM Systems with Frequency Offset in Rayleigh Fading Channels," *IEEE Commun. Lett.*, vol. 18, no. 10, pp. 1687-1690, 2014.

[21] A. M. Hamza and J. W. Mark, "Closed-Form Expressions for the BER/SER of OFDM Systems with an Integer Time Offset," *IEEE Trans. Commun.*, vol. 63, no. 11, pp. 4461 4473, 2015.

[22] A. Al-Dweik, F. Kalbat, S. Muhaidat, O. Filio, and S. M. Ali, "Robust MIMO-OFDM System for Frequency-Selective Mobile Wireless Channels," *IEEE Trans. Veh. Technol.*, vol. 64, no. 5, pp. 1739-1749, 2015.

[23] M. I. Kadir, S. Sugiura, S. Chen, and L. Hanzo, "Unified MIMO-Multicarrier Designs: A Space-Time Shift Keying Approach," *IEEE Commun. Surveys Tuts.*, vol. 17, no. 2, pp. 550-579, 2015.

[24] J. N. Laneman, D. N. Tse, and G. W. Wornell, "Cooperative Diversity in Wireless Networks: Efficient Protocols and Outage Behavior," *IEEE Trans. Inf. Theory*, vol. 50, no. 12, pp. 3062-3080, 2004.

[25] Z. Pan, K. K. Wong, and T. S. Ng, "Generalized Multiuser Orthogonal Space Division Multiplexing," *IEEE Trans. Wireless Commun.*, vol. 3, no. 6, pp. 1969-1973, 2004.

[26] L. Zheng and D. N. C. Tse, "Diversity and Multiplexing: A Fundamental Tradeoff in Multiple-Antenna Channels," *IEEE Trans. Inf. Theory*, vol. 49, no. 5, pp. 1073-1096, 2003.

[27] H. Jafarkhani, *Space-Time Coding: Theory and Practice*. Cambridge University Press, 2005.

[28] G. Bauch, "Space-Time Block Codes versus Space-Frequency Block Codes," in *Vehicular Technology Conference, 2003. VTC 2003-Spring. The 57th IEEE Semiannual*, vol. 1. IEEE, 2003, pp. 567-571.

[29] V. Tarokh, H. Jafarkhani, and A. R. Calderbank, "Space-Time Block Codes from Orthogonal Designs," *IEEE Trans. Inf. Theory*, vol. 45, no. 5, pp. 1456-1467, 1999.

[30] S. M. Alamouti, "A Simple Transmit Diversity Technique for Wireless Communications," *IEEE J. Sel. Areas Commun.*, vol. 16, no. 8, pp. 1451-1458, 1998.

[31] R. W. Chang, "Synthesis of Band-Limited Orthogonal Signals for Multichannel Data Transmission," *Bell Labs Tech. J.*, vol. 45, no. 10, pp. 1775-1796, 1966.

[32] H. Harmuth, "On the Transmission of Information by Orthogonal Time Functions," *Transactions of the American Institute of Electrical Engineers, Part I: Communication and Electronics*, vol. 79, no. 3, pp. 248-255, 1960.

[33] R. W. Chang, "Orthogonal Frequency Multiplex Data Transmission System," Jan. 1970, US Patent 3,488,445.

[34] S. Weinstein and P. Ebert, "Data Transmission by Frequency-Division Multiplexing Using the Discrete Fourier Transform," *IEEE Trans. Commun. Technol.*, vol. 19, no. 5, pp. 628-634, 1971.

[35] L. Cimini, "Analysis and Simulation of a Digital Mobile Channel using Orthogonal Frequency Division Multiplexing," *IEEE Trans. Commun.*, vol. 33, no. 7, pp. 665-675, 1985.

[36] R. Lassalle and M. Alard, "Principles of Modulation and Channel Coding for Digital Broadcasting for Mobile Receivers," *EBU Tech. Rev*, vol. 224, pp. 168-190, 1987.

[37] J. A. Bingham, "Multicarrier Modulation for Data Transmission: An Idea Whose Time has Come," *IEEE Commun. Mag.*, vol. 28, no. 5, pp. 5-14, 1990.

[38] L. Rugini and P. Banelli, "BER of OFDM Systems Impaired by Carrier Frequency Offset in Multipath Fading Channels," *IEEE Trans. Wireless Commun.*, vol. 4, no. 5, pp. 2279-2288, 2005.

[39] S. Kumari, S. K. Rai, A. Kumar, H. Joshi, A. K. Singh, and R. Saxena, "Exact BER Analysis of FRFT-OFDM System over Frequency Selective Rayleigh Fading Channel with CFO," *Electron. Lett.*, vol. 49, no. 20, pp. 1299-1301, 2013.

[40] R. Saxena and H. D. Joshi, "Performance Improvement in an OFDM System with MBH Combinational Pulse Shape," *Digital Signal Process.*, vol. 23, no. 1, pp. 314-321, 2013.

[41] R. Saxena and H. D. Joshi, "ICI Reduction in OFDM System using IMBH Pulse Shapes," *Wireless personal communications*, vol. 71, no. 4, pp. 2895-2911, 2013.

[42] A. Kumar, M. Magarini, H. D. Joshi, and R. Saxena, "Exact SER Analysis of DFRFT based QPSK OFDM System over Frequency Selective Rayleigh Fading Channel with CFO," *Journal of Computer Networks and Communications*, vol. 2016, Article ID 2804507, 7 pages, 2016.

[43] V. K. Trivedi, S. Kumari, and P. Kumar, "Generalised Error Analysis of FRFT-OFDM over Nakagami-m Fading Channel with Arbitrary m," *IET Commun.*, vol. 11, no. 9, pp. 1497-1502, 2017.

[44] A. Wittneben, "A New Bandwidth Efficient Transmit Antenna Modulation Diversity Scheme for Linear Digital Modulation," in *Communications, 1993. ICC'93 Geneva. Technical Program, Conference Record, IEEE International Conference on*, vol. 3. IEEE, 1993, pp. 1630-1634.

[45] N. Seshadri and J. H. Winters, "Two Signaling Schemes for Improving the Error Performance of Frequency Division Duplex (FDD) Transmission Systems using Transmitter Antenna Diversity," *Int. J. Wireless Inf. Networks*, vol. 1, no. 1, pp. 49-60, 1994.

[46] V. M. DaSilva and E. S. Sousa, "Fading-Resistant Modulation using Several Transmitter Antennas," *IEEE Trans. Commun.*, vol. 45, no. 10, pp. 1236-1244, 1997.

[47] V. Tarokh, N. Seshadri, and A. R. Calderbank, "Space-Time Codes for High Data Rate Wireless Communication: Performance Criterion and Code Construction," *IEEE Trans. Inf. Theory*, vol. 44, no. 2, pp. 744-765, 1998.

[48] X. B. Liang, "Orthogonal Designs with Maximal Rates," *IEEE Trans. Inf. Theory*, vol. 49, no. 10, pp. 2468-2503, 2003.

[49] A. Matache and R. D. Wesel, "Universal Trellis Codes for Diagonally Layered Space-Time Systems," *IEEE Trans. Signal Process.*, vol. 51, no. 11, pp. 2773-2783, 2003.

[50] H. Jafarkhani and N. Seshadri, "Super-Orthogonal Space-Time Trellis Codes," *IEEE Trans. Inf. Theory*, vol. 49, no. 4, pp. 937-950, 2003.

[51] H. Jafarkhani and N. Hassanpour, "Super-Quasi-Orthogonal Space-Time Trellis Codes for Four Transmit Antennas," *IEEE Trans. Wireless Commun.*, vol. 4, no. 1, pp. 215-227, 2005.

[52] C. Kose and R. D. Wesel, "Universal Space-Time Codes from Demultiplexed Trellis Codes," *IEEE Trans. Commun.*, vol. 54, no. 7, pp. 1243-1250, 2006.

[53] S. Sandhu and A. Paulraj, "Space-Time Block Codes: A Capacity Perspective," *IEEE Commun. Lett.*, vol. 4, no. 12, pp. 384-386, 2000.

[54] M. D. Ionescu, K. K. Mukkavilli, Z. Yan, and J. Lilliberg, "Improved 8-and 16-State Space Time Codes for 4PSK with Two Transmit Antennas," *IEEE Commun. Lett.*, vol. 5, pp. 301-303, 2001.

[55] R. S. Blum, "Some Analytical Tools for the Design of Space-Time Convolutional Codes," *IEEE Trans. Commun.*, vol. 50, no. 10, pp. 1593-1599, 2002.

[56] W. Su, X. G. Xia, and K. R. Liu, "A Systematic Design of High-Rate Complex Orthogonal Space-Time Block Codes," *IEEE Commun. Lett.*, vol. 8, no. 6, pp. 380-382, 2004.

[57] D. G. Brennan, "Linear Diversity Combining Techniques," *Proc. IRE*, vol. 47, no. 6, pp. 1075-1102, 1959.

[58] J. Winters, "Optimum Combining in Digital Mobile Radio with Cochannel Interference," *IEEE J. Sel. Areas Commun.*, vol. 2, no. 4, pp. 528-539, 1984.

[59] R. G. Vaughan, "On Optimum Combining at the Mobile," *IEEE Trans. Veh. Technol.*, vol. 37, no. 4, pp. 181-188, 1988.

[60] E. Ostrom, "Background on the Institutional Analysis and Development Framework," *Policy Studies Journal*, vol. 39, no. 1, pp. 7-27, 2011.

[61] G. Tsoulos, *MIMO system technology for wireless communications*. CRC press, 2006.

[62] M. C. Jeruchim, P. Balaban, and K. S. Shanmugan, *Simulation of communication systems: modeling, methodology and techniques*. Springer Science & Business Media, 2006.

[63] M. Di Renzo, F. Graziosi, and F. Santucci, "Channel Capacity over Generalized Fading Channels: A Novel MGF-based Approach for Performance Analysis and Design of Wireless Communication Systems," *IEEE Trans. Veh. Technol.*, vol. 59, no. 1, pp. 127-149, 2010.

[64] M. K. Simon and M. S. Alouini, *Digital Communication over Fading Channels*. John Wiley & Sons, 2005, vol. 95.

[65] X. N. Zeng and A. Ghrayeb, "Performance Bounds for Combined Channel Coding and Space-Time Block Coding with Receive Antenna Selection," *IEEE Trans. Veh. Technol.*, vol. 55, no. 4, pp. 1441-1446, 2006.

[66] T. Niyomsataya, A. Miri, and M. Nevins, "A New Unitary Space-Time Code with High Diversity Product," *IEEE Trans. Wireless Commun.*, vol. 5, no. 11, pp. 3045-3049, 2006.

[67] Y. Zhou and T. S. Ng, "MIMO-OFCDM Systems with Joint Iterative Detection and Optimal Power Allocation," *IEEE Trans. Wireless Commun.*, vol. 7, no. 12, pp. 5504-5516, 2008.

[68] G. A. Ropokis, A. A. Rontogiannis, P. T. Mathiopoulos, and K. Berberidis, "An Exact Performance Analysis of MRC/OSTBC over Generalized Fading Channels," *IEEE Trans. Commun.*, vol. 58, no. 9, pp. 2486-2492, 2010.

[69] L. Jacobs and M. Moeneclaey, "Accurate Closed-Form Approximation of BER for OSTBCs with Estimated CSI on Spatially Correlated Rayleigh Fading MIMO Channels," *IEEE Commun. Lett.*, vol. 17, no. 3, pp. 533-536, 2013.

[70] M. Marey and O. A. Dobre, "Blind Modulation Classification for Alamouti STBC System with Transmission Impairments," *IEEE Wireless Commun. Lett.*, vol. 4, no. 5, pp. 521-524, 2015.

[71] L. Heng and L. M. Jalloul, "Performance of the 3GPP LTE Space-Frequency Block Codes in Frequency-Selective Channels with Imperfect Channel Estimation," *IEEE Trans. Veh. Technol.*, vol. 64, no. 5, pp. 1848-1855, 2015.

[72] L. Guowei, L. Yuanan, and X. Xuefang, "Effect of Imperfect CSI on STBC-MISO System via Antenna Selection," *IET Signal Proc.*, vol. 10, no. 2, pp. 115-124, 2016.

[73] D. Ha, H. Lee, and J. Kang, "Error Performance Analysis of STBC-Alamouti and STBC-CIOD with Phase Estimation Error over Nakagami-m Fading Channels," *Electron. Lett.*, vol. 52, no. 6, pp. 452-454, 2016.

[74] Y. Acar, H. Dogan, E. Basar, and E. Panayirci, "Interpolation Based Pilot-Aided Channel Estimation for STBC Spatial Modulation and Performance Analysis under Imperfect CSI," *IET Commun.*, vol. 10, no. 14, pp. 1820-1828, 2016.

[75] S. Boualleg, K. Ghanem, B. Haraoubia, and M. Nedil, "On the Performance Enhancement when Combining STBC and Channel Estimation Techniques in Underground MIMO Channels," *IEEE Antennas Wireless Propag. Lett.*, vol. 15, pp. 394-397, 2016.

[76] H. Lee, "Exact and Asymptotic BER Analysis of 2×2 FRLR-STBC with BPSK Modulation," *Electron. Lett.*, vol. 53, no. 11, pp. 720-722, 2017.

[77] O. S. Badarneh and R. Mesleh, "Performance Analysis of Space Modulation Techniques over α-μ and κ-μ Fading Channels with Imperfect Channel Estimation," *Transactions on Emerging Telecommunications Technologies*, vol. 28, no. 2, 2017.

[78] R. S. Blum, Y. G. Li, J. H. Winters, and Q. Yan, "Improved Space-Time Coding for MIMO OFDM Wireless Communications," *IEEE Trans. Commun.*, vol. 49, no. 11, pp. 1873-1878, 2001.

[79] R. Piechocki, P. Fletcher, A. Nix, C. Canagarajah, and J. McGeehan, "Performance Evaluation of BLAST-OFDM Enhanced Hiperlan/2 using Simulated and Measured Channel Data," *Electron. Lett.*, vol. 37, no. 18, pp. 1137-1139, 2001.

[80] Y. Li, "Simplified Channel Estimation for OFDM Systems with Multiple Transmit Antennas," *IEEE Trans. Wireless Commun.*, vol. 1, no. 1, pp. 67-75, 2002.

[81] H. Bolcskei, D. Gesbert, and A. J. Paulraj, "On the Capacity of OFDM-based Spatial Multiplexing Systems," *IEEE Trans. Commun.*, vol. 50, no. 2, pp. 225-234, 2002.

[82] C. N. Chuah, D. N. C. Tse, J. M. Kahn, and R. A. Valenzuela, "Capacity Scaling in MIMO Wireless Systems under Correlated Fading," *IEEE Trans. Inf. Theory*, vol. 48, no. 3, pp. 637-650, 2002.

[83] A. Stamoulis, S. N. Diggavi, and N. Al-Dhahir, "Intercarrier Interference in MIMO OFDM," *IEEE Trans. Signal Process.*, vol. 50, no. 10, pp. 2451-2464, 2002.

[84] B. Lu, X. Wang, and K. R. Narayanan, "LDPC-based Space-Time Coded OFDM Systems over Correlated Fading Channels: Performance Analysis and Receiver Design," *IEEE Trans. Commun.*, vol. 50, no. 1, pp. 74-88, 2002.

[85] H. E. Gamal, A. R. J. Hammons, Y. Liu, M. P. Fitz, and O. Y. Takeshita, "On the Design of Space-Time and Space-Frequency Codes for MIMO Frequency-Selective Fading Channels," *IEEE Trans. Inf. Theory*, vol. 49, no. 9, pp. 2277-2292, Sep. 2003.

[86] H. Bolcskei, M. Borgmann, and A. J. Paulraj, "Impact of the Propagation Environment on the Performance of Space-Frequency Coded MIMO-OFDM," *IEEE J. Sel. Areas Commun.*, vol. 21, no. 3, pp. 427-439, 2003.

[87] Y. L. Lee, Y. H. You, W. G. Jeon, J. H. Paik, and H. K. Song, "Peak-to-Average Power Ratio in MIMO-OFDM Systems using Selective Mapping," *IEEE Commun. Lett.*, vol. 7, no. 12, pp. 575-577, 2003.

[88] G. L. Stuber, J. R. Barry, S. W. Mclaughlin, Y. Li, M. A. Ingram, and T. G. Pratt, "Broadband MIMO-OFDM Wireless Communications," *Proc. IEEE*, vol. 92, no. 2, pp. 271-294, 2004.

[89] A. J. Paulraj, D. A. Gore, R. U. Nabar, and H. Bolcskei, "An overview of MIMO Communications-A Key to Gigabit Wireless," *Proc. IEEE*, vol. 92, no. 2, pp. 198-218, 2004.

[90] W. Su, Z. Safar, and K. R. Liu, "Towards Maximum Achievable Diversity in Space, Time, and Frequency: Performance Analysis and Code Design," *IEEE Trans. Wireless Commun.*, vol. 4, no. 4, pp. 1847-1857, 2005.

[91] P. Garg, R. K. Mallik, and H. M. Gupta, "Performance Analysis of Space-Time Coding with Imperfect Channel Estimation," *IEEE Trans. Wireless Commun.*, vol. 4, no. 1, pp. 257-265, 2005.

[92] W. Su, Z. Safar, and K. R. Liu, "Full-Rate Full-Diversity Space-Frequency Codes with Optimum Coding Advantage," *IEEE Trans. Inf. Theory*, vol. 51, no. 1, pp. 229-249, 2005.

[93] A. Tarighat and A. H. Sayed, "MIMO OFDM Receivers for Systems With IQ Imbalances," *IEEE Trans. Signal Process.*, vol. 53, no. 9, pp. 3583-3596, 2005.

[94] T. H. Liew and L. Hanzo, "Space-Time Trellis and Space-Time Block Coding versus Adaptive Modulation and Coding Aided OFDM for Wideband Channels," *IEEE Trans. Veh. Technol.*, vol. 55, no. 1, pp. 173-187, 2006.

[95] M. Jiang and L. Hanzo, "Multiuser MIMO-OFDM for Next-Generation Wireless Systems," in *Proc. IEEE*, vol. 95, no. 7, pp. 1430-1469, 2007.

[96] M. Torabi, S. Aissa, and M. R. Soleymani, "On the BER Performance of Space-Frequency Block Coded OFDM Systems in Fading MIMO Channels," *IEEE Trans. Wireless Commun.*, vol. 6, no. 4, pp. 1366-1373. 2007.

[97] S. Lu, B. Narasimhan, and N. Al-Dhahir, "A Novel SFBC-OFDM Scheme for Doubly Selective Channels," *IEEE Trans. Veh. Technol.*, vol. 58, no. 5, pp. 2573-2578, 2009.

[98] P. Drotar, J. Gazda, P. Galajda, D. Kocur, and P. Pavelka, "Receiver Technique for Iterative Estimation and Cancellation of Nonlinear Distortion in MIMO SFBC-OFDM Systems," *IEEE Trans. Consum. Electron.*, vol. 56, no. 2, pp. 471-475, 2010.

[99] K. H. Kim and H. M. Kim, "An ICI Suppression Scheme Based on the Correlative Coding for Alamouti SFBC-OFDM System with Phase Noise," *IEEE Trans. Wireless Commun.*, vol. 10, no. 7, pp. 2023-2027, 2011.

[100] L. Jacobs and M. Moeneclaey, "BER Analysis of Square OSTBCs with LMMSE Channel Estimation in Arbitrarily Correlated Rayleigh Fading Channels," *IEEE Commun. Lett.*, vol. 14, no. 7, pp. 626-628, 2010.

[101] N. I. Miridakis and D. D. Vergados, "A Survey on the Successive Interference Cancellation Performance for Single-Antenna and Multiple-Antenna OFDM Systems," *IEEE Communications Surveys & Tutorials*, vol. 15, no. 1, pp. 312-335, 2013.

[102] F. Delestre, G. Owojaiye, and Y. Sun, "Efficient Space-Frequency Block Coded Pilot aided Channel Estimation Method for Multiple-Input-Multiple-Output Orthogonal Frequency Division Multiplexing Systems over Mobile Frequency-Selective Fading Channels," *IET Commun.*, vol. 8, no. 6, pp. 841-851, 2014.

[103] E. V. Zorita and M. Stojanovic, "Space-Frequency Block Coding for Underwater Acoustic Communications," *IEEE J. Ocean. Eng.*, vol. 40, no. 2, pp. 303-314, 2015.

[104] N. Kolomvakis, M. Matthaiou, and M. Coldrey, "IQ Imbalance in Multiuser Systems: Channel Estimation and Compensation," *IEEE Trans. Commun.*, vol. 64, no. 7, pp. 3039-3051, 2016.

[105] L. Chen, A. G. Helmy, G. Yue, S. Li, and N. Al-Dhahir, "Performance and Compensation of I/Q Imbalance in Differential STBC-OFDM," in *Global Communications Conference (Globecom), 2016 IEEE*. IEEE, 2016, pp. 1-7.

[106] L. Chen, A. G. Helmy, G. Yue, S. Li, and N. Al-Dhahir, "Performance Analysis and Compensation of Joint Tx/Rx I/Q Imbalance in Differential STBC-OFDM," *IEEE Trans. Veh. Technol.*, vol. 66, no. 7, pp. 6184-6200, 2017.

[107] Y. Wu, D. W. K. Ng, C. K. Wen, R. Schober, and A. Lozano, "Low-Complexity MIMO Precoding for Finite-Alphabet Signals," *IEEE Trans. Wireless Commun.*, vol. 16, no. 7, pp. 4571-4584, 2017.

[108] K. Kim, H. Park, and H. M. Kwon, "Rate-Compatible SFBC-OFDM under Rapidly Time-varying Channels," *IEEE Trans. Commun.*, vol. 59, no. 8, pp. 2070-2077, 2011.

[109] D. Singh and H. D. Joshi, "BER Performance of SFBC OFDM System over TWDP Fading Channel," *IEEE Commun. Lett.*, vol. 20, no. 12, pp. 2426-2429, 2016.

[110] D. Singh and H. D. Joshi, "Performance Analysis of SFBC-OFDM System with Channel Estimation Error over Generalized Fading Channels," *Trans. Emerg. Telecommun. Technol.*, vol. 29, no. 3, 2018.

[111] D. Singh and H. D. Joshi, "Generalized MGF Based Analysis of Line-Of-Sight Plus Scatter Fading Model and its Applications to MIMO-OFDM Systems," *Int. J. Electron. and Commun.*, vol. 91, pp. 110-117, 2018.

[112] A. A. Abu-Dayya and N. C. Beaulieu, "Outage Probabilities of Diversity Cellular Systems with Cochannel Interference in Nakagami Fading," *IEEE Trans. Veh. Technol.*, vol. 41, no. 4, pp. 343-355, 1992.

[113] V. A. Aalo, "Performance Of Maximal-Ratio Diversity Systems in a Correlated Nakagami Fading Environment," *IEEE Trans. Commun.*, vol. 43, no. 8, pp. 2360-2369, 1995.

[114] M. K. Simon and M. S. Alouini, "A Unified Approach to the Performance Analysis of Digital Communication over Generalized Fading Channels," in *Proc. IEEE*, vol. 86, no. 9, pp. 1860-1877, 1998.

[115] M. S. Alouini and A. J. Goldsmith, "Capacity of Rayleigh Fading Channels under Different Adaptive Transmission and Diversity-Combining Techniques," *IEEE Trans. Veh. Technol.*, vol. 48, no. 4, pp. 1165-1181, 1999.

[116] M. S. Alouini and M. K. Simon, "An MGF-Based Performance Analysis of Generalized Selection Combining over Rayleigh Fading Channels," *IEEE Trans. Commun.*, vol. 48, no. 3, pp. 401-415, 2000.

[117] Z. Chen, J. Yuan, and B. Vucetic, "Analysis of Transmit Antenna Selection/Maximal Ratio Combining in Rayleigh Fading Channels," *IEEE Trans. Veh. Technol.*, vol. 54, no. 4, pp. 1312-1321, 2005.

[118] K. Peppas, F. Lazarakis, A. Alexandridis, and K. Dangakis, "Error Performance of Digital Modulation Schemes with MRC Diversity Reception over η-μ Fading Channels," *IEEE Trans. Wireless Commun.*, vol. 8, no. 10, pp. 4974-4980, 2009.

[119] D. Dixit and P. Sahu, "Performance of L-branch MRC Receiver in η-μ and κ-μ Fading Channels for QAM Signals," *IEEE Wireless Commun. Lett.*, vol. 1, no. 4, pp. 316-319, 2012.

[120] P. Kumar and P. Sahu, "Analysis of *M*-PSKK with MRC Receiver over κ-μ Fading Channels with Outdated CSI," *IEEE Wireless Commun. Lett.*, vol. 3, no. 6, pp. 557-560, 2014.

[121] D. Dixit and P. Sahu, "Performance Analysis of Rectangular QAM with SC Receiver over Nakagami-*m* Fading Channels," *IEEE Commun. Lett.*, vol. 18, no. 7, pp. 1262-1265, 2014.

[122] Y. Wu, R. H. Louie, and M. R. McKay, "Asymptotic Outage Probability of MIMO-MRC Systems in Double-Correlated Rician Environments," *IEEE Trans. Wireless Commun.*, vol. 15, no. 1, pp. 367-376, 2016.

[123] M. Maleki, H. R. Bahrami, and A. Alizadeh, "On MRC-Based Detection of Spatial Modulation," *IEEE Trans. Wireless Commun.*, vol. 15, no. 4, pp. 3019-3029, 2016.

[124] S. Al-Juboori and X. Fernando, "Multi-Antenna Spectrum Sensing over Correlated Nakagami-m Channels with MRC and EGC Diversity Receptions," *IEEE Trans. Veh. Technol.*, vol. 67, no. 3, pp. 2155-2164, 2017.

[125] H. Pirzadeh and A. L. Swindlehurst, "Spectral Efficiency under Energy Constraint for Mixed ADC MRC Massive MIMO," *IEEE Signal Process. Lett.*, vol. 24, no. 12, pp. 1847-1851, 2017.

[126] Z. Wei, D. W. K. Ng, and J. Yuan, "Joint Pilot and Payload Power Control For Uplink MIMO-NOMA with MRC-SIC Receivers," *IEEE Commun. Lett.*, vol. 22, no. 4, pp. 692-695. 2018.

[127] T. Liu, H. Zhang, J. Wang, H. Fu, P. Wang, and J. Li, "Performance Analysis of Non Identically Distributed FSO Systems with Dual and Triple Branch based on MRC over Gamma-Gamma Fading Channels," *China Commun.*, vol. 15, no. 1, pp. 45-51, 2018.

[128] T. Van Luong and Y. Ko, "The BER Analysis of MRC-Aided Greedy Detection for OFDM-IM in Presence of Uncertain CSI," *IEEE Wireless Commun. Lett.*, vol. 7, no. 4, pp. 566-569, 2018.

[129] S. Wyne, A. P. Singh, F. Tufvesson, and A. F. Molisch, "A Statistical Model for Indoor Office Wireless Sensor Channels," *IEEE Trans. Wireless Commun.*, vol. 8, no. 8, pp. 4154-4164, 2009.

[130] M. D. Yacoub, "Nakagami-*m* Phase-Envelope Joint Distribution: A New Model," *IEEE Trans. Veh. Technol.*, vol. 59, no. 3, pp. 1552-1557, 2010.

[131] N. C. Beaulieu and X. Jiandong, "A Novel Fading Model for Channels with Multiple Dominant Specular Components," *IEEE Wireless Commun. Lett.*, vol. 4, no. 1, pp. 54-57, 2015.

[132] N. Youssef, C. X. Wang, and M. Patzold, "A Study on the Second Order Statistics of Nakagami-Hoyt Mobile Fading Channels," *IEEE Trans. Veh. Technol.*, vol. 54, no. 4, pp. 1259-1265, 2005.

[133] I. S. Gradshteyn and I. M. Ryzhik, *Table of integrals, series, and products*. Academic Press, 2014.

[134] M. Nakagami, "The m-Distribution-A General Formula of Intensity Distribution of Rapid Fading," in *Statistical methods in radio wave propagation*. Elsevier, 1960, pp. 3-36.

[135] P. S. Bithas, P. T. Mathiopoulos, and S. A. Kotsopoulos, "Diversity Reception over Generalized-K (KG) Fading Channels," *IEEE Trans. Wireless Commun.*, vol. 6, no. 12, pp. 4238-4243, 2007.

[136] G. D. Durgin, T. S. Rappaport, and D. A. De Wolf, "New Analytical Models and Probability Density Functions for Fading in Wireless Communications," *IEEE Trans. Commun.*, vol. 50, no. 6, pp. 1005-1015, 2002.

[137] M. Rao, F. J. Lopez-Martinez, M. S. Alouini, and A. Goldsmith, "MGF Approach to the Analysis of Generalized Two-Ray Fading Models," *IEEE Trans. Wireless Commun.*, vol. 14, no. 5, pp. 2548-2561, 2015.

[138] A. K. Papazafeiropoulos and S. A. Kotsopoulos, "The η-λ-μ: A General Fading Distribution," in *Global Telecommunications Conference, 2009. GLOBECOM 2009. IEEE*. IEEE, 2009, pp. 1-5.

[139] C. W. Lee, M. C. Chuang, M. C. Chen, and Y. S. Sun, "Seamless Handover for High Speed Trains using Femtocell-Based Multiple Egress Network Interfaces," *IEEE Trans. Wireless Commun.*, vol. 13, no. 12, pp. 6619-6628, 2014.

[140] K. Guan, Z. Zhong, B. Ai, and T. Kurner, "Propagation Measurements and Analysis for Train Stations of High-Speed Railway at 930 MHz," *IEEE Trans. Veh. Technol.*, vol. 63, no. 8, pp. 3499-3516, 2014.

[141] A. Olutayo, H. Ma, J. Cheng, and J. F. Holzman, "Level Crossing Rate and Average Fade Duration for the Beaulieu-Xie Fading Model," *IEEE Wireless Commun. Lett.*, vol. 6, no. 3 pp. 326-329, 2017.

[142] R. Subadar and A. D. Singh, "Performance of SC Receiver over TWDP Fading Channels," *IEEE Wireless Commun. Lett.*, vol. 2, no. 3, pp. 267-270, 2013.

[143] M. D. Yacoub, "The *Alpha-Mu* Distribution: A Physical Fading Model for the Stacy Distribution," *IEEE Trans. Veh. Technol.*, vol. 56, no. 1, pp. 27-34, 2007.

[144] J. F. Paris, "Statistical Characterization of *Kappa-Mu* Shadowed Fading," *IEEE Trans. Veh. Technol.*, vol. 63, no. 2, pp. 518-526, 2014.

[145] V. Asghari, D. B. da Costa, and S. Aissa, "Symbol Error Probability of Rectangular QAM in MRC Systems with Correlated *eta-mu* Fading Channels," *IEEE Trans. Veh. Technol.*, vol. 59, no. 3, pp. 1497-1503, 2010.

[146] E. Biglieri, R. Calderbank, A. Constantinides, A. Goldsmith, A. Paulraj, and H. V. Poor, *MIMO Wireless Communications*. Cambridge University Press, 2007.

[147] H. Shin and J. H. Lee, "Performance Analysis of Space-Time Block Codes over Keyhole Nakagami-m Fading Channels," *IEEE Trans. Veh. Technol.*, vol. 53, no. 2, pp. 351-362, 2004.

[148] M. K. Simon, S. M. Hinedi, and W. C. Lindsey, *Digital Communication Techniques: Signal Design and Detection*. Prentice Hall PTR, 1995.

[149] R. Pawula, S. Rice, and J. Roberts, "Distribution of the Phase Angle between Two Vectors Perturbed by Gaussian Noise," *IEEE Trans. Commun.*, vol. 30, no. 8, pp. 1828-1841, 1982.

[150] S. T. Chung and A. J. Goldsmith, "Degrees of Freedom in Adaptive Modulation: A Unified View," *IEEE Trans. Commun.*, vol. 49, no. 9, pp. 1561-1571, Sep. 2001.

[151] N. C. Beaulieu, "A Useful Integral for Wireless Communication Theory and its Application to Rectangular Signaling Constellation Error Rates," *IEEE Trans. Commun.*, vol. 54, no. 5, pp. 802-805, 2006.

[152] T. Eng and L. B. Milstein, "Coherent DS-CDMA performance in Nakagami Multipath Fading," *IEEE Trans. Commun.*, vol. 43, no. 234, pp. 1134-1143, 1995.

[153] S. Chennakeshu and J. B. Anderson, "Error Rates for Rayleigh Fading Multichannel Reception of MPSK Signals," *IEEE Trans. Commun.*, vol. 43, no. 234, pp. 338-346, 1995.

[154] C. R. Athaudage and K. Sathananthan, "Probability of Error of Space-Time Coded OFDM Systems with Frequency Offset in Frequency-Selective Rayleigh Fading Channels," in *Communications, 2005. ICC 2005. 2005 IEEE International Conference on*, vol. 4. IEEE, 2005, pp. 2593-2599.

[155] T. Yoo and A. Goldsmith, "On the Optimality of Multiantenna Broadcast Scheduling using Zero-Forcing Beamforming," *IEEE J. Sel. Areas Commun.*, vol. 24, no. 3, pp. 528-541, 2006.